For N.C.L, Liabvary

Degree awarded

354

12-9-93

TH-7490 TH-7491

04:549.73
NAI

STUDIES ON

FERRITE - MANGANITE SYSTEMS

A THESIS SUBMITTED

TO

THE UNIVERSITY OF POONA

FOR

THE DEGREE OF DOCTOR OF PHILOSOPHY

(IN CHEMISTRY)

by

BHIKAJI NARAYAN NAIK, M.Sc.
National Chemical Laboratory,
Poona-8.

JANUARY, 1967.

A C K N O W L E D G E M E N T

I am deeply indebted to Dr. A. P. B. Sinha for his keen interest, valuable guidance and encouragement during the persuit of this work.

I take this opportunity to express my sincere thanks to the Director, National Chemical Laboratory, Poona-8, for allowing me to submit the research work carried out at the National Chemical Laboratory in the form of a thesis.

B. N. Naik

(B. N. Naik)

National Chemical
Laboratory, Poona-8.

January, 1967.

C O N T E N T S

CHAPTER - III

3. Experimental Results

CHAPTER - IV

4. Discussion

GENERAL INTRODUCTION

GENERAL INTRODUCTION

The spin $CuMn_2O_4$ which was first synthesised by Sinha, Sanjana and Biswas[1] (1957) has the cubic spinel structure with the Mn ions occupying the octahedral and the Cu ions the tetrahedral sites of the structure. It is well-known that manganese when present as $Mn^{3+}(d^4)$ at the octahedral sites produces a strong Jahn-Teller distortion and the structure becomes tetragonal. The observed cubic structure of $CuMn_2O_4$ therefore appears anomalous at the first sight and was explained by Sinha et.al.[1] on the basis of the formula $Cu^{1+}[Mn^{3+}\ Mn^{4+}]\ O_4$. This formula has also been supported by the electrical properties of the compound. In this compound, the ionisation state of copper is different from that in other isomorphous compounds e.g. $CuFe_2O_4$, $CuCr_2O_4$ where it is 2+. Similarly in many other manganites, AMn_2O_4 with A = Cd^{2+}, Zn^{2+}, Mn^{2+}, Co^{2+}, Ni^{2+}, etc. manganese is present as Mn^{3+} and not as Mn^{4+}. The presence of Cu^{1+} and Mn^{4+} in $CuMn_2O_4$ appears very unique and we have therefore investigated the conditions under which this stabilization takes place.

A number of spinels of the general formula $Cu_xMe_{1-x}Mn_{2x}Fe_{2-2x}O_4$ where Me = Cu^{2+}, Ni^{2+}, Co^{2+}, Zn^{2+} and Mn^{2+} have been prepared and their structural, magnetic and electrical properties have been studied. These results

have been used to throw light on the cation distribution and the valence states of Cu and Mn in these copper manganese spinels.

In what follows we first give a review of the relevant structural, magnetic and electrical studies already done in the field of spinels. This is followed by our own experimental results on the manganite-ferrite systems.

---O---

CHAPTER - I

HISTORICAL INTRODUCTION

CHAPTER - I

1. HISTORICAL INTRODUCTION

1.1. Structural properties

The name 'spinel', originally given to a cubic mineral of composition $MgAl_2O_4$ (magnesium aluminate) whose crystal structure was determined by Bragg[2] (1915) and Nishikawa[3] (1915), now stands for the whole class of isomorphous compounds. Ferrites $MeFe_2O_4$, chromites $MeCr_2O_4$, germanates Me_2GeO_4, titanates Me_2TiO_4 (where Me = divalent metal ion viz. Mg, Cd, Zn, Fe, Co, Ni, Cu) are some well-known examples of this class. Sulphide spinels known as thiospinels (AB_2S_4) have also been synthesised.

Aminoff[4] (1926) studied the crystal structure of a related compound, Mn_3O_4. The unit cell is tetragonal and the structure can be arrived at by expanding the cubic spinel structure parallel to one of the crystal axes. A number of compounds belonging to this tetragonal structure are also known and they are called as "distorted spinels" or tetragonal spinels.

1.1.1. Cubic spinels

The unit cell is cubic with a $\simeq 8\text{Å}$. There are eight molecules of XY_2O_4 per unit cell. The structure consists of an almost perfect cubic close packing of oxygen ions, 32 of which form 64 tetrahedral interstices and 32 octahedral interstices, of which the 8 tetrahedral and 16 octahedral interstices are occupied by the 24 metal ions (Fig.1). The space group

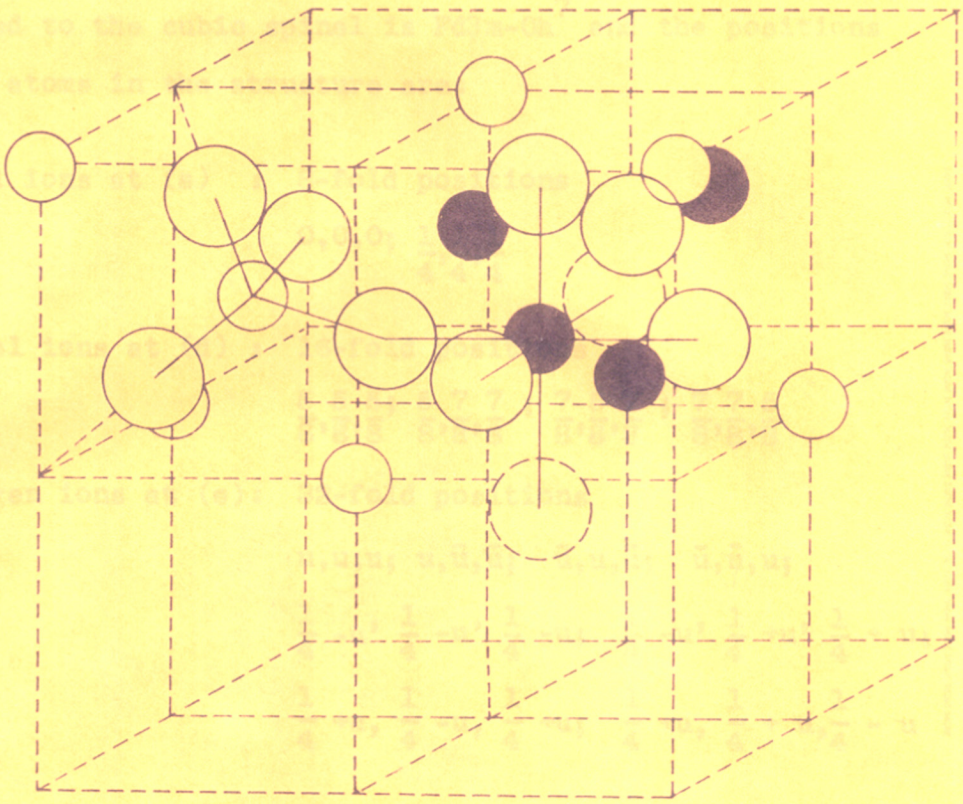

Oxygen ions.

Tetrahedral cations.

Octahedral cations.

FIG. 1.

UNIT CELL OF AN IDEAL SPINEL SHOWING ONLY TWO OCTANTS

assigned to the cubic spinel is $Fd3m\text{-}O_h^7$ and the positions of the atoms in the structure are:

8 metal ions at (a) : 8-fold positions

$0,0,0;\ \frac{1}{4},\frac{1}{4},\frac{1}{4}$

16 metal ions at (d) : 16-fold positions

$\frac{5}{8},\frac{5}{8},\frac{5}{8};\ \frac{5}{8},\frac{7}{8},\frac{7}{8};\ \frac{7}{8},\frac{5}{8},\frac{7}{8};\ \frac{7}{8},\frac{7}{8},\frac{5}{8}$

32 oxygen ions at (e): 32-fold positions

$u,u,u;\ u,\bar{u},\bar{u};\ \bar{u},u,\bar{u};\ \bar{u},\bar{u},u;$

$\frac{1}{4}-u,\ \frac{1}{4}-u,\ \frac{1}{4}-u;\ \frac{1}{4}-u,\ \frac{1}{4}+u,\ \frac{1}{4}+u;$

$\frac{1}{4}+u,\ \frac{1}{4}-u,\ \frac{1}{4}+u;\ \frac{1}{4}+u,\ \frac{1}{4}+u,\ \frac{1}{4}-u$

+

$0,0,0;$

$0,\frac{1}{2},\frac{1}{2};$

$\frac{1}{2},0,\frac{1}{2};$

$\frac{1}{2},\frac{1}{2},0.$

A 8(a) site is surrounded by 4 oxygen ions in a tetrahedral arrangement and is known as tetrahedral site and a 16- (d) position is surrounded by six oxygen ions forming a regular octahedron and is known as octahedral site. The distribution of 8 X and 16Y metal ions over the 8(a) and 16(d) sites can be in any proportion.

1.1.2. The tetragonal spinels

The unit cell is a body centred tetragon with $a \simeq 5.5\text{Å}$ and $c \simeq 9\text{Å}$. There are four XY_2O_4 molecules per unit cell. The space group is I_4/amd; D_{4h}^{19} with the positions of the atoms in unit cell as:

metal ions at 4(a) position :

$0,0,0;\quad 0,\frac{1}{2},\frac{1}{4};$

and 8(d) position :

$0,\frac{1}{4},\frac{5}{8};\quad 0,\frac{3}{4},\frac{5}{8};$

$\frac{1}{4},0,\frac{3}{8};\quad \frac{3}{4},0,\frac{3}{8};$ and

oxygen ions at 16(h) positions:

$o,\bar{x},z;\quad o,x,z;$

$o,\frac{1}{2}+x,\frac{1}{4}-z;$

$o,\frac{1}{2}-x,\frac{1}{4}-z;$

$\bar{x},o,\bar{z};\quad x,0,\bar{z};$

$x,\frac{1}{2},\frac{1}{4}+z;$ and

$\bar{x},\frac{1}{2},\frac{1}{4}+z$

+

$0,0,0$

and

$\frac{1}{2},\frac{1}{2},\frac{1}{2},$

The cations in the 8(d) position (B sites) are referred to as octahedral cations. Each one of them has six oxygen neighbours, four of which (O_1) are situated in the 'C' plane forming the square arrangement around the cations and the other two oxygens (O_2) are situated along the normal to the C plane. Ratio of Me(Oct)-O_2 distance to the Me(Oct)-O_1 distance is $\simeq C/a\sqrt{2}$. Tetrahedral cations at 4(a) positions (A sites) have four equi-distant oxygen neighbours.

The above described body-centred unit cell becomes comparable to the cubic spinel when converted into a larger C-face-centred tetragonal cell with the lattice parameters a'

and c', given by the relationship a' = a $\sqrt{2} \simeq 8\mathring{A}$ and c' = C $\simeq 9\mathring{A}$. The unit cell volume of the new cell is twice that of the body-centred cell and contains 8-molecules of XY_2O_4. In this cell there are 16 B and 8 A sites.

1.1.3. Classification on the basis of cation distribution

As mentioned above the 8X and 16Y cations in both the cubic and tetragonal spinels can be distributed in any proportion over the eight tetrahedral sites (A sites) and sixteen octahedral (B sites). Barth and Posnjak[5] (1932) have proposed the following nomenclature for the possible distributions.

(1) When the 8X ions occupy 8 tetrahedral sites and 16Y ions occupy 16 octahedral sites, the structure is said to be "Normal".

(2) When 8 of the Y-ions occupy 8 tetrahedral sites and the 8 X-ions plus the remaining 8Y ions occupy 16 octahedral sites, the structure is said to be "Inverse".

(3) If 8X and 16Y cations are distributed randomly among 8-tetrahedral and 16-octahedral positions, the structure is said to be "Random".

The convention commonly followed for writing the structure for a spinel is to put the metal ions at tetrahedral sites first, followed by the metal ions located at octahedral sites in square brackets. Thus:

$Zn\ [Al_2]\ O_4$, $Zn\ [Fe_2]\ O_4$, are "Normal spinels,

$Fe\ [MgFe]\ O_4$, $Fe\ [CuFe]\ O_4$, are "Inverse" spinels, and

$Al_{\frac{2}{3}}Ni_{\frac{1}{3}}\ [Ni_{\frac{2}{3}}Al_{\frac{4}{3}}]\ O_4$ is a "Random spinel.

During the last several years the cation distribution in many spinels has been determined and it is found that there are many intermediate cases showing various degrees of randomness. Thus in general the cations can be distributed in any proportion between two sites and the general cation distribution is as follows:

$$(A_m\ B_{1-m})_{tet} \quad \left[A_{1-m}\ B_{1+m}\right]_{oct}\ O_4 \quad (m = 0 \text{ to } 1).$$

The 'normal' (m=1), inverse (m=0) and random ($m=\frac{1}{3}$) are three special cases.

Distribution of cations is of special interest from the point of view of electrical and magnetic properties of these spinels. The X-ray method for the determination of cation distribution is often not successful because most of the spinels contains transition metal ions of equal x-ray scattering powers. In such cases neutron diffraction is a possible alternative but has not so far been applied very widely.

In ferrimagnetic spinels such as ferrites, the determination of resultant magnetic moment offers a useful method for the determination of the cation distribution. This aspect will be dealt with in detail in a later chapter.

Verwey[6] (1947) investigated the cation distribution in spinels and gave the following site preferences of the various ions:

(a) Zn^{2+}, Cd^{2+}, Ga^{3+}, In^{3+}, Ge^{4+} prefer tetrahedral site;

(b) Ni^{2+}, Cr^{3+}, Ti^{4+}, Sn^{4+}, prefer octahedral site;

(c) Mg^{2+}, Fe^{2+}, Co^{2+}, Mn^{2+}, Fe^{3+}, are indifferent ions.

Gorter[7](1954) classified such distribution on the basis of electronic configuration in the five following groups:

(1) Ions with filled 3d-shell viz., Cu^{1+}, Zn^{2+}, Cd^{2+} have tendency to form co-valent bonds using sp^3 orbital and they prefer tetrahedral sites.

(2) Ions such as Li^{1+}, Mg^{2+}, Al^{3+} which have the noble gas configuration do not show any preference for either site.

(3) Mn^{2+}, Fe^{3+}, Co^{4+} with half-filled 'd' shell have spherical symmetry and hence do not show a preference for either coordination.

(4) Transition metal ions with $3d^8$ or $3d^3$ configuration such as Ni^{2+}, Cr^{3+}, Mn^{4+} show a preference for six-fold coordination.

(5) The rest of the transition metal ions do not show any preference for either coordination.

McClure[8](1957) calculated the site preference energies of various ions in the spinel structure. This takes into account the stabilization due to the crystal field but the contributions from the Madelung energy and the Born repulsive energy are not taken into account.

Miller[9](1959) calculated the site preference energies for various ions taking the Madelung and crystal field energies into

account. The values are considerably different from those obtained by McClure[8](1957). In general these site preference energies predict the correct cation distributions.

Table 1

Octahedral site preference energies for various cations. P-k cal/g. at wt.

Ion	P	Ion	P	Ion	P	Ion	P
Li^{+}	-3.6	Mn^{++}	-14.7	Zn^{++}	-31.6	Cr^{+++}	16.6
Cu^{+}	-8.6	Fe^{++}	- 9.9	Cd^{++}	-29.1	Mn^{+++}	3.1
Ag^{+}	-19.6	Co^{++}	-10.5	Al^{+++}	- 2.5	Fe^{+++}	- 13.3
Mg^{++}	-5.0	Ni^{++}	9.0	Ti^{+++}	-21.9	Ga^{+++}	- 15.4
Ca^{++}	-30.7	Cu^{++}	- 0.1	V^{+++}	-11.9	In^{+++}	- 40.2

1.1.4. Crystal structures of ferrites and manganites

Ferrites

Ferrites having the general formula AFe_2O_4 crystallise, in general, in the spinel structure.

In case of simple ferrites, A is one of the divalent ions of the transition elements such as Mn, Fe, Co, Ni, Cu, Zn, Mg or Cd. A combination of these ions is also possible. We then speak of a solid solution of two ferrites called as 'mixed ferrites'. Metal ion distribution, lattice constant a, oxygen ion parameter u, for some of the important ferrites are tabulated below:

Table 2

Crystal data of some ferrites

No.	Ferrite	Metal ion distribution	a Å	u	d_x g/cm^3	Ref.
1.	$MnFe_2O_4$	$Mn_{0.8}Fe_{0.2}$ $[Mn_{0.2}Fe_{1.8}]$	8.5	0.384 ± 0.0003	5.00	10
2.	Fe_3O_4	Fe $[Fe^{II}Fe]$	8.39	0.379 ± 0.001	5.24	11 12
3.	$CoFe_2O_4$	Fe [CoFe]	8.38	-	5.29	13
4.	$NiFe_2O_4$	Fe [NiFe]	8.34	-	5.38	14
5.	$CuFe_2O_4$*	Fe [CuFe]	c = 8.70 a = 8.22	0.380 ± 0.005	5.35	15 16
6.	$ZnFe_2O_4$	Zn $[Fe_2]$	8.44	0.385 ± 0.002	5.33	14
7.	$MgFe_2O_4$	$Mg_{0.1}Fe_{0.9}$ $[Mg_{0.9}Fe_{1.1}]$	8.36	0.381 ± 0.001	4.52	17 18
8.	$Li_{0.5}Fe_{2.5}O_4$	Fe $[Li_{0.5}Fe_{1.5}]$	8.33	0.382 ± 0.005	4.75	19

* Copper ferrite shows a tetragonal deformation below 760°C[15].

Manganites

Several investigators have determined the structure of number of manganites and results are represented in the Table 3. It is evident from the table that many manganites crystallise in tetragonal spinel structure (Hausmannite structure):

Table 3

The structure of several manganites

No.	Compound	Structure	C(A°)	a(A°)	c/a	Cation distribution	Ref.
1.	$CuMn_2O_4$	Cubic	—	8.33	1	$Cu\left[Mn_2\right]O_4$	1
				8.30			21
				8.28			23,28
2.	$NiMn_2O_4$	Cubic	—	8.37	1	$Mn\left[NiMn\right]O_4$	1
				8.38			23
				8.39			27
3.	$MnMn_2O_4$	Tetragonal	9.44	8.15	1.16	$Mn^{2+}\left[Mn_2^{3+}\right]O_4$	1
			9.45	8.151	1.159		23
	or						
	Mn_3O_4		9.454	8.157	1.159		24,25
4.	$CdMn_2O_4$	Tetragonal	9.87	8.22	1.20	$Cd^{2+}\left[Mn_2^{3+}\right]O_4$	1
							20
5.	$ZnMn_2O_4$	Tetragonal	9.24	8.10	1.14	$Zn^{2+}\left[Mn_2^{3+}\right]O_4$	1
			9.228	8.087	1.141		23
			9.224	8.092	1.142		24
			9.254	8.087	1.144		25,26
6.	$MgMn_2O_4$	Tetragonal	9.28	8.07	1.15	$Mg^{2+}\left[Mn_2^{3+}\right]O_4$	1
			9.31		1.15		22,23
7.	$CoMn_2O_4$	Tetragonal	9.31	8.10	1.15	$Co^{2+}\left[Mn_2^{3+}\right]O_4$	23

The distortion to tetragonal structure has been explained by Dunitz and Orgel[29] (1957) on the basis of the Jahn-Teller theorem.

Jahn and Teller[31](1937) have shown that if the electronic state of a non-linear molecule is degenerate the system is unstable and a distortion to a lower energy state takes place. Jahn-Teller's theory may be illustrated by taking a particular example of Cu^{2+} ion. If the Cu^{2+} ion is situated at the octahedral site the 'd' electron configuration of the ion is $(t_{2g})^6 (eg)^3$. It gives rise to a doubly degenerate ground state, hence the regular octahedral arrangement is unstable. The system could be energetically stabilized if a distortion from regular octahedral symmetry takes place. There are various possible distortions which could remove the degeneracy. However, in case of Cu^{2+} and Mn^{3+} the tetragonal distortion of $c/a > 1$ is the one most commonly observed.

Distorted manganites transform from the tetragonal to the cubic spinel structure when heated to elevated temperatures. McMurdie and Golovato[30](1948) who studied the structure of the Mn_3O_4 at high temperatures by x-ray diffraction observed a transformation from the tetragonal to the cubic symmetry at 1170°C. Romeijn[32] (1953) had also found evidences for such a transition in his studies on the resistivity of $ZnMn_2O_4$. Irani, Sinha and Biswas[33](1962) investigated the structure of many tetragonal manganites as a function of temperature and found a transformation to cubic phase in all cases. Finch, Sinha and Sinha[34](1957) have studied the problem theoretically on the basis of an order-disorder process. This model has been investigated in detail by Wojtowicz[35] (1959). Kanamori[36] (1960) attributed the transformation as arising due to the resonance between the various possible distorted structures.

The tetragonal structure changes to the cubic structure, also when a part of the distorting ions is removed from the octahedral sites.

Finch, Sinha and Sinha[34] (1957) first studied the effect of removal of the Mn^{3+} ions on crystal distortion. They substituted the Mn^{3+} ions by non-distorting cations through the formation of solid solution of tetragonal (Mn_3O_4) and cubic (A Fe_2O_4) spinels. They analyzed the results on the assumption that the Mn^{3+} ions occupied the octahedral sites in the solid solutions as they did in the parent Mn_3O_4. Wickham and Croft[37] (1958) made similar assumption in their studies on the systems $Zn_xGe_{1-x}Mn_2O_4$, $Zn_xGe_{1-x}Co_{2-2x}Mn_{2x}O_4$ and $Zn_xLi_{1-x}Mn_2O_4$.

Irani, Sinha and Biswas[38](1960) determined the cation distribution from the x-ray diffraction intensities and plotted the unit cell dimensions as a function of the number of Mn^{3+} ions at the octahedral sites for the systems Mn_3O_4- $MgAl_2O_4$ and $MgMn_2O_4$ - $MgAl_2O_4$. They observed that c' and a' do not change linearly with compositions but remain more or less constant and then show a sudden change at a critical composition beyond which c' = a' and the systems take up the cubic spinel structure. This critical composition is one where 9.3 $\pm$ 0.2 sites out of the 16 octahedral sites are occupied by Mn^{3+} ions. Finch, Sinha and Sinha[34](1957), Wojtowicz[35](1959) and Kanamori[36](1960) have treated this transformation theoretically.

Miyahara, Muramori and Naoki Tokuda[39] (1961) have studied the tetragonal distortion in copper manganite-chromite system with general formula $CuMn_{2-a}Cr_aO_4$ (a = 0 to 2). They have reported that the system has a cubic structure in the range $0 \leqslant a \leqslant 1.0$ and a tetragonal structure with $c/a < 1$ in the range $1.0 \leqslant a \leqslant 2.0$ and in cubic region lattice parameter of specimen depends on the heat treatment and the degree of the dependence decreases with increasing chromium concentration.

Temperature dependence of the distortion of some magnetic spinels are experimentally studied in detail by Miyahara[40] (1962) and it is concluded that the transition is of the first kind. Furthermore, he reports that compound $CuMn_2O_4$ which contains both manganese and copper exhibits no tetragonal distortion due to compensation effect of cupric and manganic ions. When copper is replaced by zinc or manganese by chromium the distortion reappears.

---0---

1.2. Magnetic properties of spinels

1.2.1. Ferrimagnetism

In a ferromagnetic substance at $0^{o}K$, the magnetic dipoles are aligned parallel as a result of electron exchange interactions giving a resultant saturation moment per unit volume;

$$M = N g J \mu_B$$

where N is the number of atoms per unit volume, g is the gyromagnetic ratio, J is the total angular momentum quantum number (which includes the total orbital contribution L and the total spin contribution S) and $\mu_B = \left(\frac{eh}{4\pi mc}\right)$ is the magnetic moment of one electron. The saturation magnetization decreases with temperature and at the Curie temperature T_c, the long range order is destroyed. At higher temperatures only paramagnetism remains.

The ferromagnetic and paramagnetic behaviour of substances containing electrons of the first transition series are almost entirely due to the spins of the unpaired 3d electrons and the ferromagnetic moment of each ion is equal to $2 S \mu_B$ (S = total spin quantum number of the ion). Table 4 gives the number of 3d electrons and the value of 2 S for these ions.

Table 4

Number of 3d electrons and resulting spin moment of ions of the first transition series.

Ions	Number of 3d electrons	2 S (μ_B)
Sc^{3+} Ti^{4+}	0	0
Ti^{3+}	1	1
Ti^{2+} V^{3+}	2	2
Cr^{3+} Mn^{4+}	3	3
Mn^{3+}	4	4
Mn^{2+} Fe^{3+}	5	5
Fe^{2+} Co^{3+}	6	4
Co^{2+} Ni^{3+}	7	3
Ni^{2+}	8	2
Cu^{2+}	9	1
Cu^{1+} Zn^{2+}	10	0

In a ferromagnetic compound such as Fe_3O_4 ($Fe^{2+}Fe_2^{3+}O_4$) the moment per formula unit would be expected to be equal to the sum of the ionic moments and the saturation magnetization for Fe_3O_4 should be 4 + 2 x 5 = 14 μ_B. Weiss and Forrer[41] (1929) and Hilpert[42] (1909) however found it to be 4.08 μ_B only. Furthermore, the 'normal' ferrites e.g. $ZnFe_2O_4$ and $CdFe_2O_4$ are paramagnetic in nature. It was also known that several ferrites above Curie temperature showed a curvature of the $1/\chi$ vs T curve concave towards the T-axis, where χ is the paramagnetic susceptibility.

Using these data Neel[43] put forward the theory of antiferromagnetism in 1948. He made the basic hypothesis that a strong negative interaction i.e. a tendency to anti-parallel orientation, exists between ionic moments on tetrahedral sites on the one hand and those on the octahedral sites on the other hand. Thus the magnetic moment for $Fe^{III}\left[Fe^{II}Fe^{III}\right]O_4$ should be $(5 + 4) - 5 = 4\ \mu_B$ which is in close agreement with experiment. This behaviour is termed non-compensated antiferromagnetism or "Ferrimagnetism". At the same time, Neel calculated the paramagnetic susceptibility by extending the Weiss-molecular field theory to substances with two different lattice sites on which different amounts of magnetic ions (atoms) are found. The theory was given for a compound containing one kind of magnetic ion only e.g. $Fe^{III}_{x_a}Me_{1-x_a}\left[Fe^{III}_{x_b}Me_{2-x_b}\right]O_4$, where x_a and x_b stand for the number of ferric ions on A and B sites and Me represents non-magnetic ions and the following relationship was obtained,

$$\frac{1}{\chi} = \frac{T}{C} + \frac{1}{\chi_0} - \frac{S}{T-\theta}$$

where χ is the molar susceptibility, C_{mole} is the molar Curie constant and S, χ_0 and θ are constants related to various interaction constants.

He also found that in the ferromagnetic region the shape of the saturation magnetization vs T graph depends on the value of x_a/x_b in relation to α and β, where $\alpha = \frac{J_{AA}}{J_{AB}}$, $\beta = \frac{J_{BB}}{J_{AB}}$

and J_{AA}, J_{BB} and J_{AB} are the exchange interactions between A-A, B-B and A-B ions. The typical examples are shown in Fig.2 and condition in which one or the other curves is followed is listed in the Table No.5.

Table 5

No.	Curve	x_a/x_b
1.	b	$(1-\beta)/(1-\alpha)$
2.	c	Between 1 and $(1-\beta)/(1-\alpha)$
3.	d	1
4.	e	Between 1 and $(1+\beta)/(1+\alpha)$
5.	f	$(1+\beta)/(1+\alpha)$.

Yafet and Kittel[44] (1952) showed that a stable arrangement is also possible, if the ionic moments on the A and B sub-lattices break up into (A' and A") and (B' and B") sub-lattices respectively with the ionic moments inside each of the sub-lattices A', A", B' and B" being mutually parallel but the ionic moments in the A' and A" or in the B' and B" sub-lattices forming angles with each other as a result of the negative AA or BB interactions competing with the AB interactions. The possible arrangements of the sub-lattices magnetization are shown in the following figure.

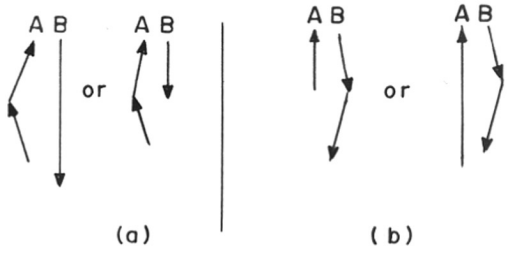

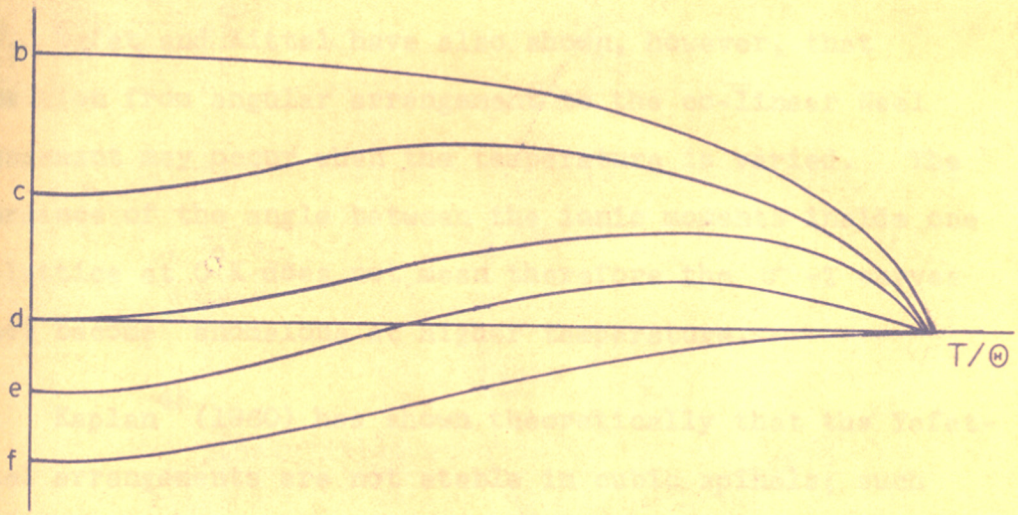

FIG. 2. SPONTANEOUS-MAGNETIZATION Vs TEMPERATURE CURVES FOR DIFFERENT RELATIONSHIPS BETWEEN THE NUMBER OF FERRIC IONS IN A AND B SITES (x_a AND x_b RESPECTIVELY) AND α AND β.

(Reproduced from Gorter.)

(a) is obtained when the interaction AA is comparable to AB, and BB is small with respect to AB, and (b) is obtained when the interaction AA is small with respect to AB and BB is comparable to AB.

Yafet and Kittel have also shown, however, that transition from angular arrangement to the co-linear Neel arrangement may occur when the temperature is varied. The occurrence of the angle between the ionic moments inside one sub-lattice at $0^{\circ}K$ does not mean therefore the σ -T curves cannot become anomalous at higher temperature.

Kaplan[45] (1960) has shown theoretically that the Yafet-Kittel arrangements are not stable in cubic spinels; such arrangements can however get stabilized in the presence of a tetragonal distortion. He has also shown that it is possible to have arrangements in which there are non-zero angles between spins on A sites simultaneously with angles between those on B sites and this is contrary to the Yafet and Kittle's results.

Kaplan, Dwight, Lyons and Menyuk[46] (1961) have shown that for B-B interaction which are sufficiently large to destabilize the Neel's configuration in the cubic spinels, a spiral spin arrangement has lower energy than Neel's or Yafet-Kittle's.

1.2.2. Magnetic properties of ferrites

The saturation moments of ferrites were first measured by Polder[47] (1949) and Gorter[48,49] (1950). More complete data on many of these materials have since been reported by other authors[50-57] giving the saturation magnetization vs temperature and susceptibility vs temperature curves.

Saturation moments and Curie temperatures of the single ferrites ($Me^{II}Fe_2^{III}O_4$) and ($Li_{0.5}Fe_{2.5}^{III}O_4$) are given below in the Table 6.

Table 6

Saturation moments (η_B) of single ferrites

No.	Ferrite	η_B	Expected value (Neel model)	T_c °C
1.	$MnFe_2O_4$	4.4	5	300
2.	$Fe^{II}Fe_2O_4$	4.08	4	585
3.	$CoFe_2O_4$	3.94	3	520
4.	$NiFe_2O_4$	2.224	2	585
5.	$CuFe_2O_4$	1.37	1	455
6.	$MgFe_2O_4$	0.86	0	440
7.	$Li_{0.5}Fe_{2.5}O_4$	2.6	2.5	670
8.	$ZnFe_2O_4$	0	0	-
9.	$CdFe_2O_4$	0	0	-

The magnetic properties of solid solutions between various ferrites have also been studied extensively and the solid solutions with $ZnFe_2O_4$ are particularly interesting. Assuming the Zn^{2+} ions to occupy the tetrahedral sites only the mixed crystals with completely inverse ferrite $Fe\left[Me^{II}Fe\right]O_4$ have the formula:

$$Zn_aFe^{III}_{1-a}\left[Me^{II}_{1-a}Fe^{III}_{1+a}\right]O_4$$

Assuming Neel's model to be valid, the saturation magnetisation n_B is given by the formula $n_B = 10\,a + (1-a)\,m_{Me}$. Gorter[58] (1954) has measured the saturation moments of the compounds

$Mn_{1-a}Zn_aFe_2O_4$

$Fe_{1-a}Zn_aFe_2O_4$

$Co_{1-a}Zn_aFe_2O_4$

$Ni_{1-a}Zn_aFe_2O_4$

$Cu_{1-a}Zn_aFe_2O_4$ (only for a = 0 and a = 0.5)

$Mg_{1-a}Zn_aFe_2O_4$

$Li_{(0.5-0.5a)}Zn_aFe_{(2.5-0.5a)}O_4$

and the results are shown graphically in Fig.3. Guillaud has also obtained similar results. The Curie points of these mixed crystals were also measured by Gorter and the results are given in Fig.4 for a $>$ 0.5,

It can be seen that the experimental curves show a strong departure from the value of n_B calculated on the basis of the above equation (dotted lines in the graph). This arises from

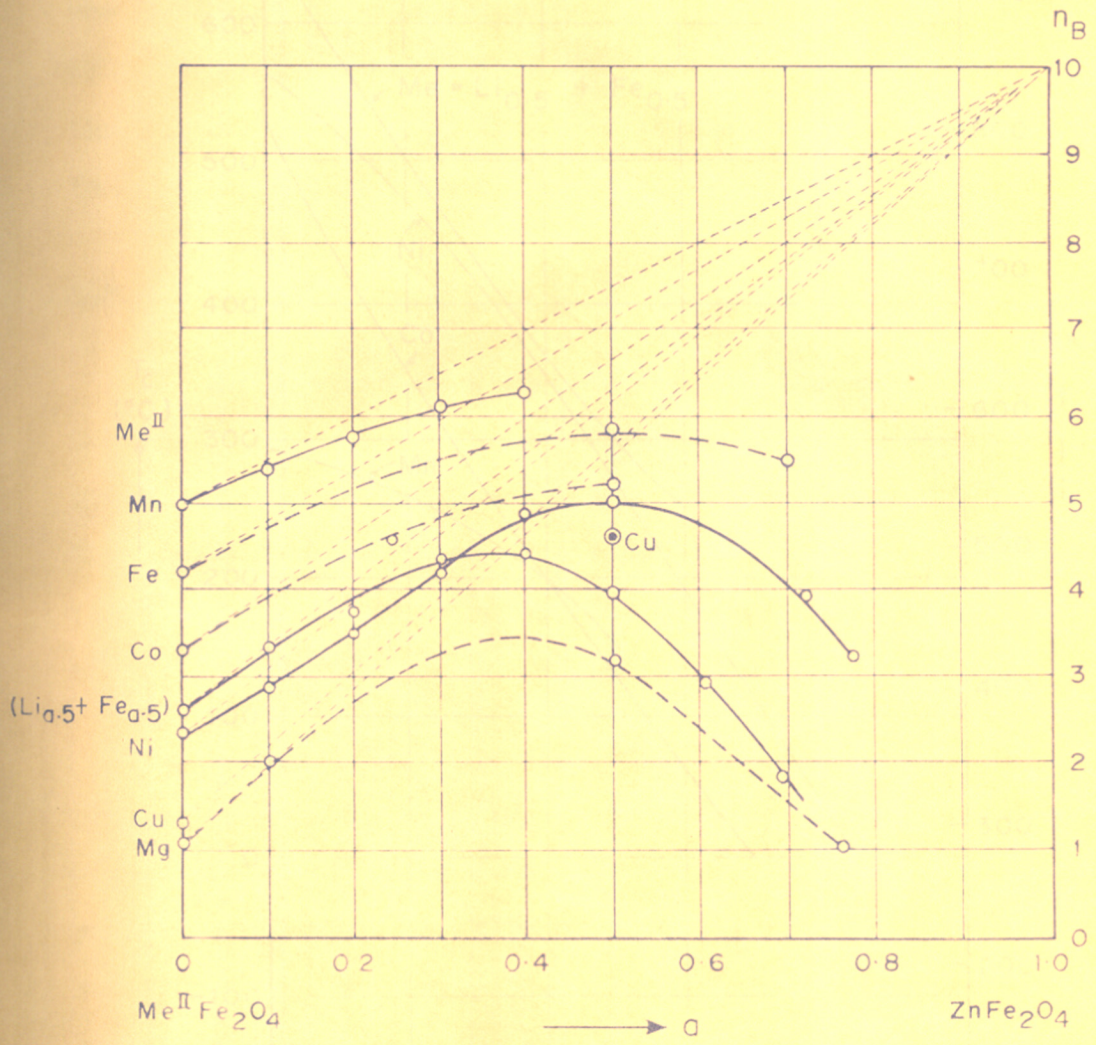

FIG. 3. SATURATION MOMENT IN BOHR MAGNETONS OF VARIOUS MIXED-CRYSTAL SERIES $Me^{II}Fe_2O_4$-$ZnFe_2O_4$.

(Reproduced from Gorter.)

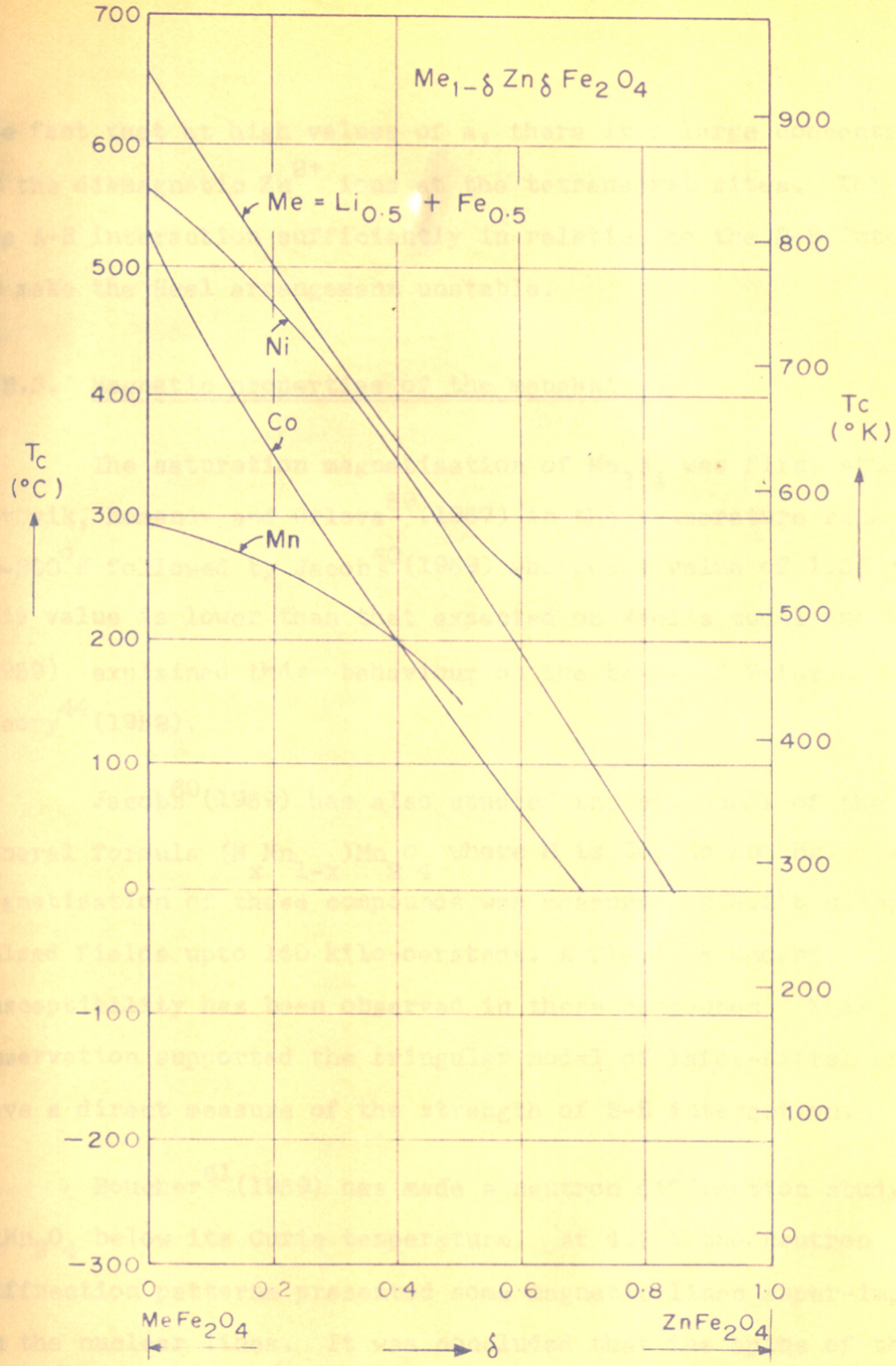

FIG. 4. CURIE POINTS OF SOME SERIES OF MIXED ZINCFERRITES $Me_{1-\delta}Zn_\delta Fe_2O_4$ AS A FUNCTION OF THE ZINC CONCENTRATION.

(Reproduced from Smit and Wijn.)

the fact that at high values of a, there is a large concentration of the diamagnetic Zn^{2+} ions at the tetrahedral sites. This decreases the A-B interaction sufficiently in relation to the B-B interaction to make the Neel arrangement unstable.

1.2.3. Magnetic properties of the manganites

The saturation magnetisation of Mn_3O_4 was first studied by Borovik, Romanov and Orlova[59] (1957) in the temperature range 20-300°K followed by Jacobs[60] (1959) who got a value of 1.56 ± .04 μ_B. This value is lower than that expected on Neel's model and Jacobs[60] (1959) explained this behaviour on the basis of Yafet-Kittel's theory[44] (1952).

Jacobs[60] (1959) has also studied the compounds of the general formula $(M_xMn_{1-x})Mn_2O_4$ where M is Co, Zn and Mg. The magnetization of these compounds was measured at 4.2°K using pulsed fields upto 140 kilo-oersteds. A field dependent susceptibility has been observed in these compounds. This observation supported the tringular model of Yafet-Kittel and gave a direct measure of the strength of B-B interaction.

Boucher[61] (1959) has made a neutron diffraction study of $NiMn_2O_4$ below its Curie temperature. At 4.2°K the neutron diffraction patterns presented some magnetic lines super-imposed on the nuclear lines. It was concluded that the spins of the tetrahedral Mn^{3+} ions are all parallel whereas those on the octahedral sites form four sets, possibly forming a pyramidal configuration or an oblique configuration in one plane.

Wickham and Croft[62](1958) studied the crystallographic and magnetic properties of several spinels containing manganese. They studied a complete range of solid solutions in the system $Co_{3-x}Mn_xO_4$. The configuration for values of 'x' between 0 and 2 appeared to be $Co^{2+}\left[Co^{3+}_{2-x}Mn^{3+}_{x}\right]O_4$. The observed magnetic properties (saturation magnetization measured at 4.2°K and Curie temperature) could be interpreted in terms of the above configuration. The magnetization measured for cubic materials was assumed to be the result of Neel-type magnetic coupling between Co^{2+} ions on tetrahedral sites and Mn^{3+} ions on octahedral sites. Tetragonal materials apparently had a more complex magnetic structure. The configuration of $Co_{3-x}Mn_xO_4$ for values of 'x' between 2 and 3 appears to be $Co^{2+}_{3-x}Mn^{2+}_{x-2}\left[Mn^{3+}_{2}\right]O_4$. They also gave the saturation magnetization at 4.2°K and Curie temperature (T_c) for a number of materials including $GeMn_2O_4$, $LiMn_2O_4$, Co_3O_4, $MnCo_2O_4$, $CoMn_2O_4$ and Mn_3O_4. Thus in the case of Mn_3O_4 an appreciable magnetic moment appeared for values of 'x' greater than 2.1 reaching a maximum of 1.4 B for pure Mn_3O_4. The Curie temperature for Mn_3O_4 was reported to be 30°K as against 43°K reported by Borovic et.al.[59](1957).

Recently, Jocobs and Kouvel[63](1961) have extended the magnetic studies on these mixed manganites. They have observed a unidirectional anisotropy which was detected by the observation of hysteresis loops displaced along the field axis when the materials were cooled to low temperature in magnetic field of several kilo-oersteds, further the unidirectional behaviour is

stable to reverse field pulses of 140 kilo-oersteds. An exchange anisotropy model is proposed involving interactions between ferrimagnetic and nearly antiferromagnetic region, brought about by the random distribution of the diamagnetic ions among the tetrahedral sites.

Dwight and Menyuk[64] (1960), investigated the magnetic properties of single crystals of Mn_3O_4 between 4.2°K and 41.9°K (Curie temperature). Their results showed that although the concept of canted spins appeared to be essentially correct, Yafet-Kittel theory was over-simplified and the conclusions based on this did not agree quantitatively with their experimental results.

Sabane[65] (1960) has carried out the paramagnetic susceptibility measurements at different temperatures for $CdMn_2O_4$, $ZnMn_2O_4$, $MgMn_2O_4$, Mn_3O_4, $CoMn_2O_4$, $NiMn_2O_4$ and $CuMn_2O_4$; $\frac{1}{\chi}$ - T plots for $MgMn_2O_4$, Mn_3O_4, $CoMn_2O_4$, $NiMn_2O_4$ and $CuMn_2O_4$ were hyperbolic showing that these compounds are ferrimagnetic at low temperatures.

Jogalekar[66] (1965) measured the paramagnetic susceptibility of Zn $(Li^{1+}_{2x}Mn^{3+}_{2-6x}Mn^{4+}_{4x})O_4$ systems (x = 0.05 to 0.30) in the temperature range of 90°K to 350°K. At $x \leqslant 0.1$ (small Mn^{4+} concentration) the compounds are paramagnetic and obey Curie-Weiss Law and in the range $0.15 \leqslant x \leqslant 0.25$ i.e. when Mn^{3+} and Mn^{4+} ion concentrations are nearly equal, the compounds are ferrimagnetic.

G. Blasse[67,68](1965,1966) reported a new type of ferrimagnetism in oxygen spinels. The spinels $Cu^{1+}[Mg_{0.5}Mn_{1.5}]O_4$ and $Li_{0.5}Zn_{0.5}[Li_{0.5}Mn_{1.5}]O_4$ become ferromagnetic below 570°K and 22°K respectively at least in fields larger than 2 kilo-oersteds. This is ascribed to ferromagnetic 90° (Mn^{4+} - O^{2-} - Mn^{4+}) interaction. The spinel $Cu^{1+}[Ni^{2+}_{0.5}Mn^{4+}_{1.5}]O_4$ becomes ferrimagnetic below 150°K due to an antiferromagnetic coupling between the crystallographically ordered Ni^{2+} and Mn^{4+} ions.

1.2.4. Studies on ferrite-manganite systems

Baltzer and White[69](1958) studied the $(NiFe_2O_4)_{1-x}$ + $(NiMn_2O_4)_x$ solid solutions. They were found to have the cubic spinel structure and the lattice parameter increased with x from 8.34 to 8.39 Å. The authors found that in the range $0 \leq x \leq 0.5$, manganese progressively replaced iron on the octahedral sites whereas in the range $0.5 \leq x \leq 1$ the manganese replaced iron on the four coordinated sites.

Magnetic moment was measured by vibrating sample magnetometer in a 15,000 oersteds field down to liquid nitrogen temperature. It was concluded that all of manganese was trivalent in the range $0 \leq x \leq 0.5$, but in pure $NiMn_2O_4$ the manganese was divalent and quadrivalent on tetrahedral and octahedral sites respectively. $NiMn_2O_4$ appeared to become ferrimagnetic at approximately 100°K.

Eschenfelder[70](1958) reported the value of magnetic moment as a function of composition for manganese, iron spinels of the composition $Mn_xFe_{3-x}O_4$. They explained the variation of

the magnetic moment η_B and the Curie temperature (T_c) as a function of 'x' in terms of a model in which excess of manganese replaced Fe^{3+} as Mn^{4+} and equal amount of iron was converted to Fe^{2+}. When the manganese content became so high that all the iron became Fe^{2+} (Mn_2FeO_4), manganese then replaced the iron as Mn^{3+} and converted an equal amount of Mn^{4+} to Mn^{3+}.

Miller[71](1960) observed anomalous values of magnetic moment for ferrospinel containing manganese. He suggested that on octahedrally ligated spinel site the ion pair Fe^{2+}, Mn^{3+} was more stable than Fe^{3+}, Mn^{2+}.

Moruzzi[72](1961) qualitatively explained the anamalously low magnetic moment for $Mn_xFe_{3-2x}O_4$ spinel by a Yafet-Kittel triangular moment arrangement. Values of β, n and α were calculated from the measurement of magnetic moment; high field susceptibility and Curie temperature. The measurements on Mn_3O_4 yielded a moment of 1.73 Bohr-magnetons and a susceptibility of 3.5×10^{-4} gauss/oersted. Transition from triangular state to a Neel type arrangement was found to occur for X = 1.25, x = 1.55 and X = 1.80.

Mo'Keeffe[73] (1961) studied the cation valencies and distribution in spinels containing manganese. He reported that the amount of Mn^{3+} on octahedral site required to produce tetragonal distortion in spinel depends upon nature of the other ions present. Crystallographic and magnetic results were reported for

spinels in which A site was occupied solely by Zn^{2+} or $Zn^{2+} + Ge^{4+}$. By means of this it was shown that $Mn^{3+} + Fe^{2+}$ rather than $Mn^{2+} + Fe^{3+}$ was the stable configuration on octahedral site of the spinel. The predicted valency and distribution in $FeMn_2O_4$, $CuMn_2O_4$ and system $x\ Mn_3O_4 + (1-x)NiMn_2O_4$ were

$$Mn^{2+}\left[Fe^{3+}Mn^{3+}\right]O_4\ ,\ Cu^{2+}\left[Mn^{3+}\right]_2O_4$$

$$Mn^{2+}_{x}Mn^{3+}_{1-x}\left[Ni^{2+}_{1-x}Mn^{3+}_{1+x}\right]O_4$$

respectively.

1.3. Electrical properties of spinels

1.3.1. Experimental studies on ferrites and manganites

The electrical properties of ferrites have been studied very extensively and there is a large amount of published literature. Recently, Smit and Wijn[74](1959) have reviewed the work done in this field. It has been a general observation that the resistivity of ferrites decreases with increasing temperature according to the relationship

$$\rho = \rho_0 \exp \Delta E/KT$$

Furthermore, it is also known that the resistivity at room temperature can very from $> 10^{11}$ to 10^{-2} ohm x cm depending on the chemical composition. Verwey[75] as long ago as 1936, had observed that Fe_3O_4 is a good conductor and Co_3O_4 an insulator. On the basis of the stability of ions he postulated that

Fe_3O_4 contained Fe^{2+} and Fe^{3+} ions while Co_3O_4 had the Co^{2+} and Co^{4+} ions. Electron transport from Fe^{2+} to Fe^{3+} required very little activation energy because this did not change the overall electronic configuration of the system. On the other hand in Co_3O_4 large activation energy was required, because the electron exchange between Co^{2+} and Co^{4+} changed the overall ionisation states of ions. Similarly γ-oxides are not good conductors because of the presence of only trivalent cation in the lattice.

A low resistivity due to simultaneous presence of Fe^{2+} and Fe^{3+} ions at the octahedral site has also been observed by Van Uitert[76](1956) in Ni-Zn ferrite and by Jonker[82] in cobalt-ferrite containing excess iron.

The temperature dependence of the resistivity of the manganese ferrite has been determined by Guillaud and Bertrand[77] (1950) and Belov and Nikitin[78](1961). Belov's measurements were carried on single crystals of nearly stoichiometric compounds whereas those of Guillaud's were on polycrystalline materials which were free from divalent iron but did contain some trivalent manganese. The resistivity at $300^{\circ}K$ in both cases is approximately 10^4 ohm x cm.

Recently, Lotgering[79](1964) studied the semiconducting properties of the mixed crystals Fe_3O_4- $MnFe_2O_4$- Mn_2FeO_4 along with Seebeck voltages. He concluded that the conductivity arises exclusively from ferric and ferrous ions on octahedral sites

according to the Verwey hopping mechanism and that the reaction $Mn^{2+} + Fe^{3+} \longrightarrow Mn^{3+} + Fe^{2+}$ is endothermic involving an energy approximately 0.30 ev.

The resistivity of nickel ferrite has been studied as a function of temperature byGuilland and Bertrand[75] but it appears that their sample contained some divalent iron. Van Uitert[76] has studied the effect of composition and firing temperature of the resistivity of nickel ferrite in a great detail. He has found out that the resistivity of iron deficient nickel ferrite is not very sensitive to firing temperature whereas iron rich nickel ferrite is. For the second class the resistivity decreases with increasing temperature first slowly and then very abruptly around $300^{\circ}K$. The author explained this behaviour as due to excess iron present in the ferrite. At temperature below $1300^{\circ}C$ it is presumed to be present as Fe^{3+} whereas above $1300^{\circ}C$ it is present as Fe^{2+}. In later case conduction is facilitated due to electronic exchange between Fe^{2+} and Fe^{3+}. For a stoichiometric sample fired at temperature less than $1300^{\circ}C$ room temperature resistance is approximately 10^{5}-10^{6} and $\triangle E = 0.32$ e.v.

Morin and Geballe[80] (1955) measured the electrical conductivity and Seebeck effect in $Ni_{0.8}Fe_{2.2}O_4$ as a function of temperature on single crystals. A thermal hysteresis was observed in conductivity but not in Seebeck effect. This suggests that the hysteresis involves the

charge carrier transfer process but not the production of carriers. The activation energy associated with the transfer is estimated to be 0.10 e.v. in the high temperature state and 0.06 e.v. in the low temperature state.

Elwell, Parker and Sharkey[81](1963) reported the measurements of electrical resistivity for nickel ferrite with a Ni:Fe ratio ranging from 1:2 to 1:1.88 with manganese content of upto 2%. Specimens were prepared at sintering temperature between 1100 to 1250°C under oxygen pressure ranging from 3 to 456 cm. of mercury.

It is concluded that the large increase in resistivity resulting from the manganese impurity which was reported by Van Uitert[76] arises from the contribution of the impurity energy levels, which lies approximately half way between those of Ni^{2+} and Fe^{2+}.

The electrical conductivity of cobalt ferrite has been measured by Jonker[82](1959). The room temperature resistivity for pure stoichiometric cobalt ferrite is 10^4 ohms x cm. and $\triangle E = 0.23$ e.v.

The electrical properties of manganites have not been studied so extensively. Sabane[65](1960) was the first to make a systematic study of the variation of electrical conductivity

of the manganites $CuMn_2O_4$, $NiMn_2O_4$, $Mn^{2+}Mn_2O_4(Mn_3O_4)$, $CoMn_2O_4$, $MgMn_2O_4$, $ZnMn_2O_4$ and $CdMn_2O_4$, as a function of temperature. He has observed that at higher temperature Wilson's Law is obeyed for all these manganites. He has also studied the electrical conductivity in the solid solutions: $NiMn_2O_4$- $CuMn_2O_4$, $NiMn_2O_4$ - Mn_3O_4, $NiMn_2O_4$ - $CoMn_2O_4$, $NiMn_2O_4$ - $MgMn_2O_4$, Mn_3O_4 - $CoMn_2O_4$, Mn_3O_4 - $CuMn_2O_4$, $CoMn_2O_4$ - $CuMn_2O_4$ and $CuMn_2O_4$ - $MgMn_2O_4$.

The results on the thermoelectric coefficient measurement indicate that all the manganites except $NiMn_2O_4$ showed p-type conduction. He has also discussed the mechanism of electrical conductivity on the basis of the electron transport process.

Larson, Arnott and Wickham[83](1962) have prepared a series of compounds with the general formula $Ni_{1-x}Mn_{2+x}O_4$. They have studied the semiconduction and low temperature magnetization of this system. The compounds with the values of 'x' less than 0.42 crystallize with cubic symmetry and others with the values of x, greater than 0.42 exhibit tetragonal symmetry. From the results of Seebeck coefficient measurements, they observed that n-type conduction occurs in cases of compounds with $x < 0.46$ and p-type conduction occurs when $x > 0.46$. A sharp change in low temperature magnetization takes place as the value of x is increased from 0.36 to 0.42. According to them, the formula of the above systems is:

$$(1-\beta)Mn_x^{2+}Mn_{1-x}^{3+}\left[Ni_{1-x}^{2+}Mn_{1+x}^{3+}\right]O_4$$

$$+\ \beta Mn^{2+}\left[Ni_{1-x}^{2+}Mn_{2x}^{3+}Mn_{1-x}^{4+}\right]O_4$$

The electrical conductivity results from the transfer of electrons from 'B' site Mn^{3+} ions to the neighbouring 'B' site Mn^{4+} ions. The possible contribution to the conductivity from A site ions is neglected because the distance between them is too great to allow a comparable transfer of charge by a hopping mechanism according to which an electron jumps directly from one cation to a neighbouring cation.

Recently, Rosenberg, Nicolou, Manaila and Pausescu[84] (1963) have prepared $Cu_xMn_{3-x}O_4$ ($0 \leqslant x \leqslant 0.2$), $Zn_{1+x}Mn_{2-x}O_4$ ($0 \leqslant x \leqslant 0.2$), $Mg_xMn_{3-x}O_4$ ($0 \leqslant x \leqslant 1$) and $Zn_xMn_{3-x}O_4$ ($0 \leqslant x \leqslant 1$) by co-precipitation methods and studied their electrical conductivity. From the studies of the crystal symmetry as a function of composition and of electrical conductivity as a function of composition and temperature, they have concluded that the electrical conductivity involves the hopping mechanism of electrons between Mn^{3+} and Mn^{4+} ions at octahedral sites.

Jogalekar[66] (1965) has studied the electrical properties of compounds of the general formula $ZnLi_{2x}^{1+}Mn_{2-6x}^{3+}Mn_{4x}^{4+}O_4$ ($ZnLi_{2x}Mn_{2-2x}O_4$), where x = 0.05 to 0.30 and σ follows the relationship $\sigma = \sigma_0 \exp - \Delta E/kT$. The thermoelectric properties indicated that compound in which the number of

Mn^{4+} ions is small ($0 \leqslant x \leqslant 0.1$) are p-type while those with $0.15 \leqslant x \leqslant 0.3$ are n-type semiconductor.

1.3.2. Mechanism of electrical conductivity in the transition metal oxides

De Boer and Verwey[85] (1937) made first attempt to explain the electron transport in the oxide semiconductors. They pointed out that the collective electron treatment of Bloch[86,87] (1928, 1930) and Wilson[88] (1931), although very successful in explaining the electrical behaviour of metals, is not a correct approximation for the oxide semiconductors. Mott[89] (1949) has also shown that the band picture of solids does not satisfactorily explain the electron transport in oxide semiconductors such as NiO. The Heitler-London approximation should be used here which is based on localised atomic wave functions.

Yamashita and Kurosawa[90-92] (1958, 1960, 1961) have discussed the problem of conduction in semiconductors with incomplete 'd' shells. They have proposed the Heitler-London approach to explain the conduction in such compounds and have assumed that the wave function of the electron is localized closely around an ion. However, the localized state is a stationary state only in the first approximation. The electron jumps from an ion to its nearest neighbour ion with a certain probability due to the perturbing influence of the neighbouring ions. Considering the conservation of energy, this transition of the electron must be accompanied by emission and absorption of many phonons. This therefore becomes a thermally activated

process and the mobility is associated with activation energy term. Yamashita concluded that when mobility is much larger than 1 cm^2/sec x volt, the usual Block theory could be used; while the H-L approach might be good when the mobility is much smaller than 1 cm^2/ sec x volt. If the mobility is smaller, activation energy becomes larger. Also, if the density of donors is low, the main part of the activation energy comes from the work required to separate an electron from the vicinity of the donor to a distant point in the lattice.

Recently, Sinha and Sinha[93] (1963) have studied the electronic conduction in some polar semiconductors where the carriers are assumed to be localised the electron lattice coupling is separated in to two parts, one dependent and the other independent of the coordinates of the excess charge carriers. The independent part gives rise to lattice polarization while the dependent part, treated as the perturbation, superposes some excited orbital states on the ground orbital state of the carrier located at the metal ion. The static potential of the other ions, treated as the perturbation, causes transition of the carrier from one site to another. This formulation automatically takes into account the role of the intermediate excited states in the hopping process. They have found that; under favourable conditions these intermediate states give an easier path for conduction. In the higher temperature region the dependence of carrier mobility on temperature is nearly exponential. This behaviour is in agreement with the experimental observations of some transition metal compounds.

CHAPTER - II

EXPERIMENTAL TECHNIQUES

C H A P T E R - II

2. EXPERIMENTAL TECHNIQUES

In this section we discuss the experimental techniques used for the preparation of the samples and for the measurements of their physical properties. First the individual spinels (Ferrites and manganites), then their appropriate solid solutions were prepared by solid state reactions. The x-ray powder diffraction, Curie temperature and saturation magnetization measurements were carried out on powder materials. For electrical conductivity and thermoelectric coefficient measurements sintered pellets were prepared. The permeabilities μ' and μ'' were measured on sintered toroids with the help of a Q-meter.

2.1. Preparation of the samples

The spinels $CuMn_2O_4$, $CuFe_2O_4$, $ZnFe_2O_4$, $NiFe_2O_4$, $CoFe_2O_4$, and $MnFe_2O_4$, were prepared by the high temperature solid state reaction between the respective oxides, mentioned in column 2, Table 3.

Table 9

No.	Compound	Starting materials	Reaction temp.($T^{o}C$)	Atm.
1.	$CuMn_2O_4$	$CuO + Mn_2O_3$ (1:1)	950	Air
2.	$CuFe_2O_4$	$CuO + Fe_2O_3$ (1:1)	1000	Air
3.	$ZnFe_2O_4$	$ZnO + Fe_2O_3$ (1:1)	1250	Air
4.	$NiFe_2O_4$	$NiO + Fe_2O_3$ (1:1)	1250	Air
5.	$CoFe_2O_4$	$CoCO_3 + Fe_2O_3$ (1:1)	1250	Air
6.	$MnFe_2O_4$	$MnCO_3 + Fe_2O_3$ (1:1)	1250	Nitrogen gas

Mn_2O_3 was obtained by heating A.R. grade manganese dioxide (MnO_2) in a platinum crucible at 900°C for 4-5 hours in air and quenching to room temperature. The other materials (AR grade) were used as supplied by manufacturers.

The starting compounds were intimately mixed in the equimolecular ratio in an agate mortar and pestle for one hour under ethanol. The mixture was dried and heated in a platinum crucible at the reaction temperature given in column III of Table 9. The temperature of the furnace was controlled within ± 5°C with a chopper arrangement and was measured by means of a calibrated Pt/Pt-Rh thermocouple. After about 5 hours of heating, the furnace was switched off and the compounds were cooled in the furnace. The product thus obtained was then analysed by x-ray

diffraction using a 14 cm. Debye-Scherrer camera and Mo-K α (λ= 0.7080Å) radiation, filtered through a zirconium foil. There were no diffraction lines due to unreacted oxides indicating the completion of the reaction. From the Debye-Scherrer powder patterns the 'd' values were calculated in the usual manner and unit cell parameters determined.

The hard mass obtained after the reaction was broken into small pieces in an agate mortar. The product was ball milled under alcohol for 16 hours in a cylindrical stainless steel ball mill (length 8" and dia. 6") containing ten stainless steel balls of one inch diameter. The can was rotated at a speed of sixty revolutions per minute by a half H.P. continuous operation motor. On completion of the grinding, the compound was poured out in a stainless steel plate and dried in a oven at 110°C.

Starting from these individual spinels, the following binary solid mixtures were prepared:

(1) $(CuMn_2O_4)_x + (CuFe_2O_4)_{1-x}$

(2) $(CuMn_2O_4)_x + (NiFe_2O_4)_{1-x}$

(3) $(CuMn_2O_4)_x + (CoFe_2O_4)_{1-x}$

(4) $(CuMn_2O_4)_x + (ZnFe_2O_4)_{1-x}$

(5) $(CuMn_2O_4)_x + (MnFe_2O_4)_{1-x}$

where x = 0, 0.1, 0.2, 0.3, 0.4, 0.5, 0.6, 0.7, 0.8, 0.9, and 1.0. The appropriate oxides were mixed for three hours in ethanol medium in an agate ~~and~~ mortar and pestle mounted on an automatic grinding machine. They were then transferred in a platinum crucible and heated under the conditions described below for each system:

(1) $(CuMn_2O_4)_x + (CuFe_2O_4)_{1-x}$

x = 0 to 0.5 reacted at 1100°C
x = 0.6 to 1.0 reacted at 1050°C } in air for 5 hours.

Samples were annealed slowly from 1050°C to 200°C in 20 hours.

(2) $(CuMn_2O_4)_x + (NiFe_2O_4)_{1-x}$

x = 0 to 0.5 reacted at 1150°C
x = 0.6 to 1.0 reacted at 1100°C } in air for 5 hours.

Samples were cooled in the furnace.

(3) $(CuMn_2O_4)_x + (CoFe_2O_4)_{1-x}$

x = 0 to 0.5 reacted at 1150-1160°C
x = 0.6 to 1.0 reacted at 1100-1110°C } in air for 5 hours.

Samples were cooled in the furnace.

(4) $(CuMn_2O_4)_x + (ZnFe_2O_4)_{1-x}$

x = 0 to 0.5 reacted at 1200°C
x = 0.6 to 1.0 reacted at 1100°C } in air for 5 hours.

Samples were cooled in the furnace.

(5) $(CuMn_2O_4)_x + (MnFe_2O_4)_{1-x}$

x = 0 to 0.3 reacted at 1150°C
x = 0.4 to x = 0.6 reacted at 1100°C
x = 0.7 to x = 1.0 reacted at 1050°C } in nitrogen (N_2) atmosphere for 5 hours.

Samples were cooled in the furnace.

For electrical conductivity measurement, pellets (0.8 cm. in dia. and 0.2 to 0.4 cm. thick) were made by the standard ceramic technique of powdering, mixing, grinding, moulding, sintering, etc.

The compound was finely ground and in agate mortar and pestle and sieved through a standard 325 ASTM sieve. 1.5 cc. of 2% solution of the polyvinyl acetate in acetone was added per gram of powder and the mixture was homogenised and dried in an oven. The appropriate amount of the dry powder was filled in a die and a pressure of 8000 to 9000 p.s.i. was applied by means of a Carvar Laboratory Press fitted with a calibrated pressure gauge.

The pellets thus obtained were slowly heated in air [N_2 for ($CuMn_2O_4$ + $MnFe_2O_4$)] at 800°C for about 2 hours when the binder was burnt completely. The temperature of the furnace was then increased gradually and the sintering was carried out at 1100°C for 3 hours. After sintering the furnace was switched off and the sample was cooled in air in the furnace. It took 3 hours to reach 600°C and 6 hours from 600°C to room temperature. The end faces were made parallel by careful grinding on various grades of emery paper.

Toroids of inner diameter = 2.5 cm., outer diameter = 3.5 cm. and thickness = 0.3 - 0.5 cm. were also prepared by the above technique for the measurements of μ' and μ''.

2.2. X-ray examinations

In addition to checking the completion of reactions, the x-ray powder diffraction technique was also employed to determine the crystal structure of the solid solutions formed. The samples were filled in thin glass capillaries and Debye-Scherrer patterns were taken on a Philips X-ray machine using Mo-K_α radiations (λ = 0.708 Å) filtered through a zirconium foil in a 14 cm. camera. The 'd' values were obtained from the powder diffraction data in the usual way. The patterns were indexed with the help of the standard charts and the lattice parameters were calculated from the observed 'd' values.

2.3. Curie temperature

For determination of Curie temperature of the ferrites, the test sample was kept in a thin walled platinum bucket suspended with the aid of a steel spring and a quartz rod into a vertical tube furnace of one inch diameter. The purpose of the quartz rod was to keep the steel spring out of the furnace to avoid its heating.

A ten inch long mild steel rod with diameter slightly less than one inch was introduced into the furnace from its end. The distance between the upper end of the rod and the sample was kept at about 1/2 cm.

The mild steel rod was magnetized by passing a current of 5 amps. through a coil of 1500 turns of copper wire fitted at

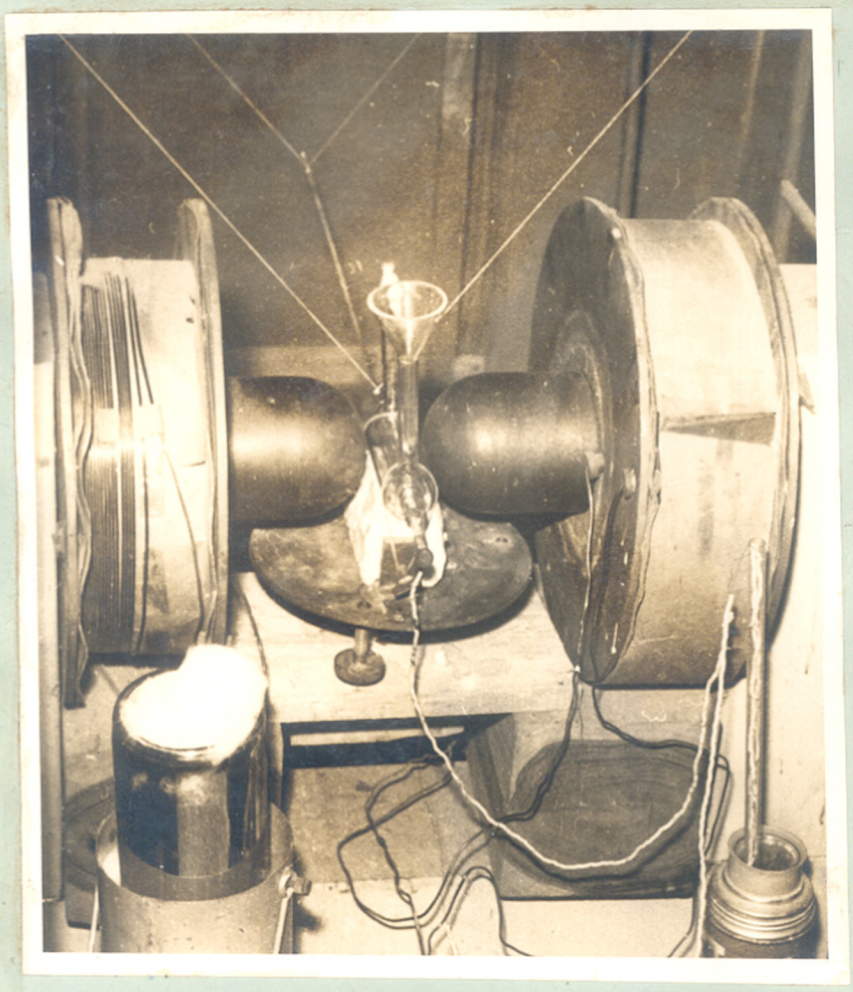

FIG. 5.

THE APPARATUS USED FOR THE SATURATION MAGNETIZATION.

its lower end. The magnetised rod pulled the sample towards itself making an electrical contact between the platinum foil and the mild steel rod. This, in turn, completed the circuit of an indicator lamp (bulb) which was made on and off as the contact was made or broken respectively.

The magnetic sample which remained attached to the magnetized rod got released at the Curie point and the indicator lamp went off. The furnace was heated at a rate of approximately 5 degree per minute in the region of Curie temperature. The temperature of the sample was determined by means of a chromel-alumel thermocouple kept close to it inside the platinum bucket. The uncertainty in the value of Curie temperature measured by this method was estimated as $\pm$ 5^{o}C.

2.4. Saturation magnetization

The measurements of saturation magnetization(σ) were carried out by Ponderomotor method described by Rathenau and Snoek[94] (Fig.5). Here the material was fixed at the end of a horizontal pendulum p (made of silica rod). The pendulum was suspended from four wires (W) moving perpendicular to an inhomogeneous field. The field varied nearly as $H = H_o - \frac{1}{2} ax^2$ in the direction 'x' of the oscillation. This type of variation was brought about by the special shape of the pole pieces 'N' and 'S'. The constant of the resisting force on the magnetic material in this inhomogeneous field was $(a \sigma m)$ where σ = saturation magnetization in $C_{gS_{magn}}$ cm^3/grams m = the weight of the sample.

Thus the saturation magnetization 'σ' was found from the formula :

$$\sigma = \frac{4\pi^2 M}{a\ m}\left[\frac{1}{t^2} - \frac{1}{t_o^2}\right] = \frac{C}{m}\left[\frac{1}{t^2} - \frac{1}{t_o^2}\right]$$

where

$C = \frac{4\pi^2 M}{a}$

M = the weight of the pendulum,

t_o = the period of oscillation in a magnetic field without the material fixed to the pendulum,

t = the period of oscillation when the magnetic material was present.

The constant $4\pi^2 M/a$ was determined by calibrating with very pure nickel metal.

The saturation magnetization 'σ' has been measured at various temperatures in the range of 77°K ~~and~~ t_o 300°K for all the ferrite-manganite systems.

The experimental set up consisted essentially of an electromagnet having hemispherical pole-pieces of 10 cms. diameter. The Yoke was ⊔ shaped where the horizontal portion was 30" long and the vertical limbs were each 22" long. The area of cross section was 6 x 6 sq. inches. A suitable D.C.stabilized power supply unit supplied by Automatic Electric Private Ltd. was used to energise the coil. The gap between the magnetic pole pieces was fixed at about 3.8 cm. A steady magnetic field of 6500 oersted was obtained by controlling the current through the coil of electromagnet.

A silica pendulum consisting of a silica rod 3 mm. diameter and 56 cm. length tied with four strings as shown in the figure 5 was used. At one end of silica rod sample tube of 3.5 mm. dia. and4 cm. length was attached. The sample was kept exactly at the centre of the pole-pieces. A double wall pyrex circular flask (evacuated outer space) was used for low temperature ($77^{\circ}K$ to $273^{\circ}K$). For temperatures greater than room temperature a suitable heating assembly was used. The temperature was measured by a previously calibrated copper-constantan thermocouple and a potentiometer.

For calibration of the apparatus, pure Ni metal (supplied by Johnson Mathey, England) was used as the standard substance for which the value of ' σ ' is known to be 54.39 gauss-cm^3/g. at $20^{\circ}C$.

The tube constant 'c' for the specimen tube at room temperature was calculated from the

$$C = \frac{\sigma(Ni)}{1/t^2 - 1/t_o^2} \times \text{wt. of substance (Ni)}.$$

By using this constant the saturation magnetization for pure $NiFe_2O_4$ and $CuFe_2O_4$ was measured at different temperatures. Values for $NiFe_2O_4$ and $CuFe_2O_4$ (annealed) at different temperatures agreed with those reported.

Thus the values for ' σ ' of unknown substance was obtained by using the constant 'C', time periods t, t_o and the weight of the substance taken:

$$\sigma = C \frac{(1/t^2 - 1/t_o^2)}{\text{Wt. of the substance}}$$

From these results the value of $\sigma (T = 0^{\circ}K)$ could be obtained by extrapolation of the graph of the σ vs temperature.

The saturation magnetisation in the Bohr magneton units was calculated using the relationship:

$$n_B = \frac{\sigma_o \times \text{molecular weight}}{5585} \qquad \left[\sigma_o = \sigma (T^2 = 0^{\circ}K)\right.$$

2.5. Electrical conductivity

The electrical conductivity of sintered pellets was studied as a function of temperature. A suitable furnace was constructed for these measurements.

The standard resistor Kanthal (A) wire was wound over an opaque silica tube of 6 cms. in diameter, 45 cm. in length. This was kept in a box of asbestos cement and lagged with magnesia as insulating material. From one end of the furnace another silica tube of 3 cms. diameter and 45 cm. length was inserted together with a calibrated chromel-alumel thermocouple (covered with insulating beads) in such a way that the measuring junction of thermocouple was at the centre of the furnace where the pellet in the sample holder assembly was also located. A small automatic controller (chopper bar type) was used to control the heating of the furnace. The temperature could be controlledto $\pm 5^{\circ}$C.

Sample assembly

A zirconia tube of 20 cms. in length and 1 cm. dia. with an 'U' type notch at one end was taken. The ferrite was coated with aqua dag on the two circular faces. A silica plate was placed on the notch at the lower part of the zirconia tube. On this plate a clean Pt-foil followed by the sample, another Pt-foil and finally a silica plate were placed and a mild pressure was applied from the top with the help of a spring loaded silica rod (3 mm. dia. x 25 cm. length) as shown in Figure 6. The Pt-foils had welded Pt-wire leads which were taken out of the tube and connected to the vacuum tube voltmeter.

The sample assembly was introduced in the furnace and the platinum wire leads were connected to a vacuum tube voltmeter (electronic volt - Ohm-meter-Eico), the chromel-alumel thermocouple leads were connected to potentiometer to measure the thermocouple e.m.f. The accuracy of this e.m.f. measurement was $\simeq \pm 0.1\%$.

The A.C. conductivity has been measured at various temperatures from 35°C to 450°C. Whenever temperature was changed, sufficient time was allowed for attaining equilibrium.

If Wilson's Law is obeyed the conductivity of these compounds should be given by a simple relation:

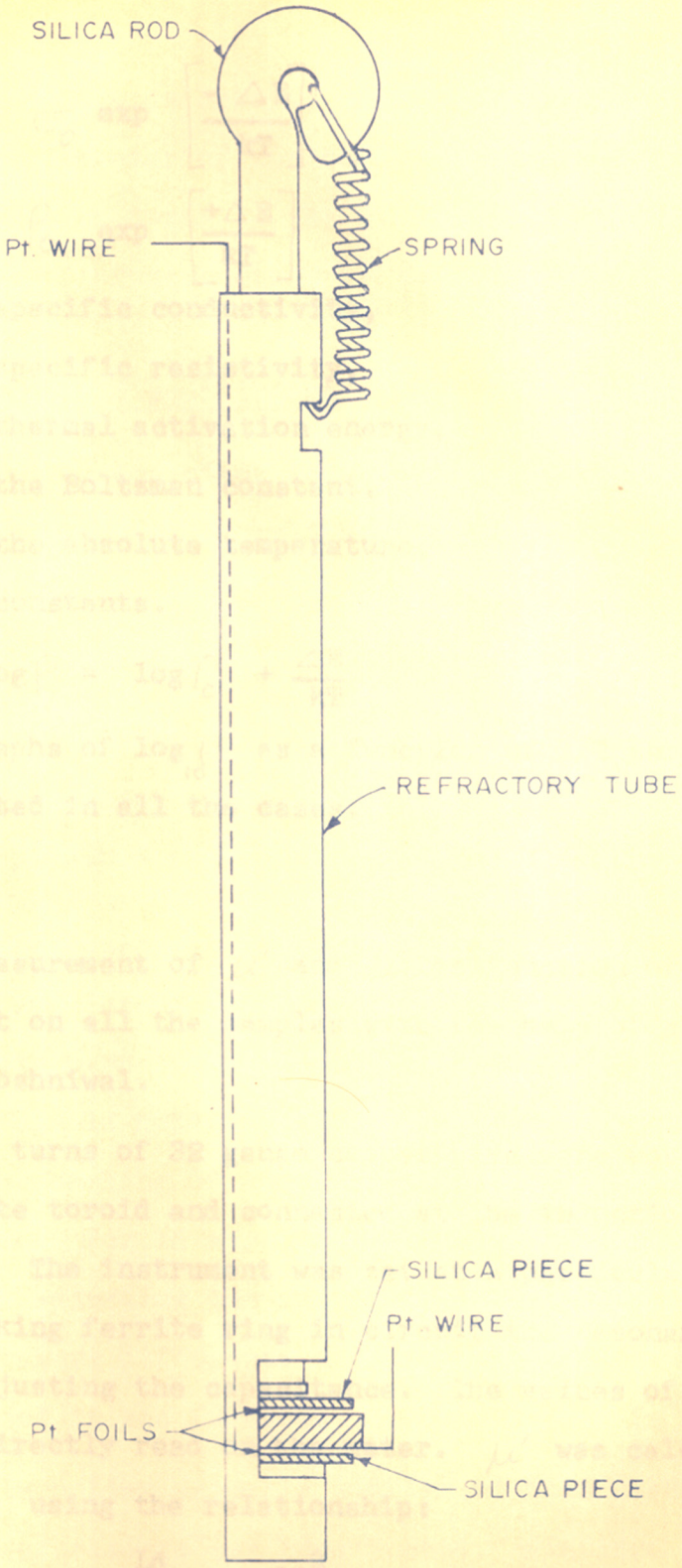

FIG. 6. SAMPLE HOLDER ASSEMBLY FOR PELLETS.

$$\sigma = \sigma_0 \exp\left[\frac{-\Delta E}{kT}\right]$$

or

$$\rho = \rho_0 \exp\left[\frac{+\Delta E}{kT}\right]$$

where: σ = specific conductivity,

ρ = specific resistivity,

ΔE = thermal activation energy,

k = the Boltzman constant,

T = the absolute temperature,

σ_0, ρ_0 = constants.

Thus $\log \rho = \log \rho_0 + \frac{\Delta E}{kT}$

The graphs of $\log_{10} \rho$ as a function of 1/T were therefore plotted in all the cases.

2.6 Permeability

The measurement of μ' and μ'' as function of frequency was carried out on all the samples with the help of a Q-meter made by M/s. Toshniwal.

Twenty turns of 32 gauge copper wire were wound on the sintered ferrite toroid and connected at the induction terminals of the meter. The instrument was set at a particular frequency and then by taking ferrite ring in circuit the resonance was obtained by adjusting the capacitance. The values of Q (= μ'/μ'') and Lf^2 were directly read on the meter. μ' was calculated from the value of L using the relationship:

$$\mu = \frac{Ld}{4N^2A} \times 10^9$$

where L = inductance in henrys,

d = mean diameter of the toroid,

N = number of turns in the winding,

A = area of cross section of the toroid($cm.^2$).

2.7. Thermoelectric coefficient

An apparatus described below was constructed to measure the thermoelectric e.m.f. of cylindrical pellets at various temperatures.

The electric furnace was made by winding standard resistor Kanthal wire over a 2 inch diameter opaque silica tube. The sample was located close to one end of the tube furnace so that there was a temperature gradient between two ends of the tube.

The silica tube was placed in a box made up of asbestos cement sheet. The furnace was thermally insulated by packing the box with magnesia asbestos powder. One end of the silica tube was closed and the sample holder assembly was introduced from the other end. The heating of the furnace was controlled by means of a variac (rated for 15 amps., 220-270 volts) and a temperature controller. By adjusting the voltage supply it was possible to obtain a temperature difference of 10-40^{o}C between two ends of the sample placed in the furnace.

A sample holder assembly similar to that used for conductivity measurements was constructed. Platinum foils were

employed for electrical contacts. The platinum wires (23 s.w.g. ~~gauge~~) were fused to the platinum foils. These wires were electrically insulated with porcelain leads and were brought out of the furnace for the e.m.f. measurements.

Temperature measurements were done by two different previously calibrated chromel-alumel thermocouples of 26 gauge wire and placed in contact at the centre of the end faces of the pellet. The temperature difference between the two ends of the pellet was measured by connecting these two thermocouples in opposition.

A potentiometer, which reads upto 10 micro volts was used to measure thermocouple e.m.f. as well as thermoelectric e.m.f. The average temperature of the sample was obtained by taking the mean of the temperatures at the two ends.

The thermoelectric coefficient has been measured at various temperatures ranging from 30-200^{o}C.

----0----

CHAPTER - III

EXPERIMENTAL RESULTS

CHAPTER - III

3.EXPERIMENTAL RESULTS

3.1. Saturation magnetization

3.1.1. $CuMn_2O_4$- $CuFe_2O_4$($CuMn_{2x}Fe_{2-2x}O_4$)

Saturation magnetization of the compounds having the general formula $CuMn_{2x}Fe_{2-2x}O_4$ (where x ranges from 0 to 1 in interval of 0.1) were measured in the temperature range of 77°K to 300°K. The value of σ (T = 0°K) was obtained by extrapolation of σ vs T plot to T = 0°K. Saturation magnetization in Bohr magneton (n_B) per molecule was calculated from the formula:

$$n_B = \frac{\sigma(T = 0^\circ K) \times M}{5585}$$

where M is the molecular weight of the compound.

For pure $CuFe_2O_4$ (x = 0) the saturation magnetization was found to be 25.30 cgs units at room temperature. It increased with decrease in temperature and at 77°K the value was 29.35 gauss-$\frac{cm.^3}{g}$ The extrapolated value to T = 0°K is 31.2 units gauss-$\frac{cm.^3}{g}$ or 1.33 μ_B which is in good agreement with that reported by Gorter[58]. The ~~plot~~ σ - T plot is shown in Fig.7. For other compositions also (x > 0) we get an increase in the saturation magnetization on decrease in temperature. The values of σ at 300°K, 77°K and 0°K (extrapolated) are presented in Table 10 and σ - T plots are shown in Figures 7 to 12. It

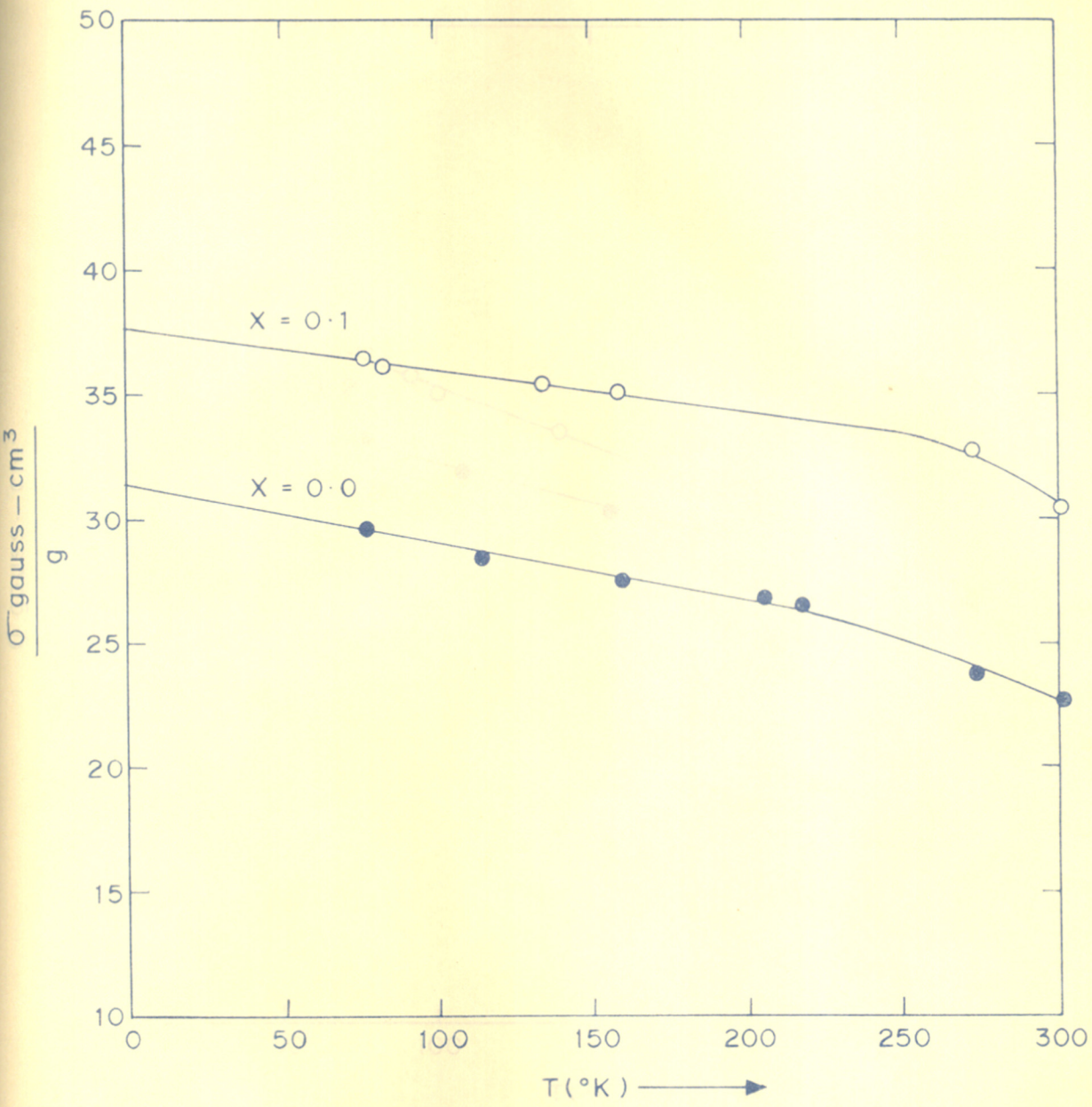

FIG. 7.

SATURATION MAGNETIZATION PER GRAM 'σ' AS A FUNCTION OF TEMPERATURE 'T' FOR THE SYSTEM $CuMn_{2x}Fe_{2-2x}O_4$.

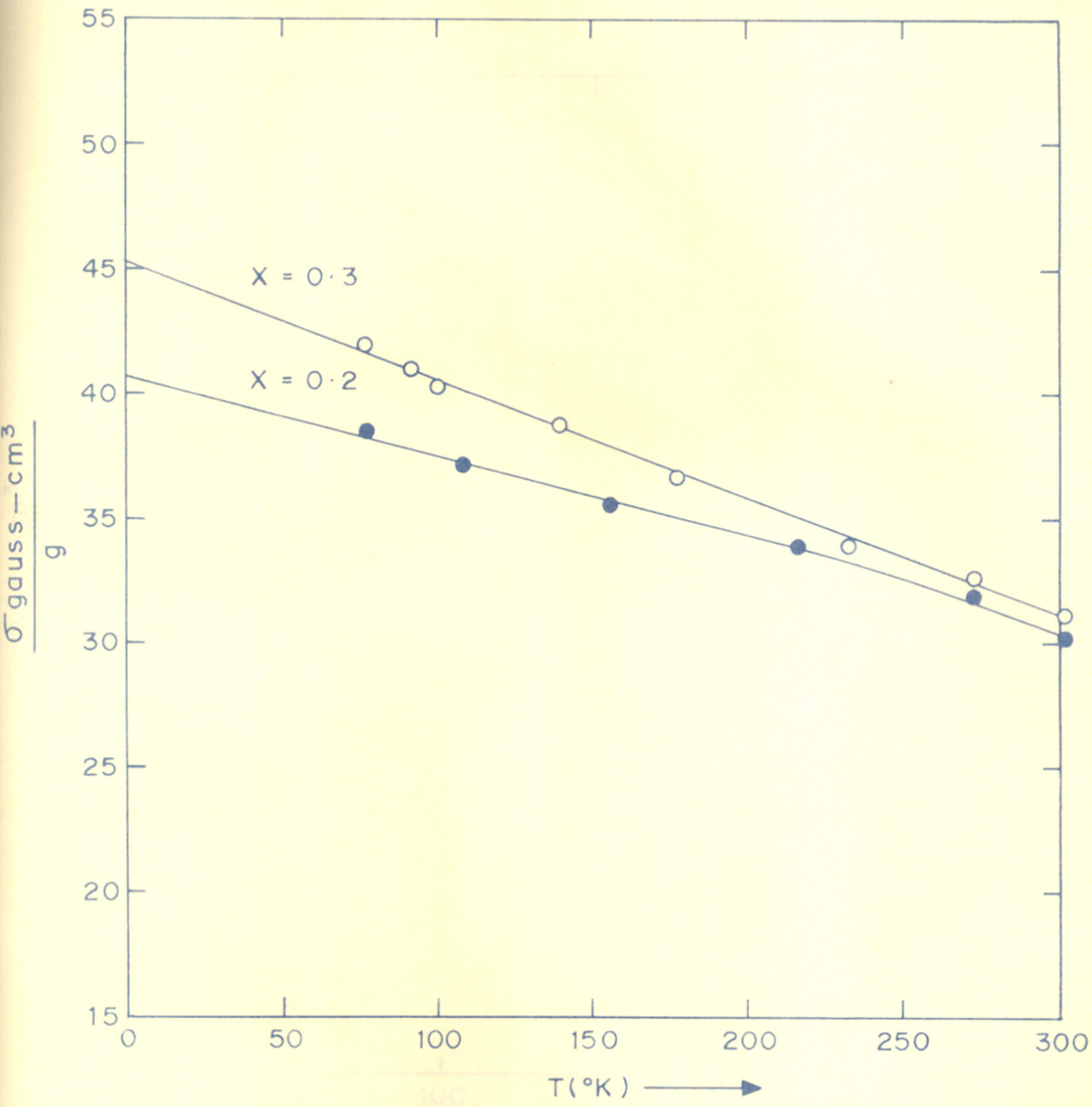

FIG. 8.

SATURATION MAGNETIZATION PER GRAM 'σ' AS A FUNCTION OF TEMPERATURE 'T' FOR THE SYSTEM $CuMn_{2x}Fe_{2-2x}O_4$.

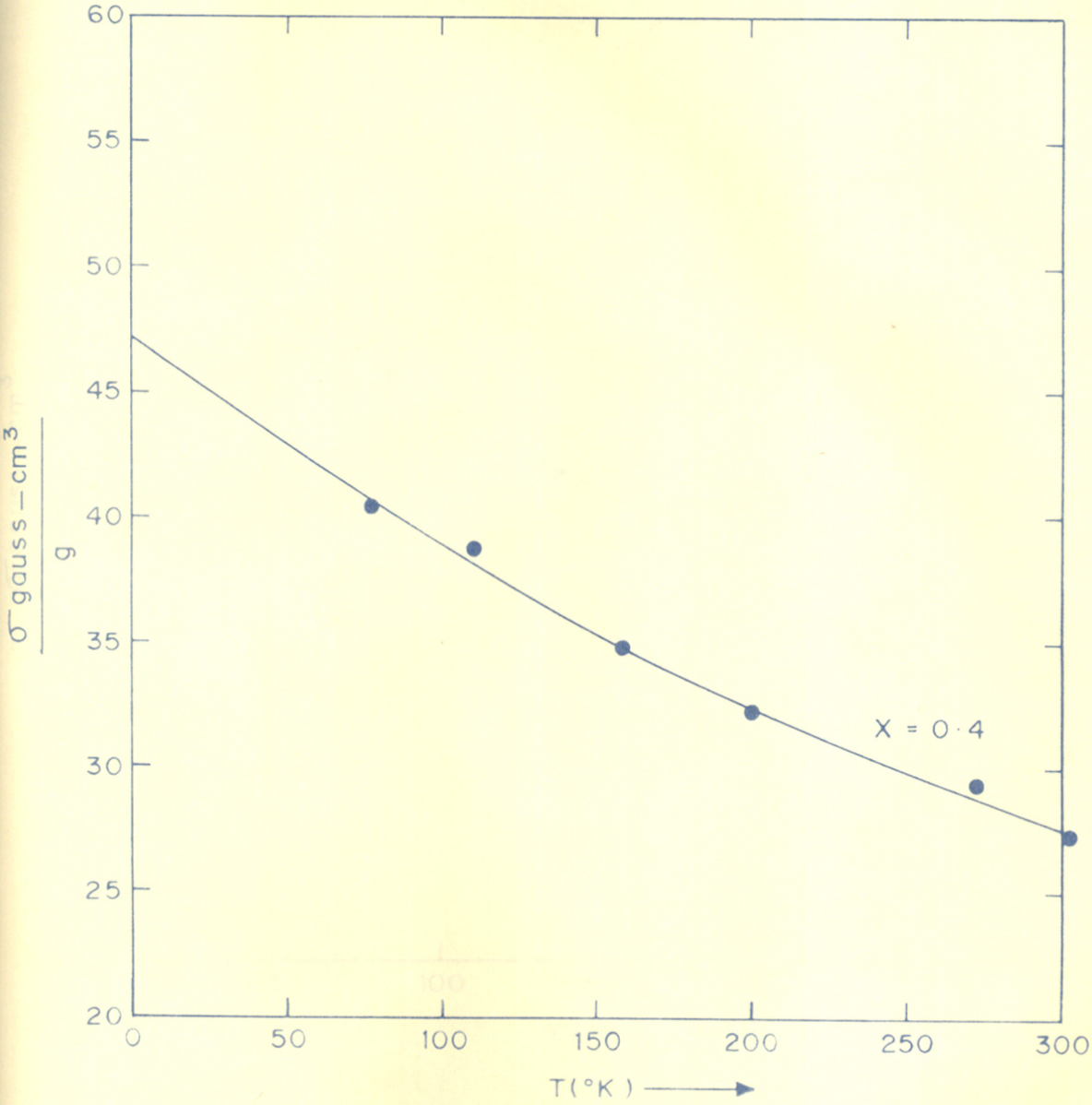

FIG. 9.

SATURATION MAGNETIZATION PER GRAM 'σ' AS A FUNCTION OF TEMPERATURE 'T' FOR THE SYSTEM $CuMn_{2x}Fe_{2-2x}O_4$

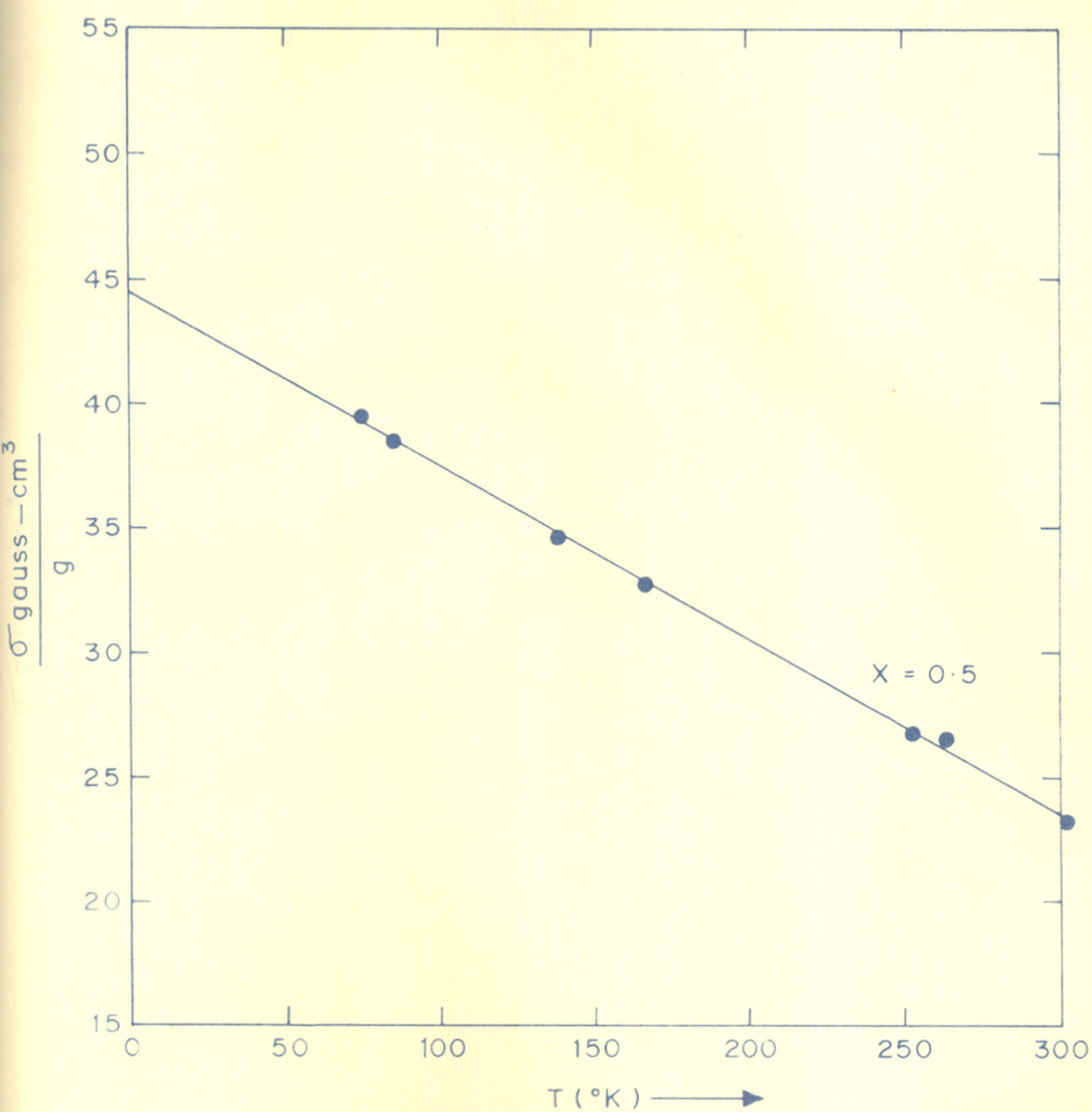

FIG. 10.

SATURATION MAGNETIZATION PER GRAM 'σ' AS A FUNCTION OF TEMPERATURE 'T' FOR THE SYSTEM $CuMn_{2x}Fe_{2-2x}O_4$

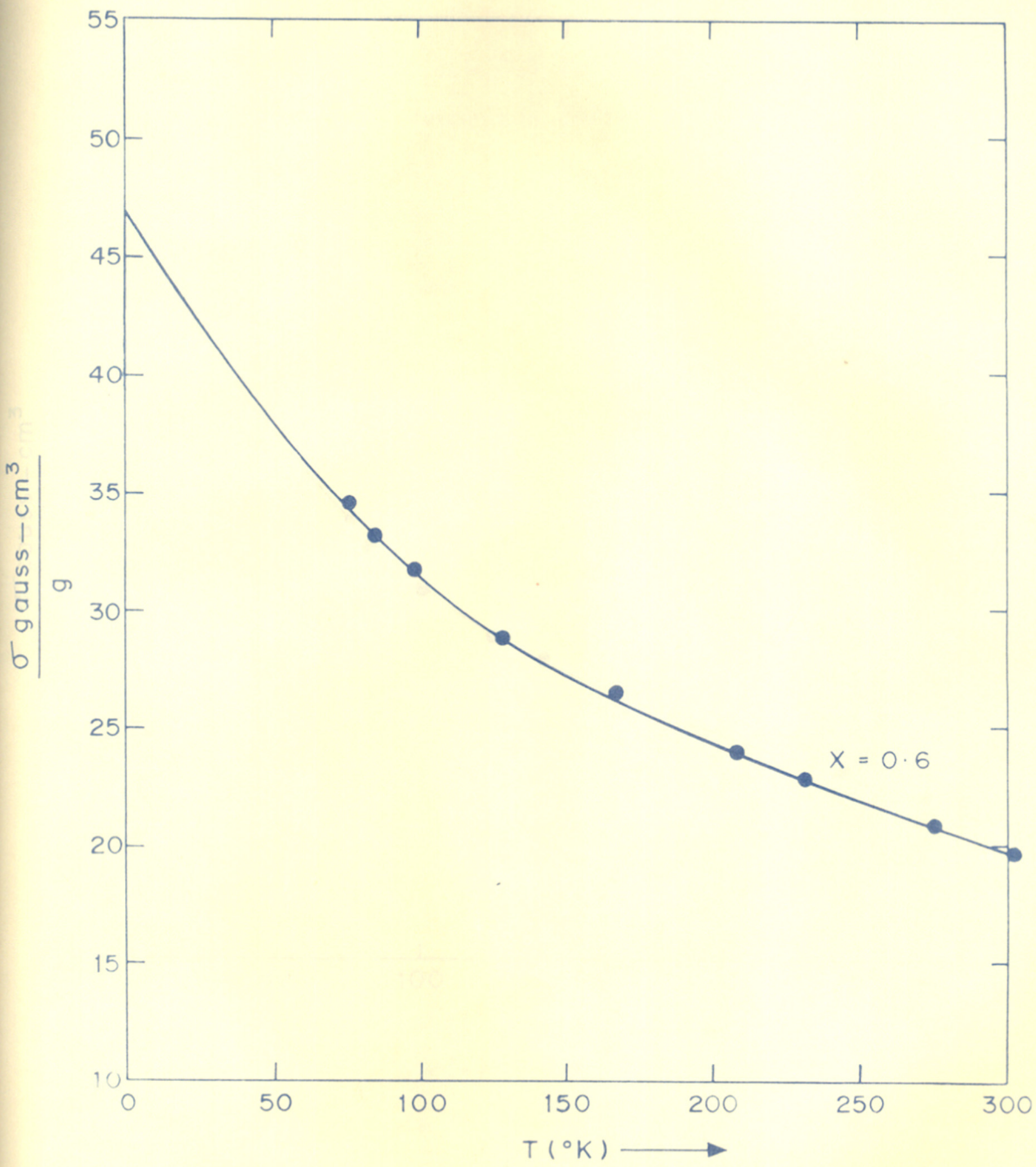

FIG. 11.

SATURATION MAGNETIZATION PER GRAM 'σ' AS A FUNCTION OF TEMPERATURE 'T' FOR THE SYSTEM $CuMn_{2x}Fe_{2-2x}O_4$.

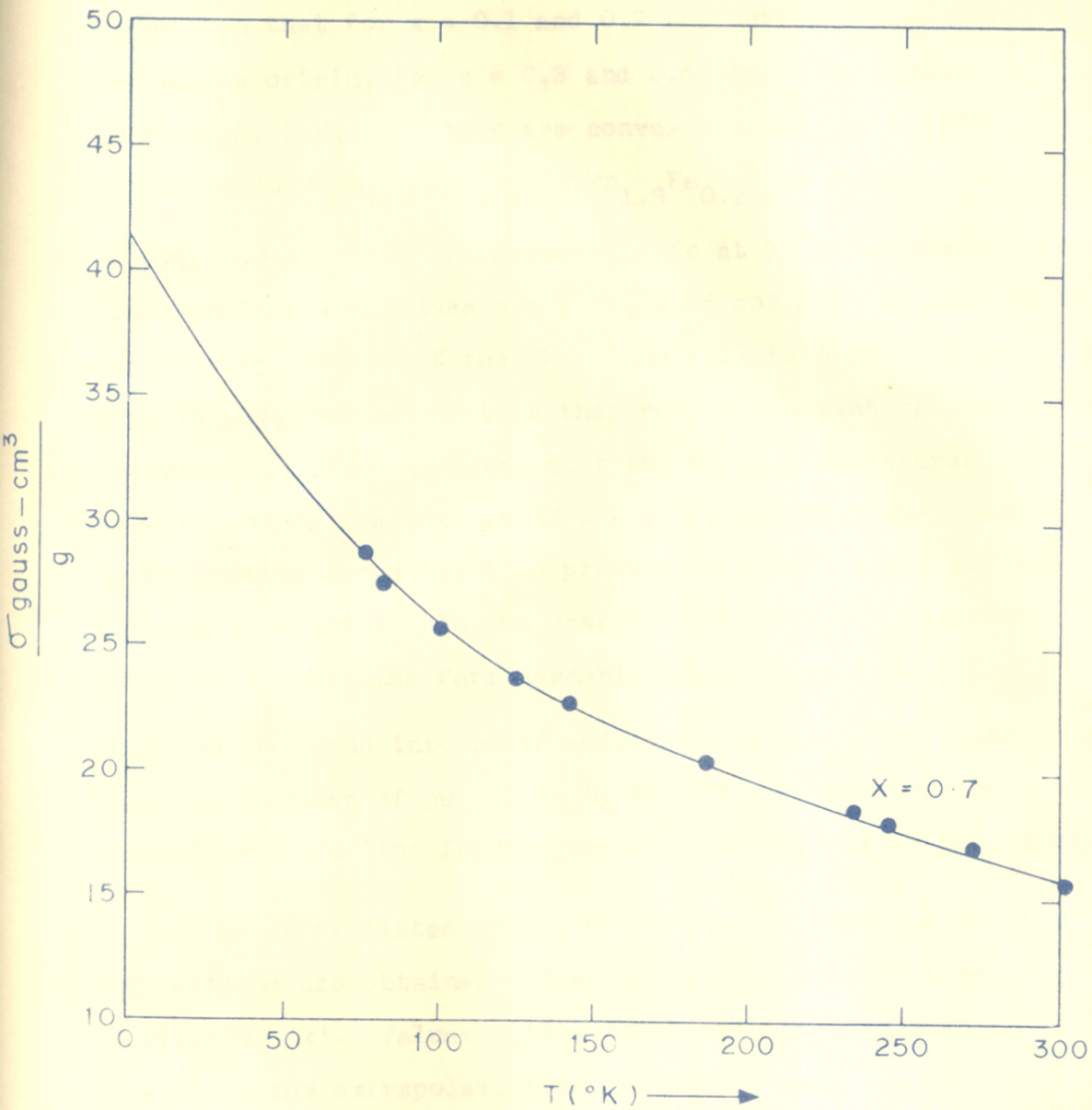

FIG. 12.

SATURATION MAGNETIZATION PER GRAM 'σ' AS A FUNCTION OF TEMPERATURE 'T' FOR THE SYSTEM $CuMn_{2x}Fe_{2-2x}O_4$

can be seen that for x = 0.1 and 0.2 the curves are concave towards the origin, for x = 0.3 and 0.4, they are linear and for x = 0.5, 0.6, 0.7, they are convex towards the origin. The compounds $CuMn_{1.6}Fe_{0.4}O_4$, $CuMn_{1.8}Fe_{0.2}O_4$ and $CuMn_2O_4$(i.e. x = 0.8, 0.9 and 1.0) are ferromagnetic at 77°K and the saturation magnetization values are 7.78, 4.05 and 5.2 (in cgs. units) respectively. At 140°K the σ values fall to 6.75, 1.0 and 0.75 respectively, but beyond this they remain constant upto room temperature. This indicates that the Curie temperatures for these compounds lie between 77°K - 140°K and that the small ferromagnetism above 140°K is presumably due to trace ferromagnetic impurities. In the case of the first two compounds it is likely that the ferromagnetic compound is free $CuFe_2O_4$ which has not gone into solid solution. However, it could not be so in the case of pure $CuMn_2O_4$ and further work on the identification of the ferromagnetic impurities is in progress.

The extrapolated values of $\sigma(T = 0°K)$ for the various compositions are obtained and n_B values are plotted as a function of 'x'. Values upto x = 0.7 only are included in Fig. 29 as the extrapolation in the other cases was not possible in view of a very limited number of points below the Curie temperature. It canbe seen that the magnetic moment (n_B) increases as 'x' decreases from x = 1.0 and reaches the maximum value at x = 0.5 (n_B = 1.95) beyond which it starts falling.

3.1.2. $CuMn_2O_4$ - $NiFe_2O_4$ ($Cu_xNi_{1-x}Mn_{2x}Fe_{2-2x}O_4$)

Saturation magnetization of the compounds having the general formula $Cu_xNi_{1-x}Mn_{2x}Fe_{2-2x}O_4$ was measured in the temperature range of 80 - 300°K and as usual the values of $\sigma_{(T = 0^\circ K)}$ were obtained by extrapolation of σ vs T plot to T = 0°K. Saturation magnetization in Bohr magneton (n_B) per mole was calculated.

For pure $NiFe_2O_4$ (x = 0) the saturation magnetization was found to be 51.52 $\frac{\text{gauss-cm}^3}{\text{g}}$ at room temperature which increased with decrease in temperature and the extrapolated value to T = 0°K is 55.2 $\frac{\text{gauss-cm}^3}{\text{g}}$ (= 2.3 μ_B) which is in good agreement with that reported by Gorter[58]. The σ - T plot is shown in Fig.13. For other compositions in the range x < .9 we get a similar increase in saturation magnetization on decrease in temperature. The values of σ at 300°K, 82°K and 0°K (extrapolated) are represented in Table 11 and σ - T plots are shown in Fig. 14 to 19.

For x = .9, σ - T plot is linear in the range between 120 - 210°K, falls abruptly between 210-250°K and then remains nearly constant till room temperature.

This shows that the Curie temperature for the compound $Cu_{0.9}Ni_{0.1}Mn_{1.8}Fe_{0.2}O_4$ (i.e. x = 0.9) lies between 240-250°K and that it may contain some other ferromagnetic phase as trace impurity.

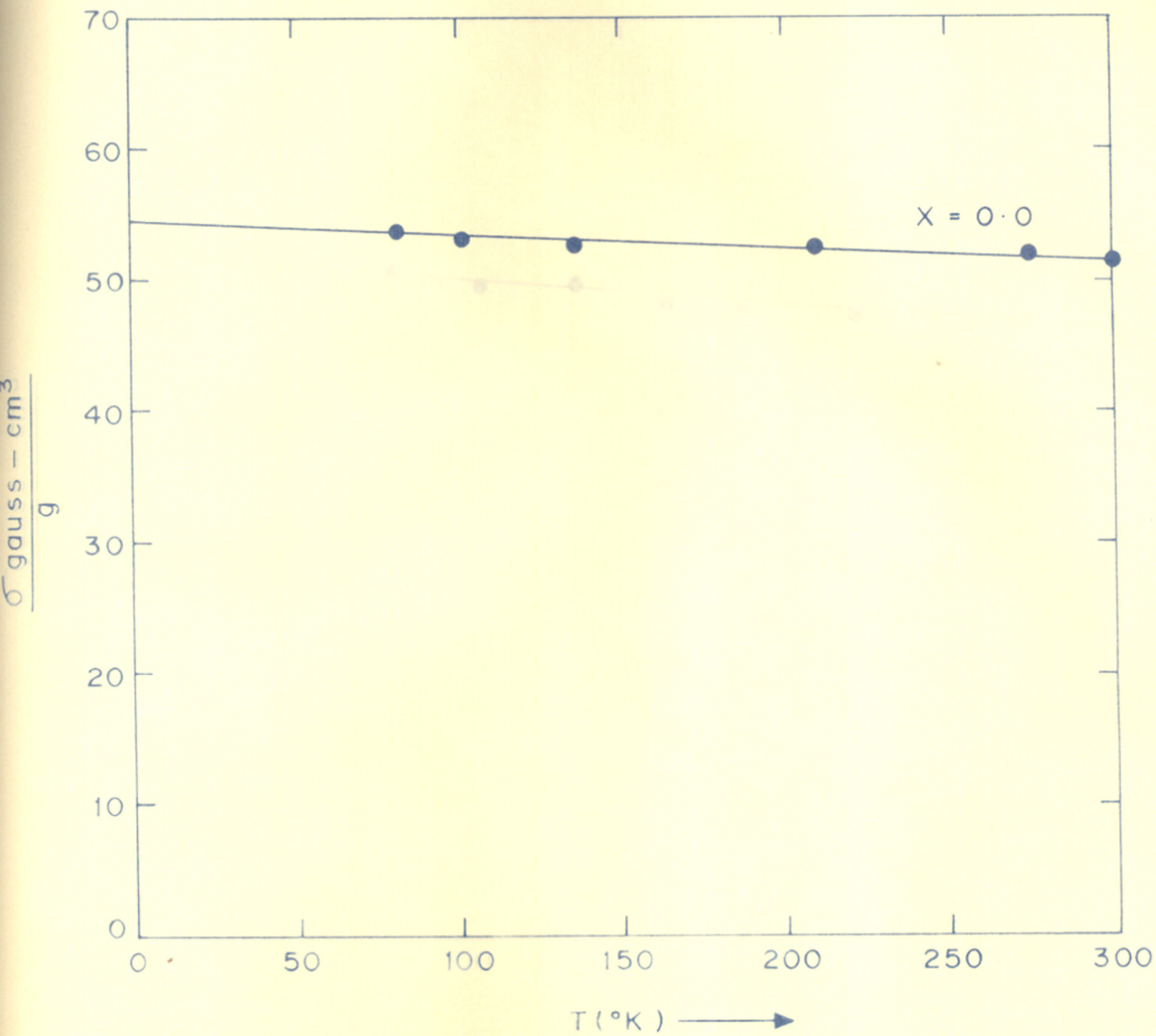

FIG. 13.

SATURATION MAGNETIZATION PER GRAM 'σ' AS A FUNCTION OF TEMPERATURE 'T' FOR THE SYSTEM $Cu_xNi_{1-x}Mn_{2x}Fe_{2-2x}O_4$

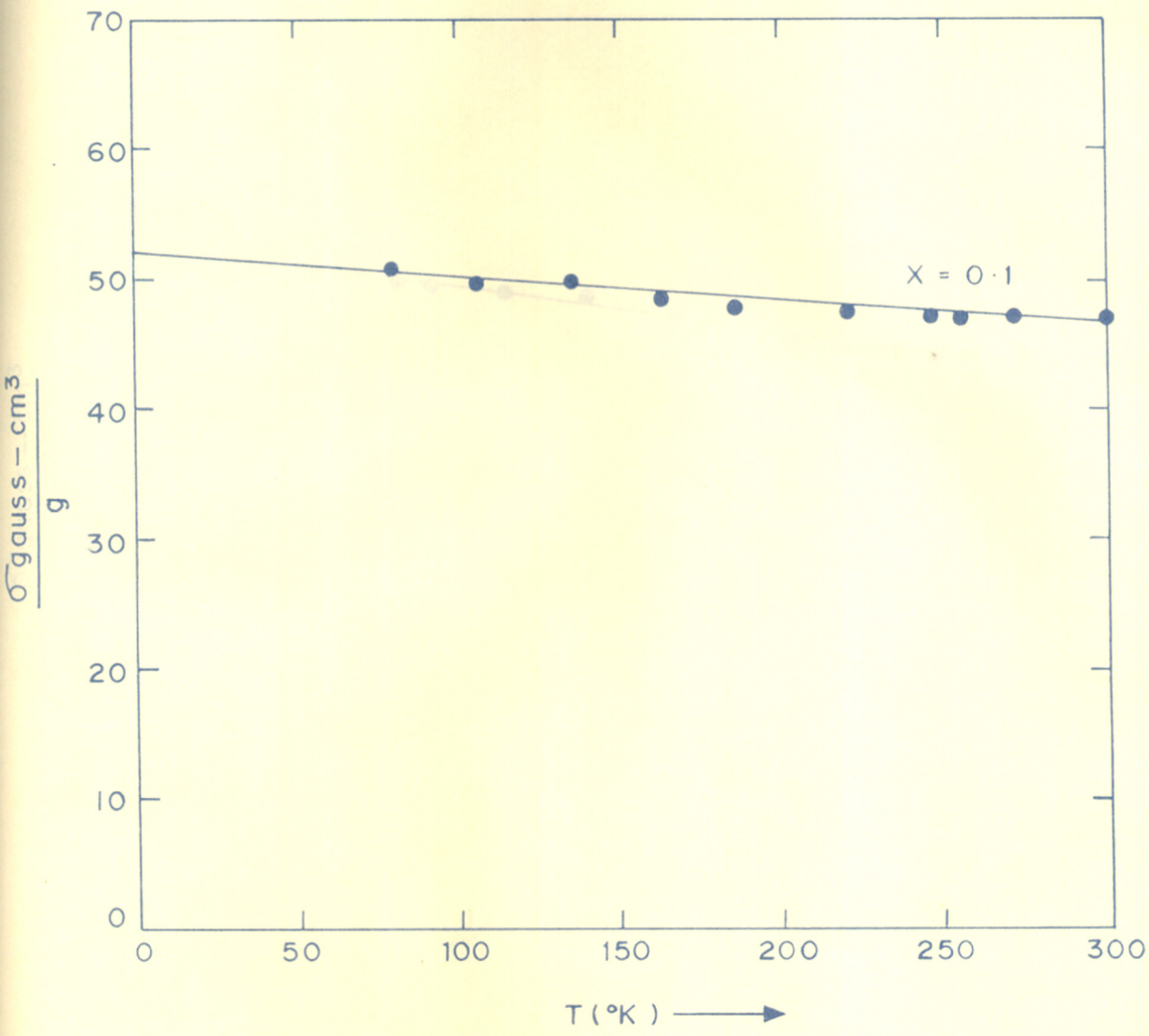

FIG.14.

SATURATION MAGNETIZATION PER GRAM 'σ' AS A FUNCTION OF TEMPERATURE 'T' FOR THE SYSTEM $Cu_xNi_{1-x}Mn_{2x}Fe_{2-2x}O_4$.

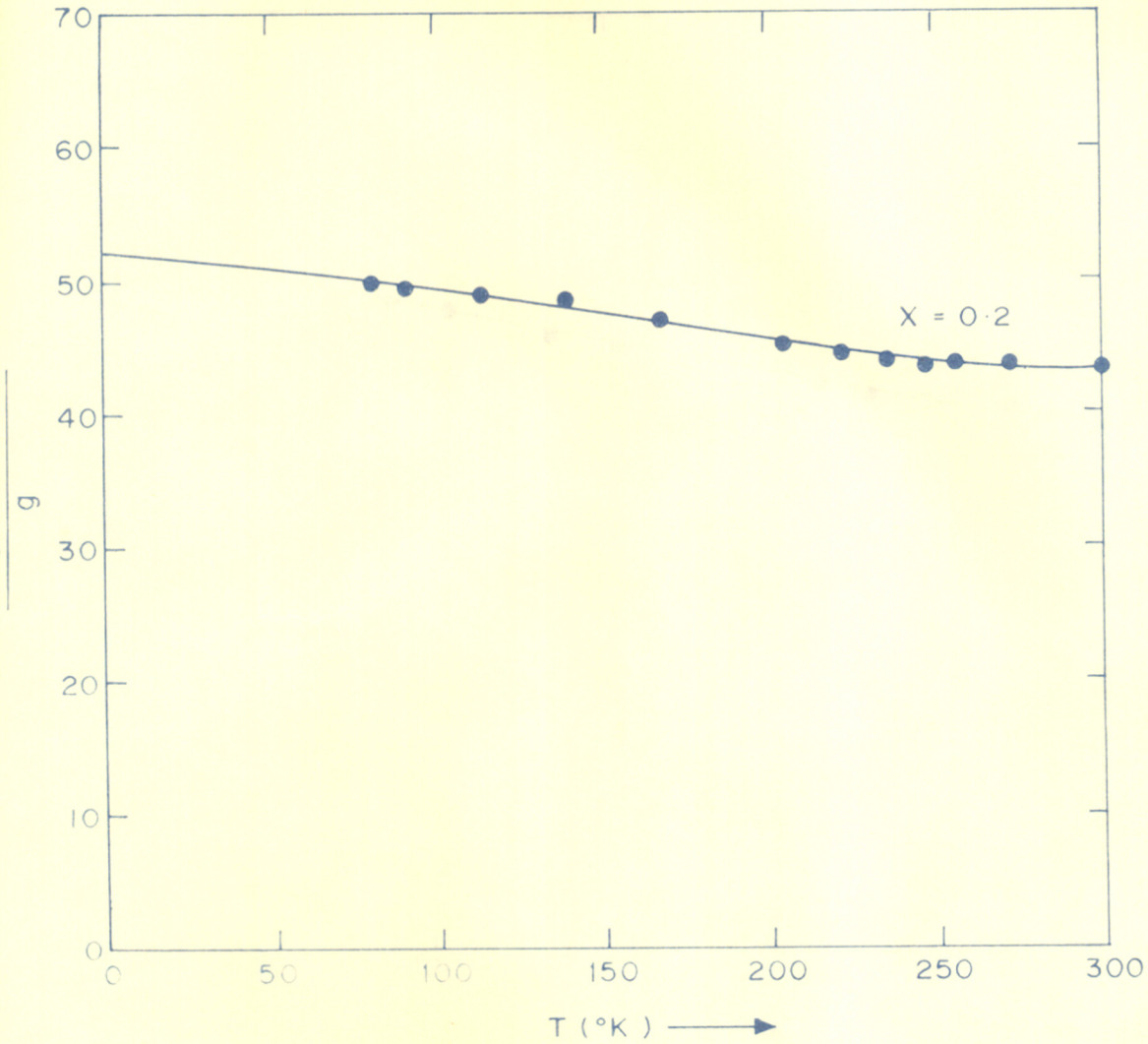

FIG. 15.

SATURATION MAGNETIZATION PER GRAM 'σ' AS A FUNCTION OF TEMPERATURE 'T' FOR THE SYSTEM $Cu_xNi_{1-x}Mn_{2x}Fe_{2-2x}O_4$

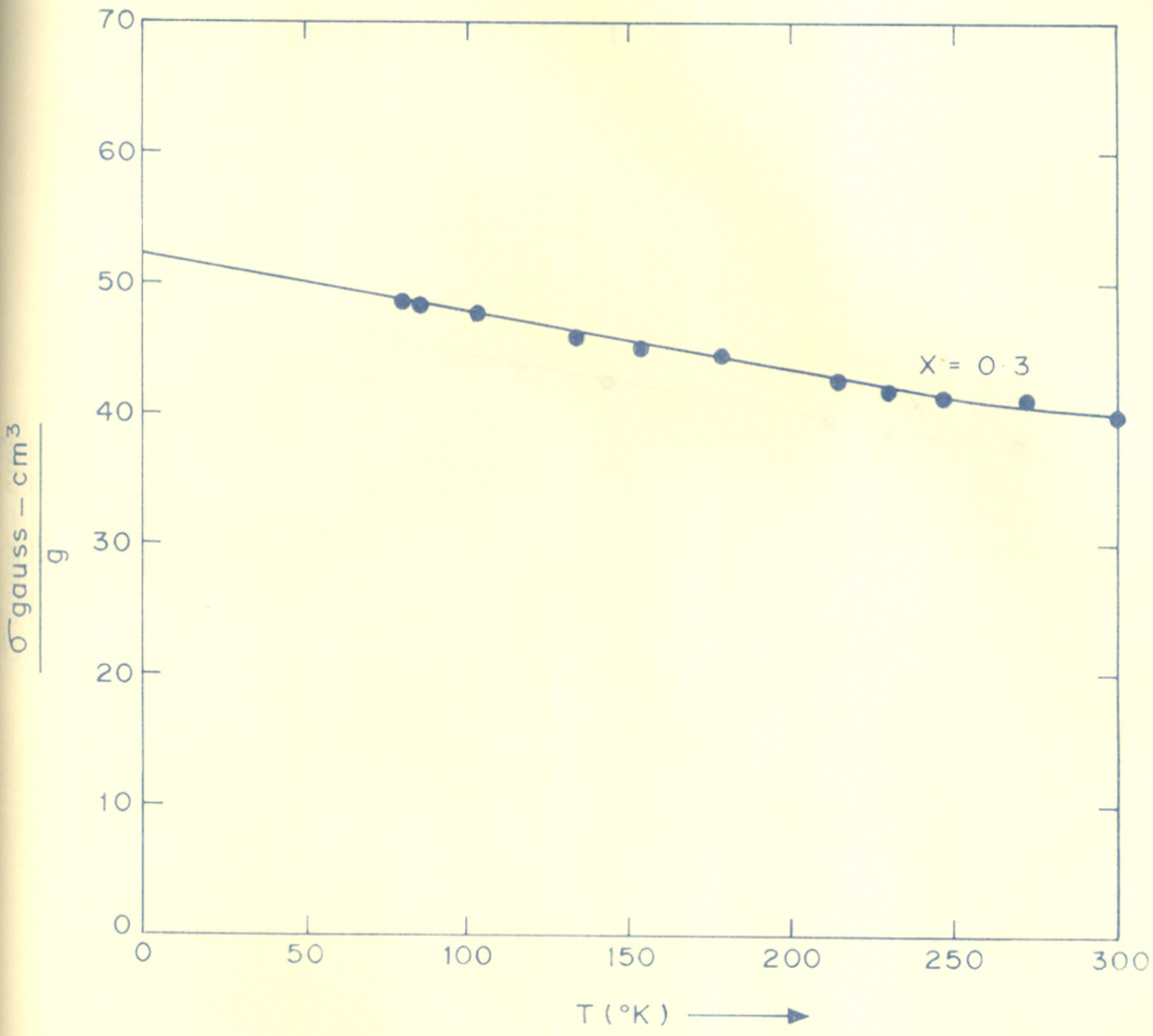

FIG 16.

SATURATION MAGNETIZATION PER GRAM 'σ' AS A FUNCTION OF TEMPERATURE 'T' FOR THE SYSTEM $Cu_xNi_{1-x}Mn_{2x}Fe_{2-2x}O_4$.

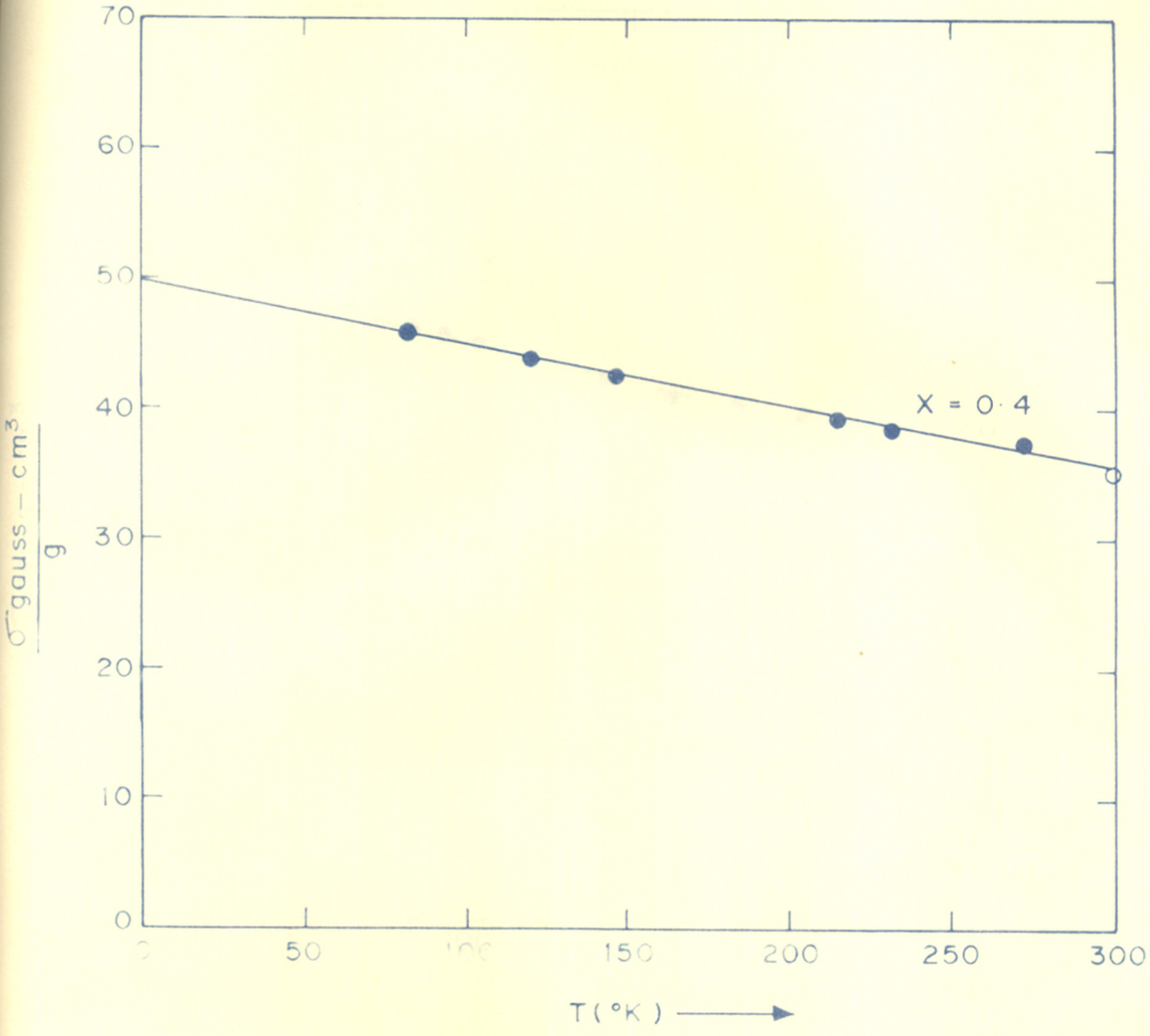

FIG. 17

SATURATION MAGNETIZATION PER GRAM 'σ' AS A FUNCTION OF TEMPERATURE 'T' FOR THE SYSTEM $Cu_xNi_{1-x}Mn_{2x}Fe_{2-2x}O_4$.

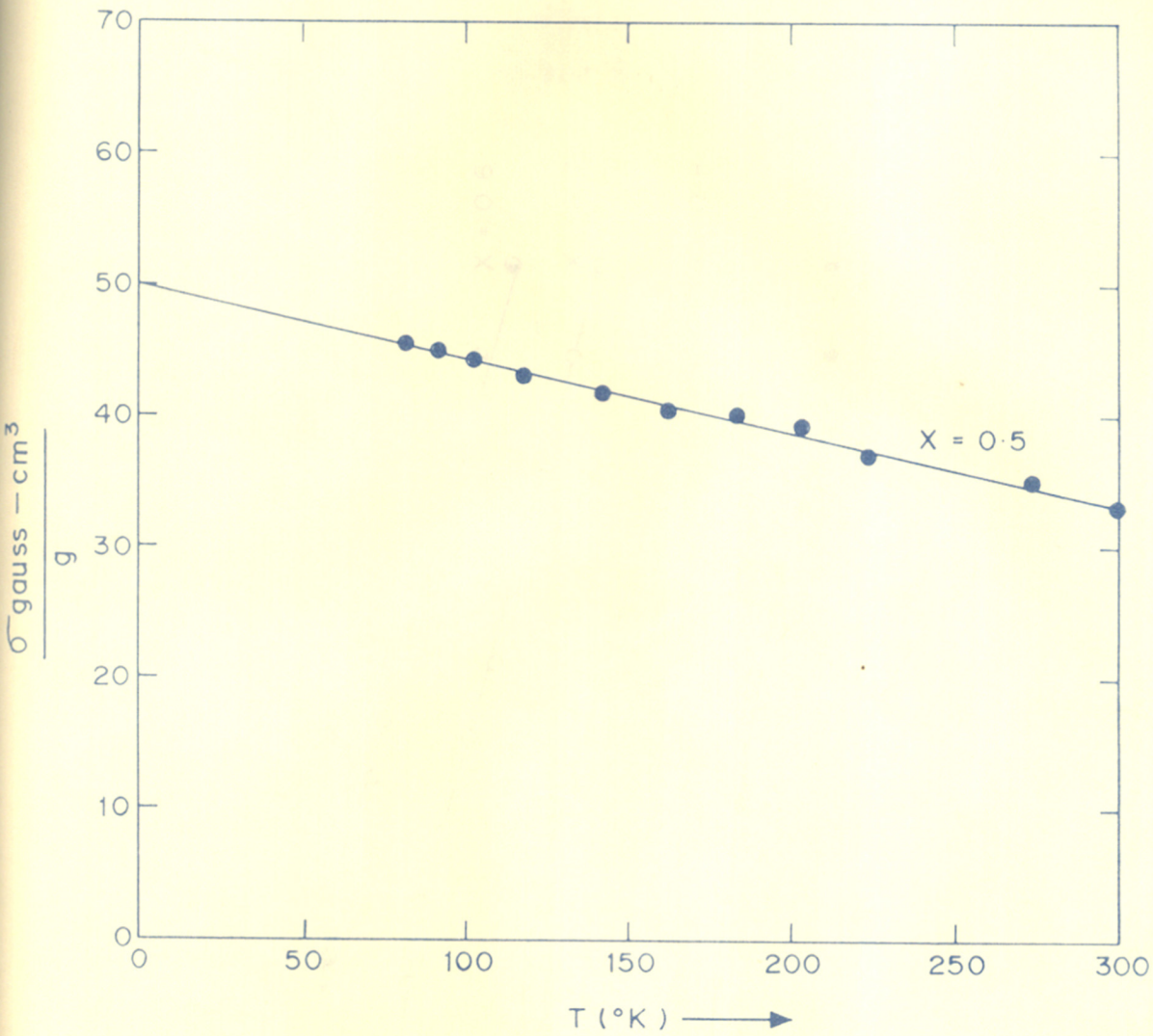

FIG. 18.

SATURATION MAGNETIZATION PER GRAM 'σ' AS A FUNCTION OF TEMPERATURE 'T' FOR THE SYSTEM $Cu_xNi_{1-x}Mn_{2x}Fe_{2-2x}O_4$.

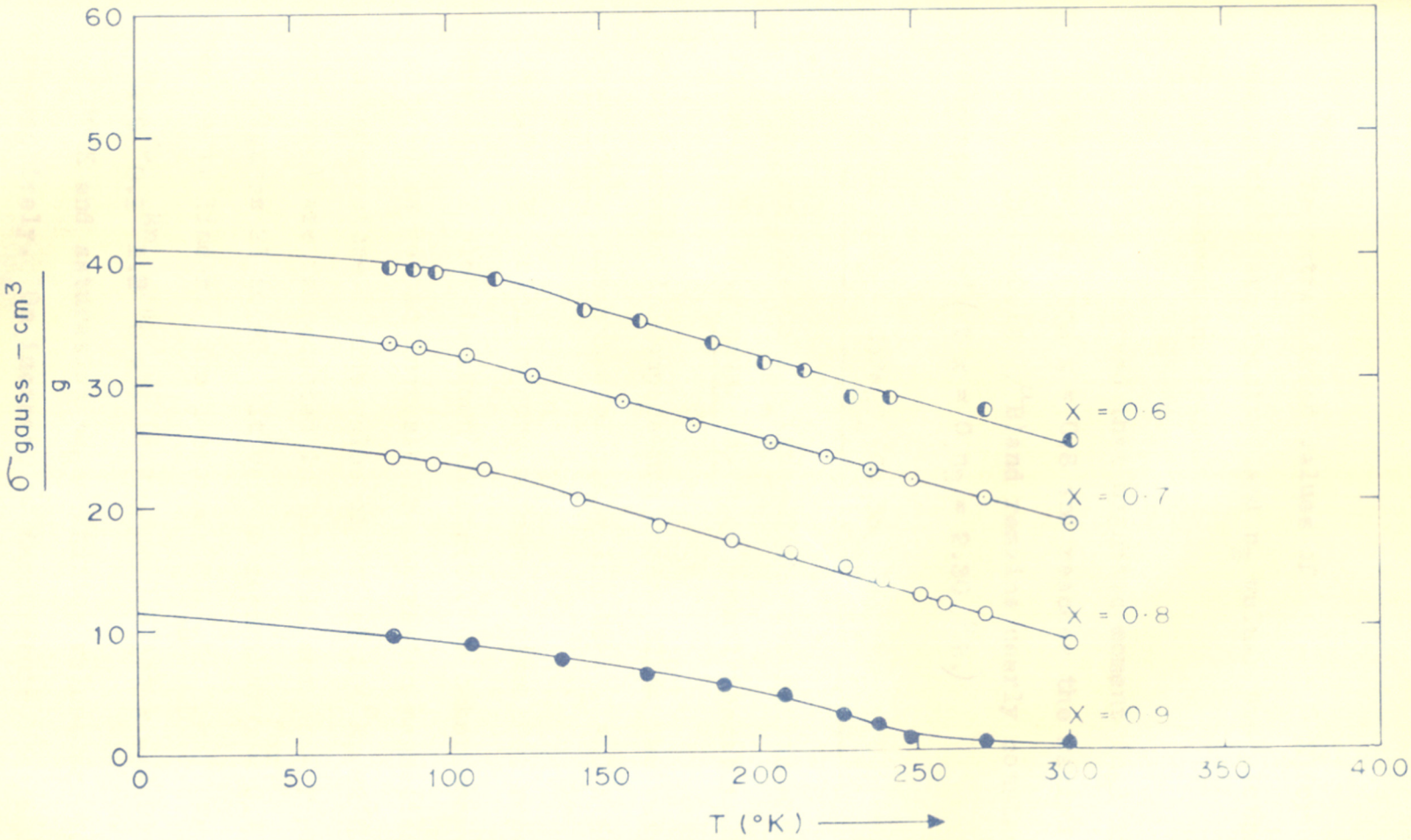

FIG. 19. SATURATION MAGNETIZATION PER GRAM 'σ' AS A FUNCTION OF TEMPERATURE 'T' FOR THE SYSTEM $Cu_xNi_{1-x}Mn_{2x}Fe_{2-2x}O_4$

The extrapolated values of $\sigma_{(T = 0^{\circ}K)}$ for the various compositions are obtained and n_B values are plotted as a function of 'x' as shown in Fig.30.

It is observed that magnetic moment (n_B) increases as 'x' decreases from x = 0.8 and reaches the maximum value at x = 0.5 (n_B = 2.12 μ_B) and remains nearly constant for further decrease in 'x' (at x = 0, n_B = 2.30 μ_B.)

3.1.3. $CuMn_2O_4$ - $CoFe_2O_4$ ($Cu_xCo_{1-x}Mn_{2x}Fe_{2-2x}O_4$)

For pure $CoFe_2O_4$ (x = 0) the saturation magnetization was found to be 67.0 $\frac{\text{gauss-cm.}^3}{g}$ at room temperature and increased with decrease in temperature and at 81°K. The value was 74.52 $\frac{\text{gauss-cm}^3.}{g}$ the extrapolated value of $\sigma_{(T = 0^{\circ}K)}$ is 78.0 $\frac{\text{gauss-cm.}^3}{g}$ (= 3.3 μ_B) which is in good agreement with that reported by Gorter[58]. The σ - T plot is shown in Fig.20. For other compositions also (x > 0) we get an increase in saturation magnetization on decrease in temperature. The value of σ at 300°K, 82°K and 0°K (extrapolated) are represented in Table 12 and σ - T plots are shown in Figures 21 to 23. It can be seen that for x = 0.1 to 0.7, the curve is linear. The compounds $Cu_{0.8}Co_{0.2}Mn_{1.6}Fe_{0.4}O_4$, and $Cu_{0.9}Co_{0.1}Mn_{1.8}Fe_{0.2}O_4$ (i.e. x = 0.8 and x = 0.9) are ferromagnetic at 82°K and saturation magnetization values are 20.65 and 10.02 respectively. On increase of temperature, σ values fall very rapidly and are 13.5 $\frac{\text{gauss-cm.}^3}{g}$ and 4.0 $\frac{\text{gauss-cm.}^3}{g}$ respectively

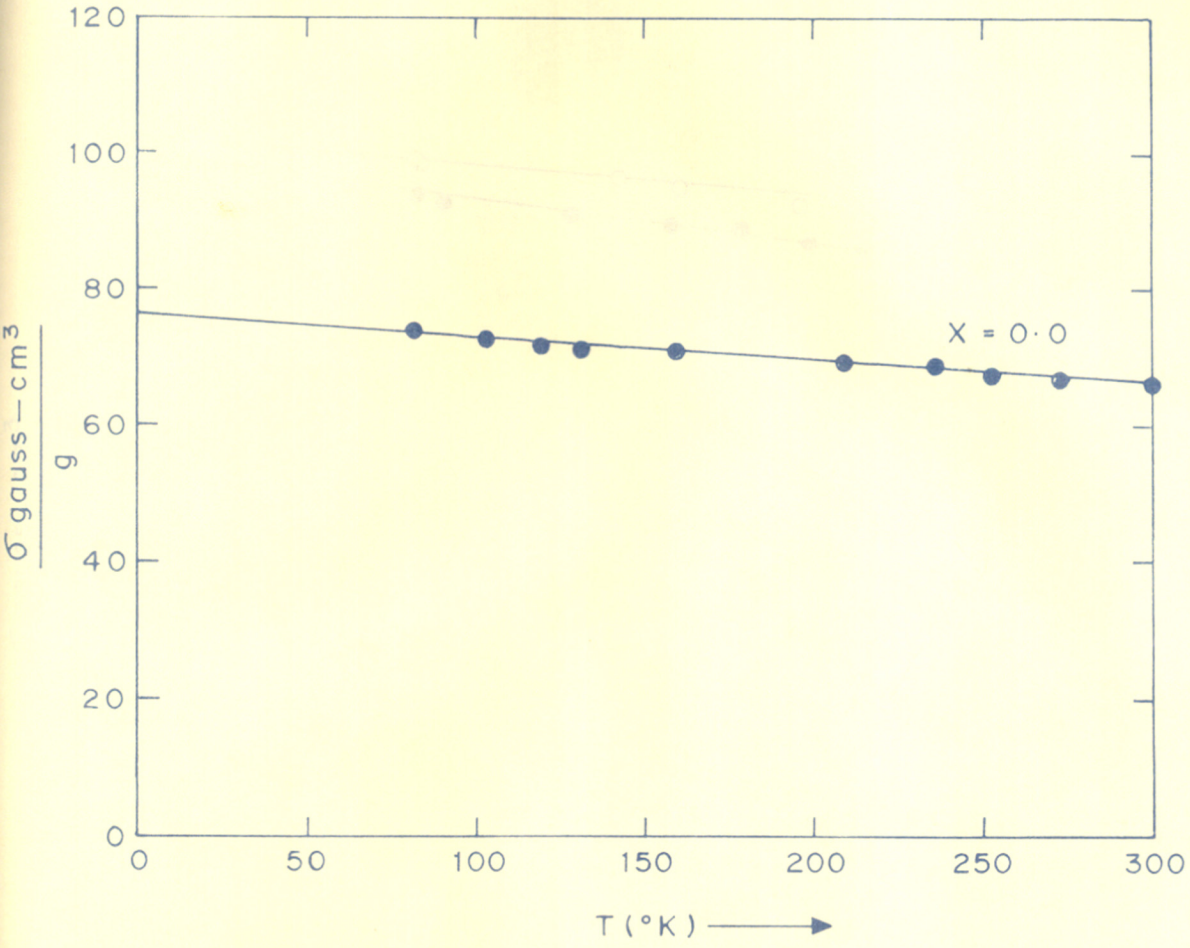

FIG. 20.

SATURATION MAGNETIZATION PER GRAM 'σ' AS A FUNCTION OF TEMPERATURE 'T' FOR THE SYSTEM $Cu_xCo_{1-x}Mn_{2x}Fe_{2-2x}O_4$.

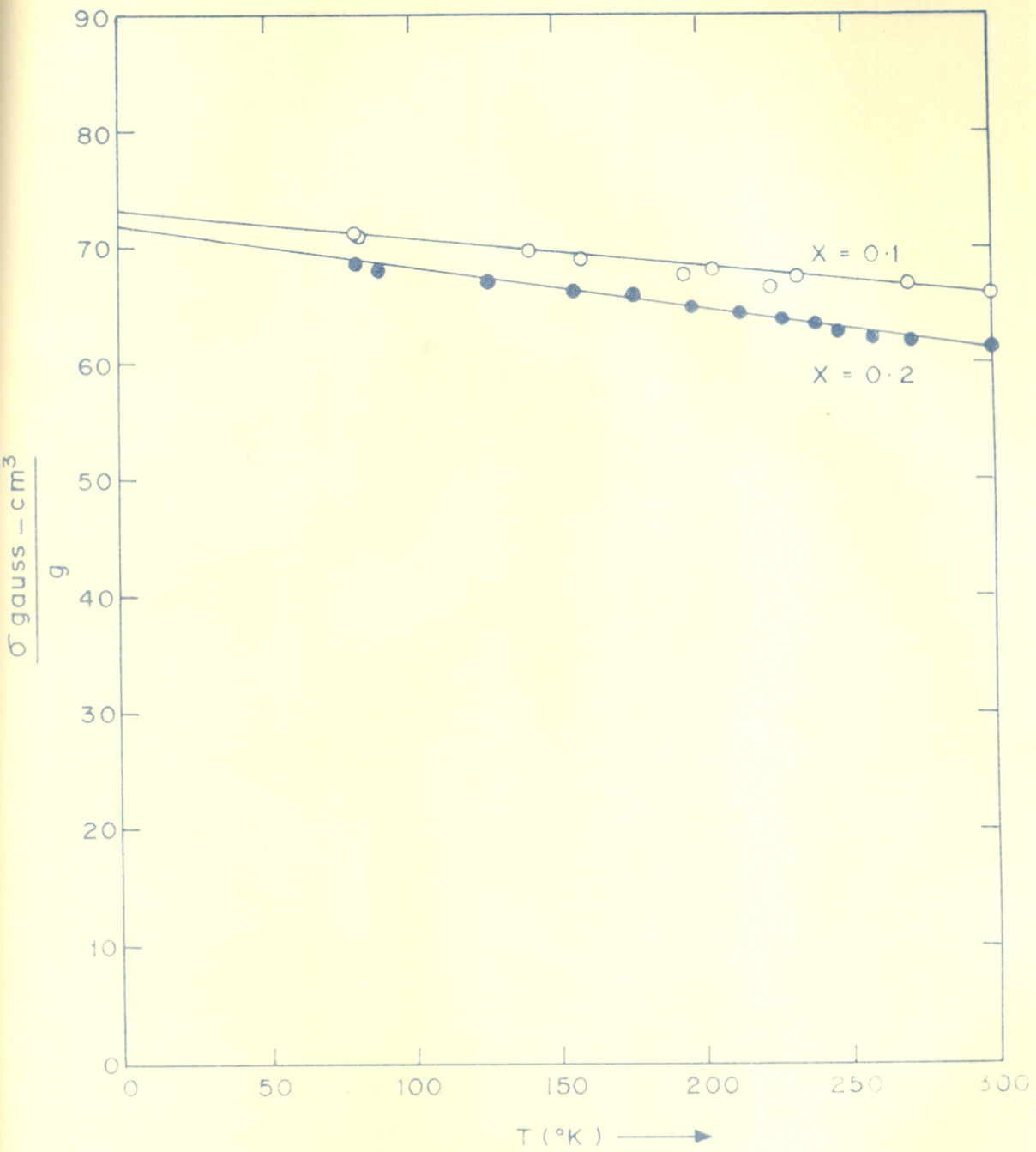

FIG 21.

SATURATION MAGNETIZATION PER GRAM 'σ' AS A FUNCTION OF TEMPERATURE 'T' FOR THE SYSTEM $Cu_xCo_{1-x}Mn_{2x}Fe_{2-2x}O_4$

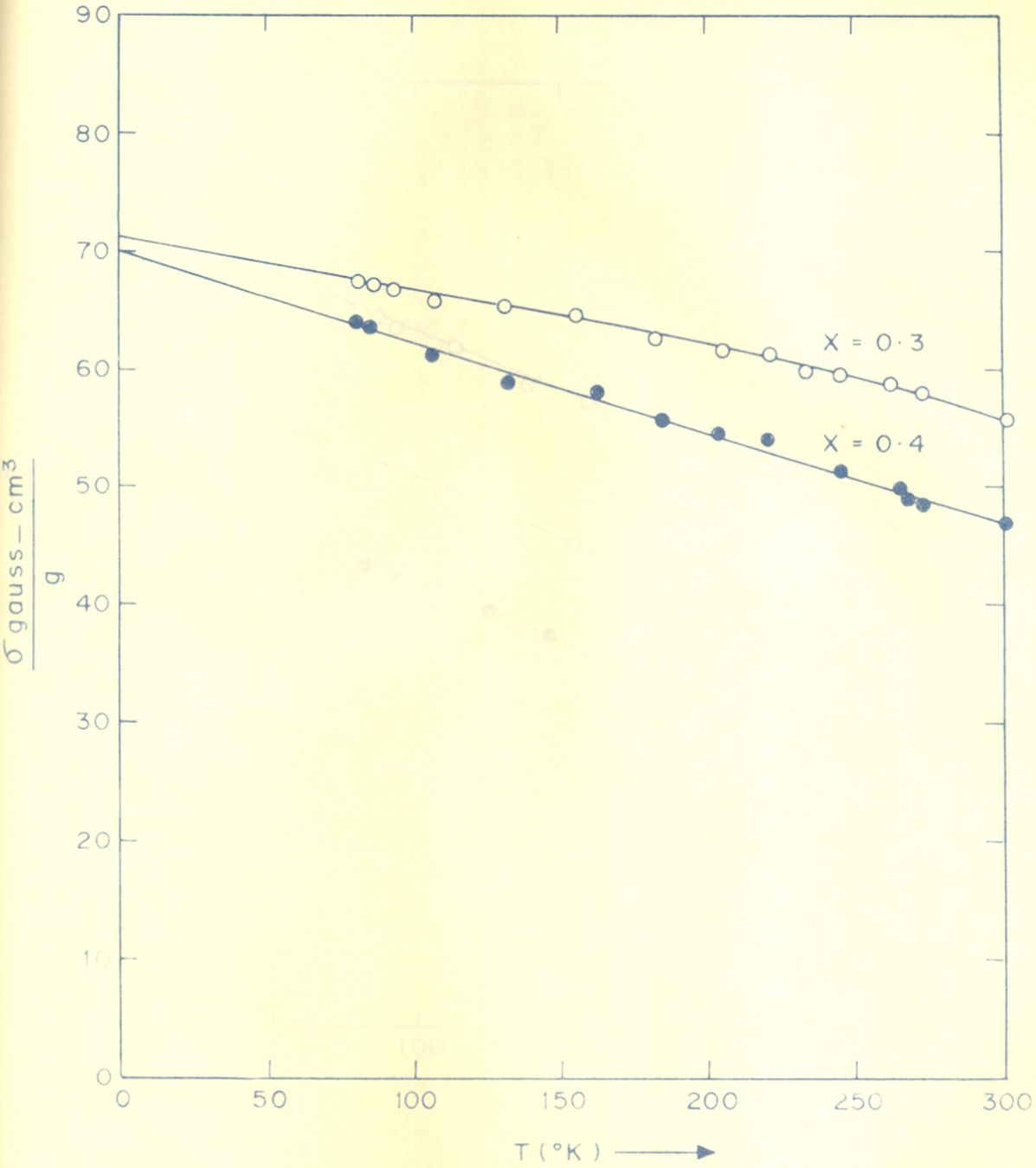

FIG. 22.

SATURATION MAGNETIZATION PER GRAM 'σ' AS A FUNCTION OF TEMPERATURE 'T' FOR THE SYSTEM $Cu_xCo_{1-x}Mn_{2x}Fe_{2-2x}O_4$.

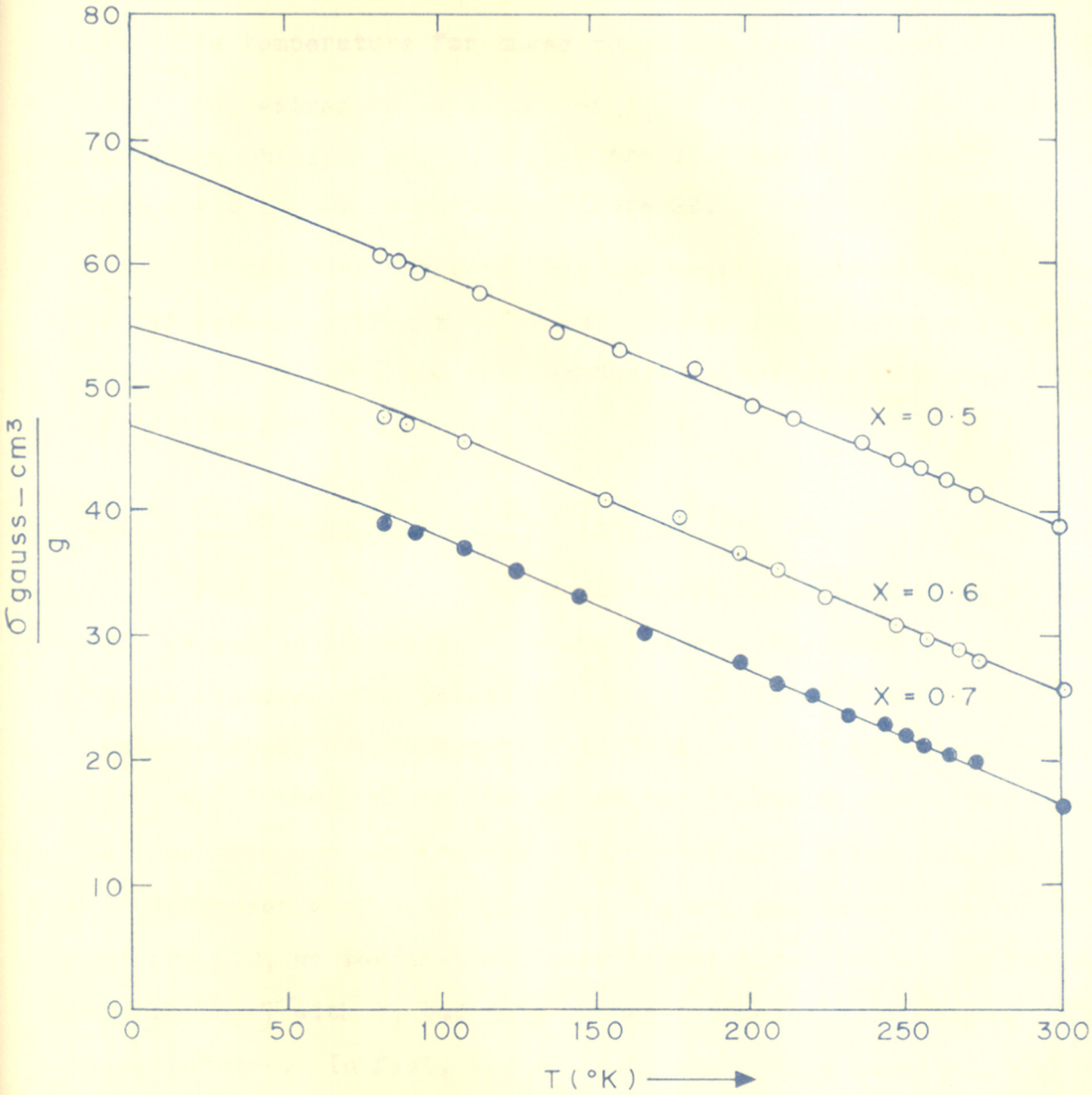

FIG. 23.

SATURATION MAGNETIZATION PER GRAM 'σ' AS A FUNCTION OF TEMPERATURE 'T' FOR THE SYSTEM $Cu_xCo_{1-x}Mn_{2x}Fe_{2-2x}O_4$.

at 160°K and 7.0 and 2.0 at room temperature. It appears that the Curie temperature for these compounds lies between 150-250°K.

The extrapolated values of $\sigma_{(T = 0^{\circ}K)}$ for various compositions are obtained and n_B values are plotted as a function of 'x' from x = 0 to 0.7 as shown in Figure 29.

It has been observed that the magnetic moment (n_B) increases as 'x' decreases from x = 0.7 and reaches the maximum value at x = 0.5 (n_B = 2.95) and remains nearly constant on further decrease in 'x' (at x = 0, n_B = 3.30).

3.1.4. $CuMn_2O_4$ - $ZnFe_2O_4$ ($Cu_xZn_{1-x}Mn_{2x}Fe_{2-2x}O_4$)

For $x \geq 0.1$ the σ - T plots are shown in Figures 24 to 26. We get an increase in saturation magnetization on decrease in temperature. The values of σ at 300°K, 82°K and 0°K (extrapolated) are represented in Table 13. It is observed that for x = 0.1 the plot is linear but for higher values of x, it becomes more and more convex. For x = 0.5, 0.6 and 0.7, σ increases very rapidly as temperature decreases. For x = 0.7, 0.8 and 0.9, we see that at lower temperatures there is a rapid change in σ with T, but this change becomes slow at higher temperatures. In fact, for x = 0.9, there is a long tail and the transition from ferro to paramagnetic state is very gradual. The magnetic moment (n_B) was calculated from the extrapolated values of $\sigma_{(T = 0^{\circ}K)}$ for various compositions, and n_B values are plotted as a function of 'x' (Fig.30).

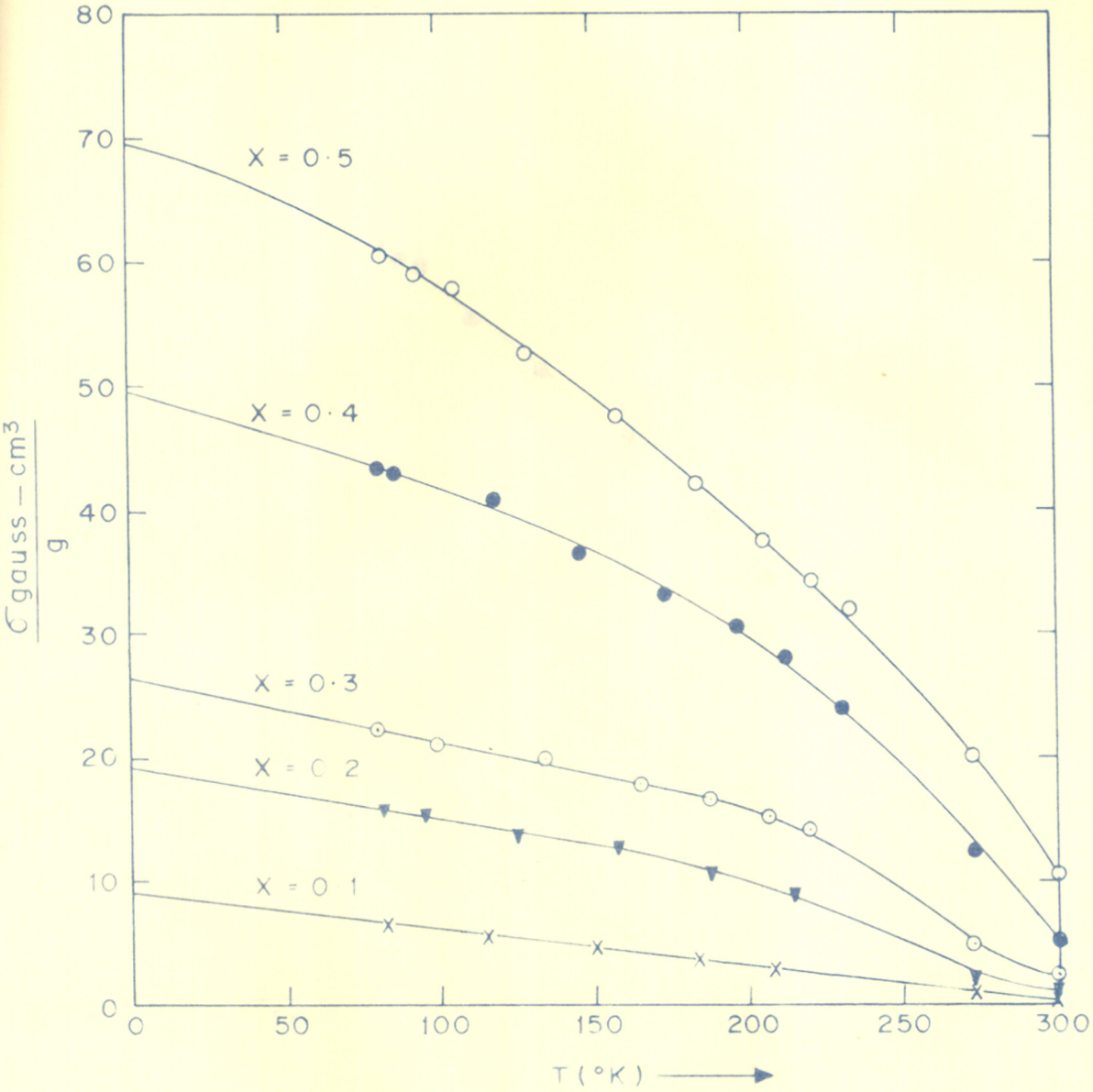

FIG. 24

SATURATION MAGNETIZATION PER GRAM 'σ' AS A FUNCTION OF TEMPERATURE 'T' FOR THE SYSTEM $Cu_xZn_{1-x}Mn_{2x}Fe_{2-2x}O_4$

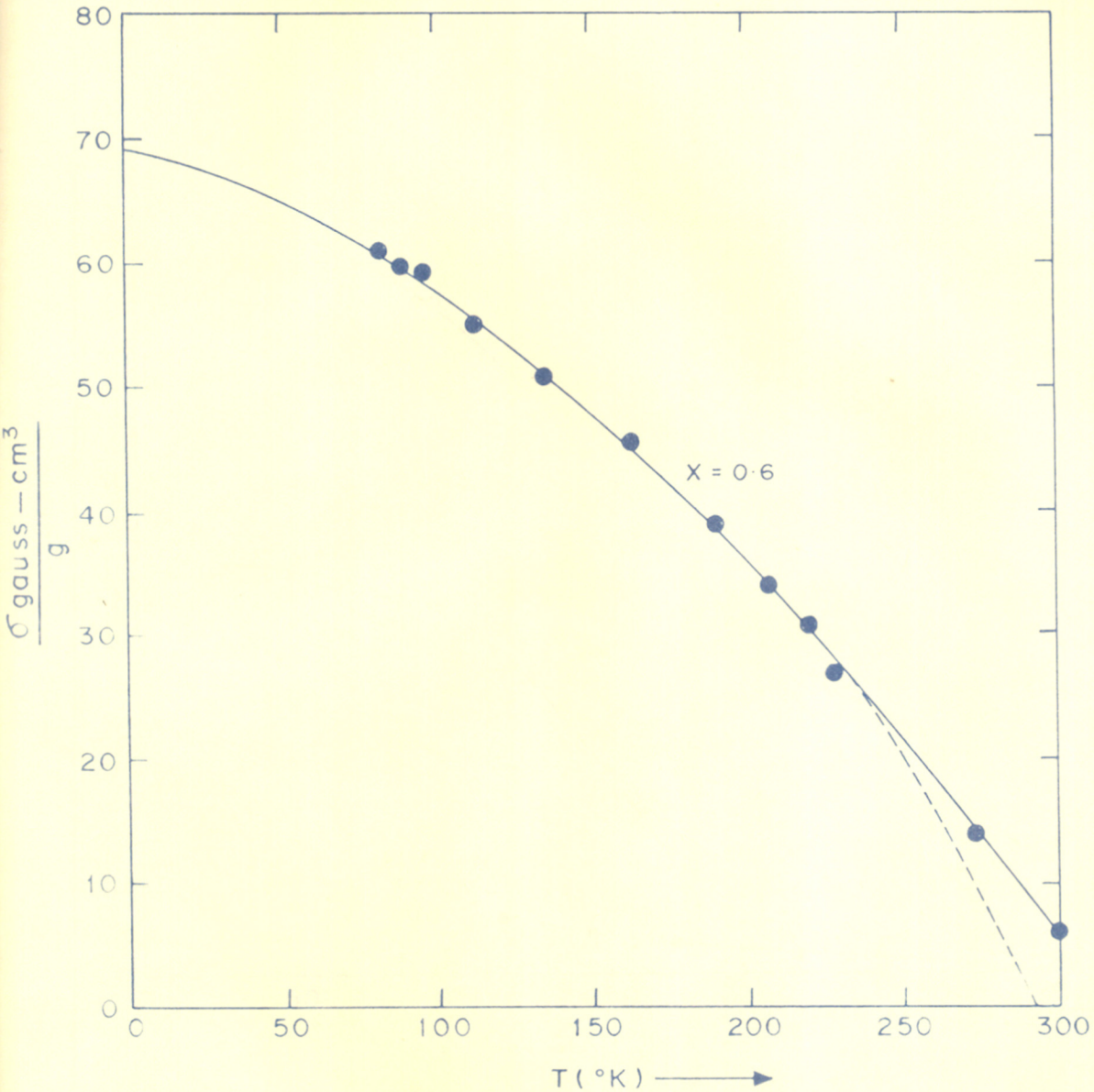

FIG. 25

SATURATION MAGNETIZATION PER GRAM 'σ' AS A FUNCTION OF TEMPERATURE 'T' FOR THE SYSTEM $Cu_xZn_{1-x}Mn_{2x}Fe_{2-2x}O_4$.

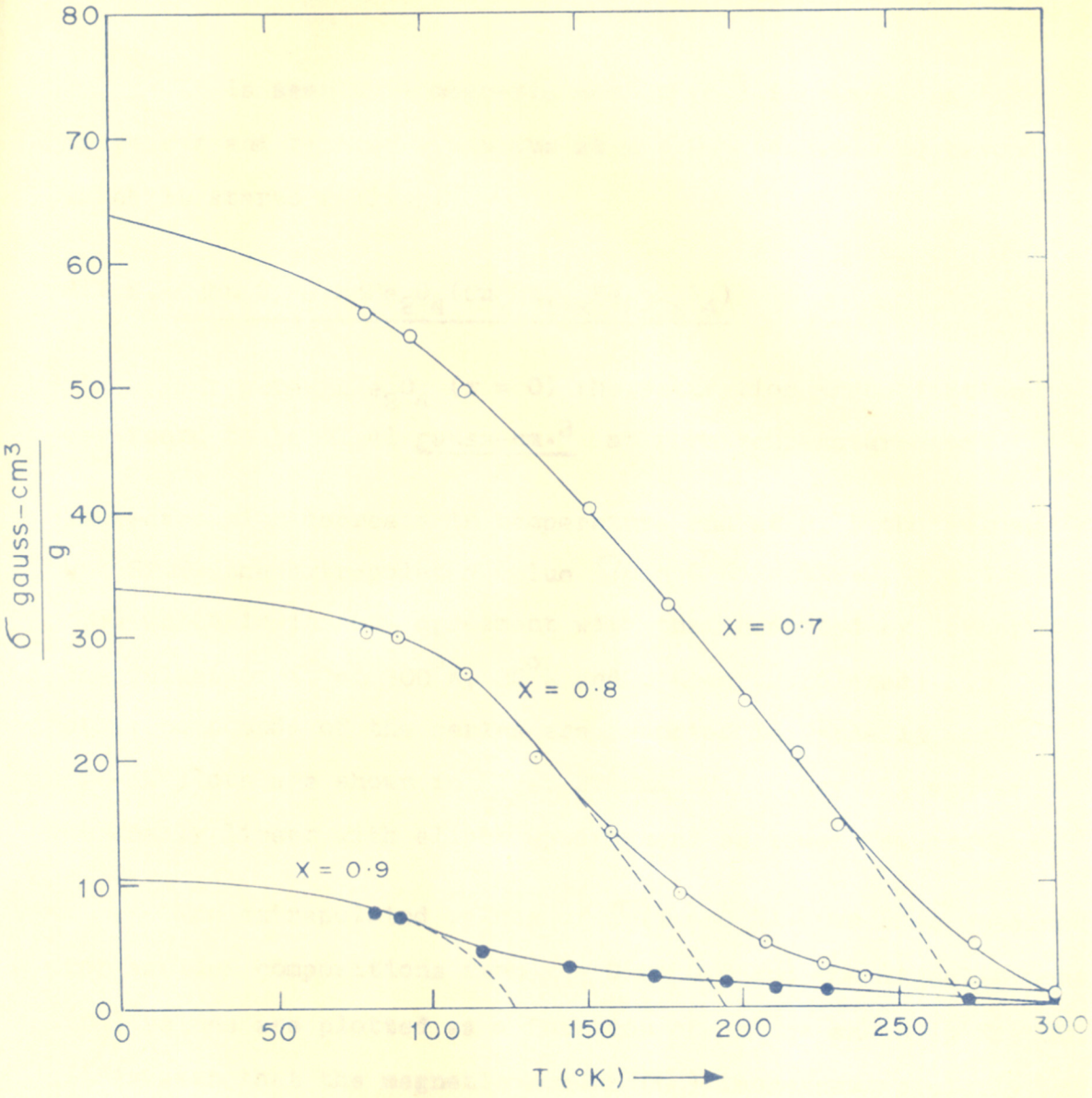

FIG. 26. SATURATION MAGNETIZATION PER GRAM 'σ' AS A FUNCTION OF TEMPERATURE 'T' FOR THE SYSTEM $Cu_xZn_{1-x}Mn_{2x}Fe_{2-2x}O_4$

It is seen that magnetic moment (n_B) increases as 'x' decreases and reaches a maximum at x = 0.6 (= 3.01 μ_B) beyond which it starts falling.

3.1.5. $CuMn_2O_4$ - $MnFe_2O_4$ ($Cu_xMn_{1+x}Fe_{2-2x}O_4$)

For pure $MnFe_2O_4$ (x = 0) the saturation magnetization was found to be 61.41 $\frac{\text{gauss-cm.}^3}{g}$ at room temperature and increased with decrease in temperature and at 81°K the value was 82.19, the extrapolated value (σ_T = 0°K) is 112.0 (= 4.6 μ_B) which is in good agreement with that reported by Gorter[58]. The values of σ at 300°K, 82°K and 0°K (extrapolated) for other compounds of the series are reported in Table 14 and σ - T plots are shown in Figs. 27 and 28. They all appear to be nearly linear with slight upward bend at lower temperatures.

The extrapolated values of σ(T = 0°K) have been obtained for various compositions from x = 0 to 0.9 and the magnetic moment (n_B) values are plotted as a function of 'x' as shown in Fig.30. It is seen that the magnetic moment (n_B) increases regularly as 'x' decreases from x = 0.9 to 0.

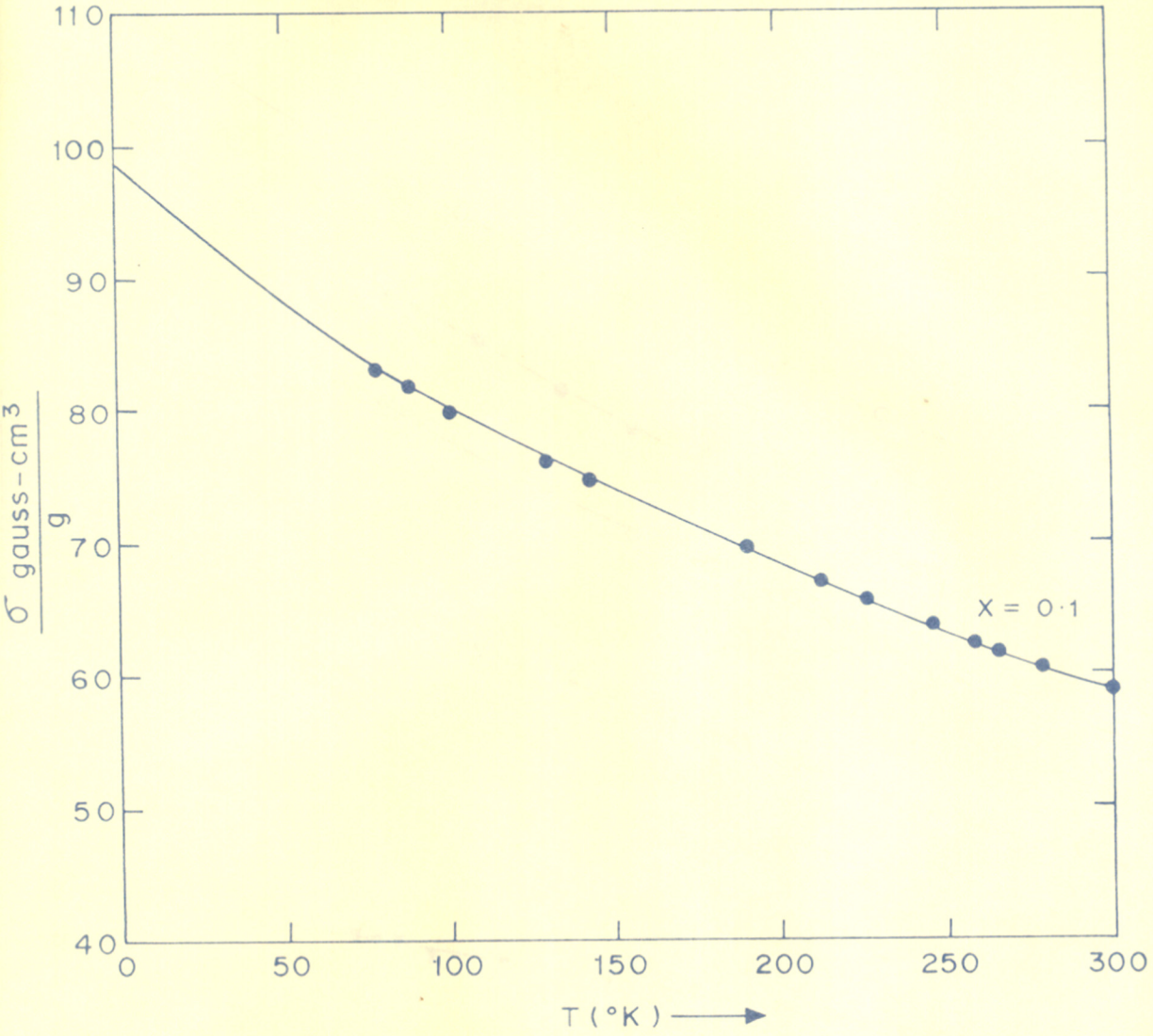

FIG. 27. SATURATION MAGNETIZATION PER GRAM 'σ' AS A FUNCTION OF TEMPERATURE 'T' FOR THE SYSTEM $Cu_xMn_{1+x}Fe_{2-2x}O_4$

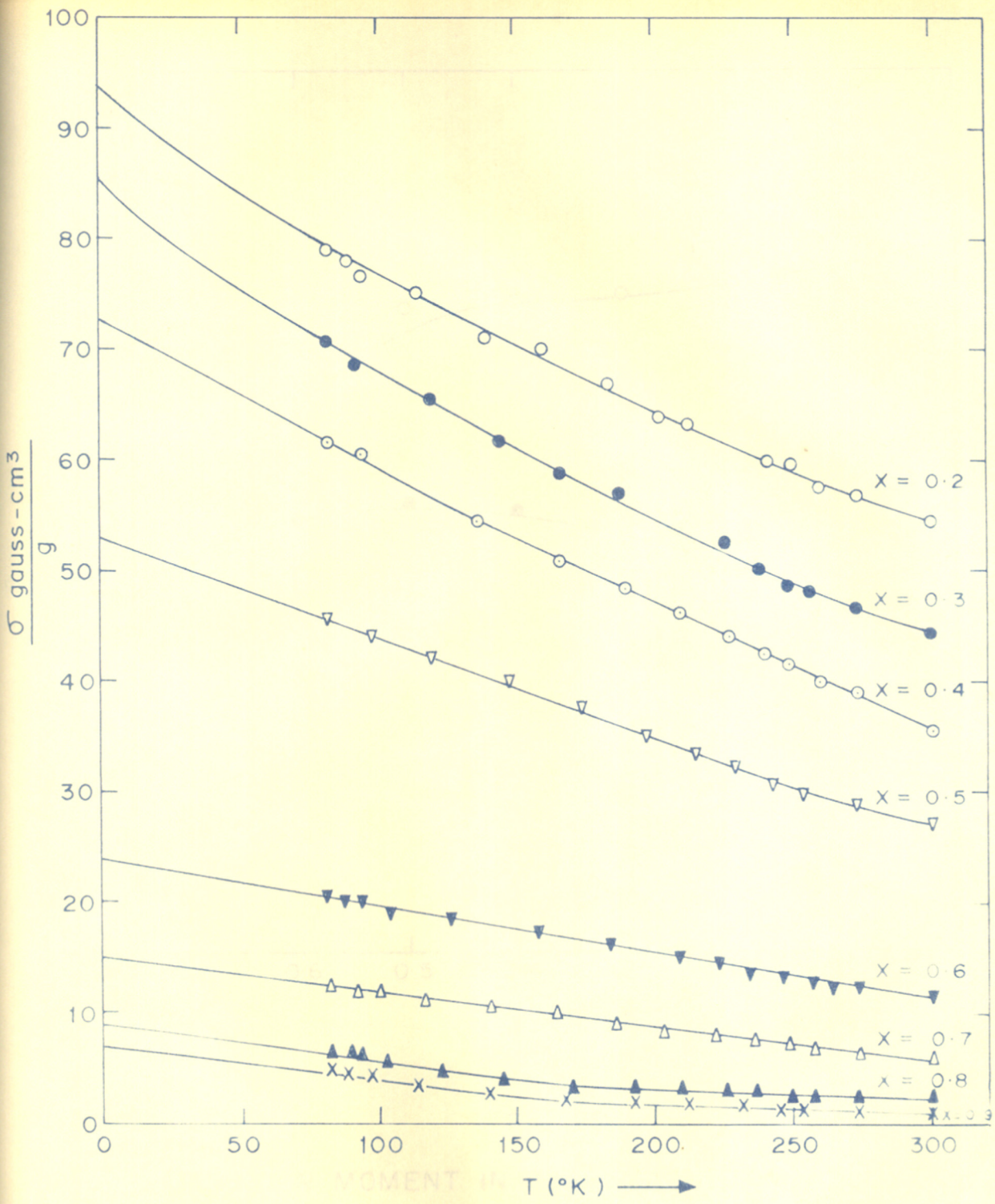

FIG. 28. SATURATION MAGNETIZATION PER GRAM 'σ' AS A FUNCTION OF TEMPERATURE 'T' FOR THE SYSTEM $Cu_x Mn_{1+x} Fe_{2-2x} O_4$

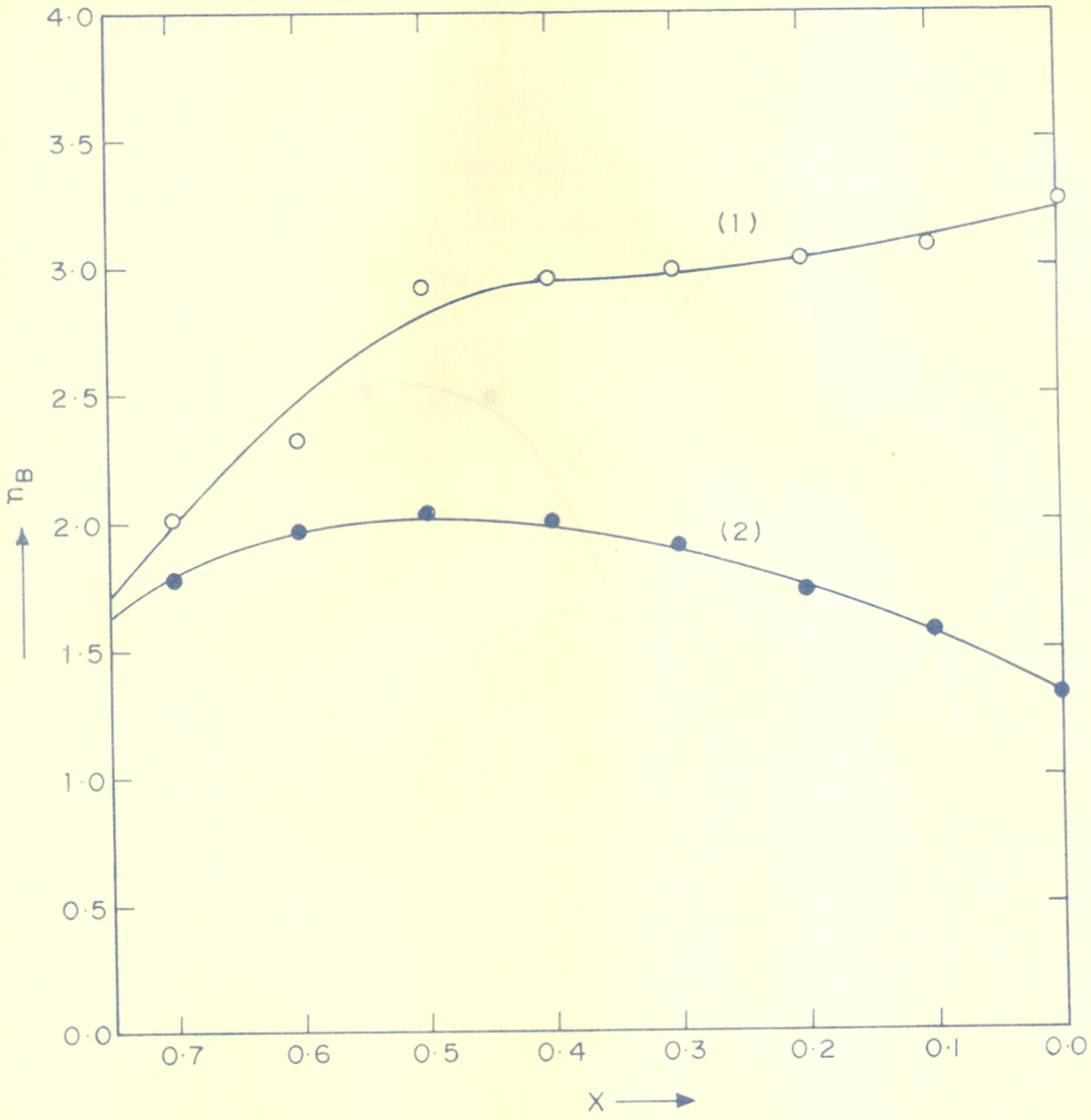

FIG. 29.

SATURATION MOMENT IN BOHR MAGNETONS 'n_B' AT 0 °K FOR MIXED CRYSTAL SERIES.

(1) $Cu_xCo_{1-x}Mn_{2x}Fe_{2-2x}O_4$

(2) $CuMn_{2x}Fe_{2-2x}O_4$

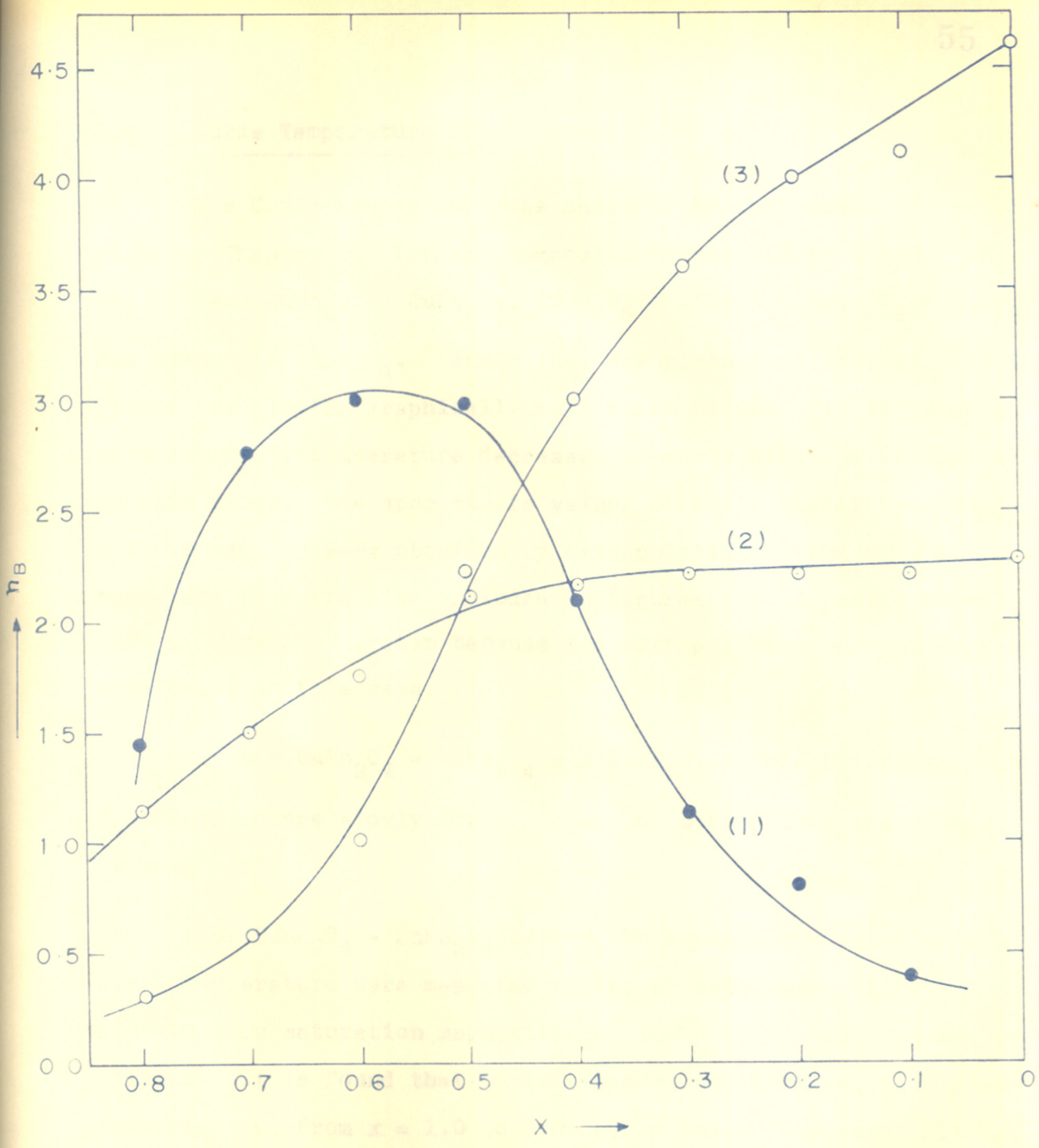

FIG. 30.

SATURATION MOMENT IN BOHR MAGNETONS 'n_B' AT 0 °K FOR MIXED CRYSTAL SERIES

1) $Cu_xZn_{1-x}Mn_{2x}Fe_{2-2x}O_4$
2) $Cu_xNi_{1-x}Mn_{2x}Fe_{2-2x}O_4$
3) $Cu_xMn_{1+x}Fe_{2-2x}O_4$.

3.2. Curie Temperature (T_c)

The Curie temperature was measured by the method described earlier (Chapter II) for the compositions x = 0.0 to x = 0.7 of the systems $CuMn_2O_4$ - $CuFe_2O_4$, $CuMn_2O_4$ - $NiFe_2O_4$, $CuMn_2O_4$ - $CoFe_2O_4$ and $CuMn_2O_4$ - $MnFe_2O_4$. The values are given in Tables 10, 11, 12, 14 and are plotted graphically in Figures 31 and 32. It is seen that the Curie temperature decreases linearly with increasing 'x' in this range. The approximate values of Curie temperature for x = 0.8 and 0.9 were obtained by extrapolation of the σ - T curve and they are also included in figures for all cases except $CuMn_2O_4$ - $CuFe_2O_4$ system because the extrapolation was not very conclusive in this case.

In the $CuMn_2O_4$ - $NiFe_2O_4$ and $CuMn_2O_4$ - $MnFe_2O_4$ systems the T_c values change slowly for $x < 0.7$ but beyond this, the change is very rapid.

For $CuMn_2O_4$ - $ZnFe_2O_4$ system the approximate value of the Curie temperature were measured by the extrapolation of σ - T plot to zero saturation magnetization ($\sigma = 0$) for all the compositions. It is found that Curie temperature increases slowly as 'x' decreases from x = 1.0 to 0.5 beyond which it starts falling. The plot of T_c vs x is shown in Figure 33.

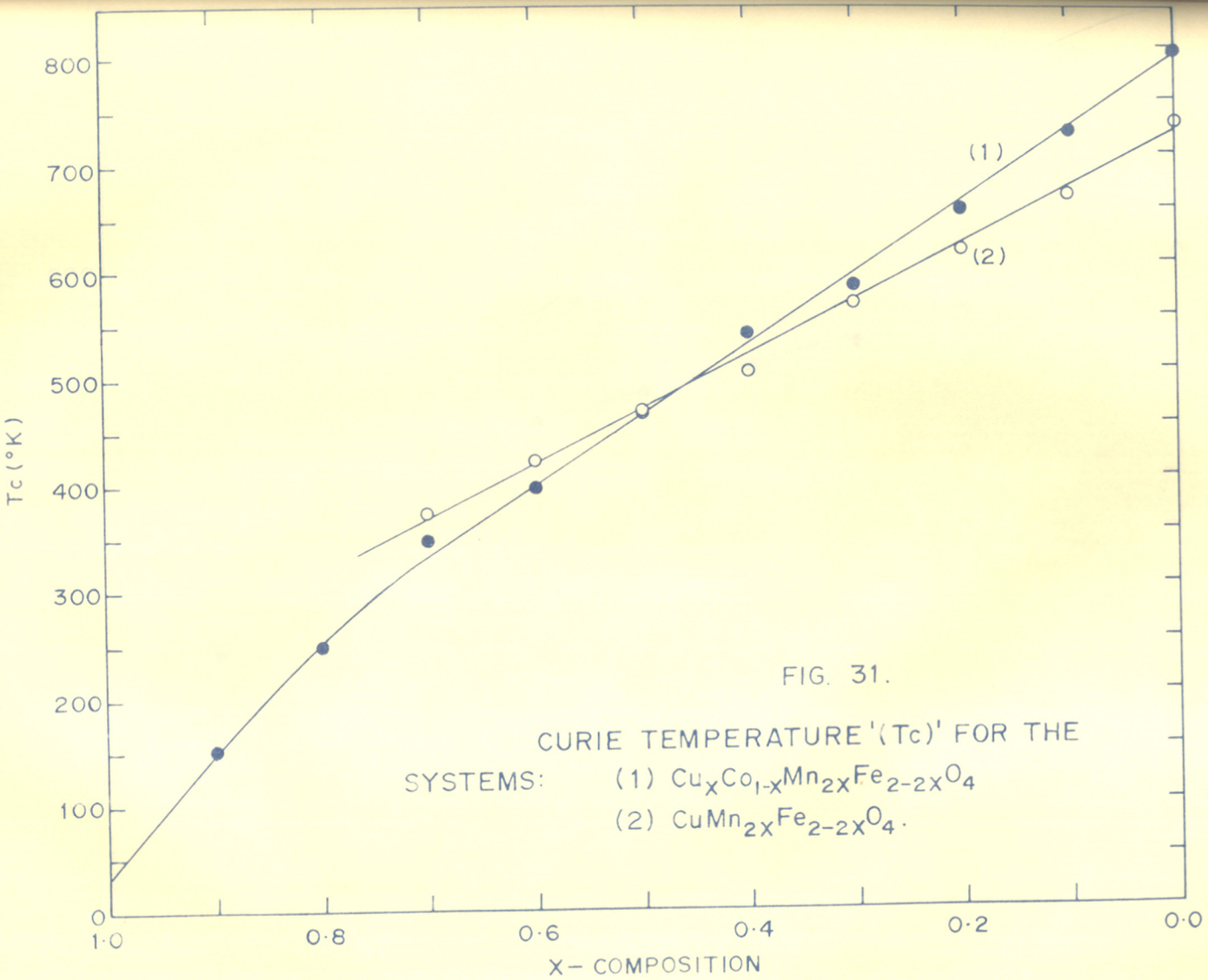

FIG. 31.

CURIE TEMPERATURE '(Tc)' FOR THE SYSTEMS: (1) $Cu_xCo_{1-x}Mn_{2x}Fe_{2-2x}O_4$

(2) $CuMn_{2x}Fe_{2-2x}O_4$.

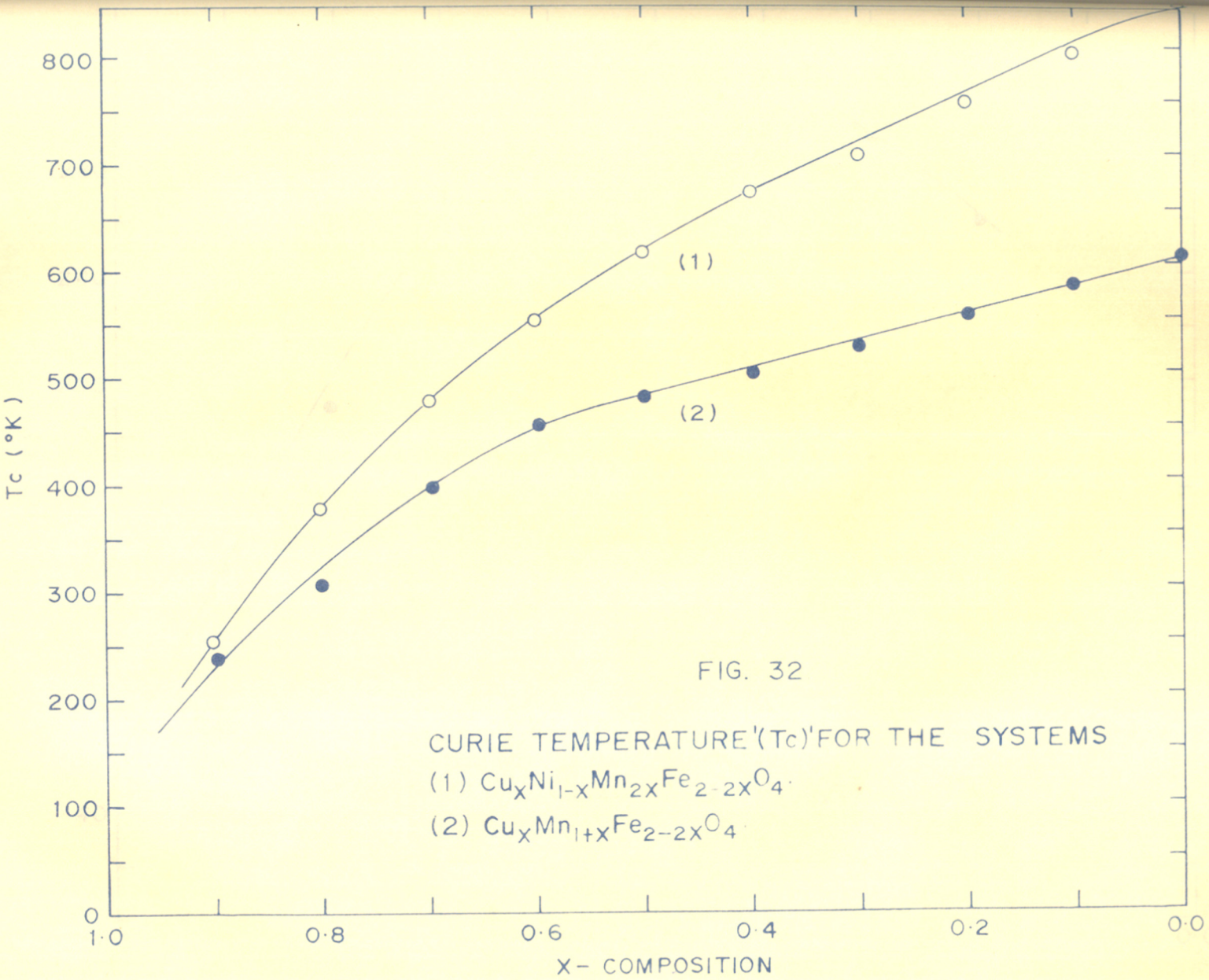

FIG. 32

CURIE TEMPERATURE '(Tc)' FOR THE SYSTEMS

(1) $Cu_xNi_{1-x}Mn_{2x}Fe_{2-2x}O_4$

(2) $Cu_xMn_{1+x}Fe_{2-2x}O_4$

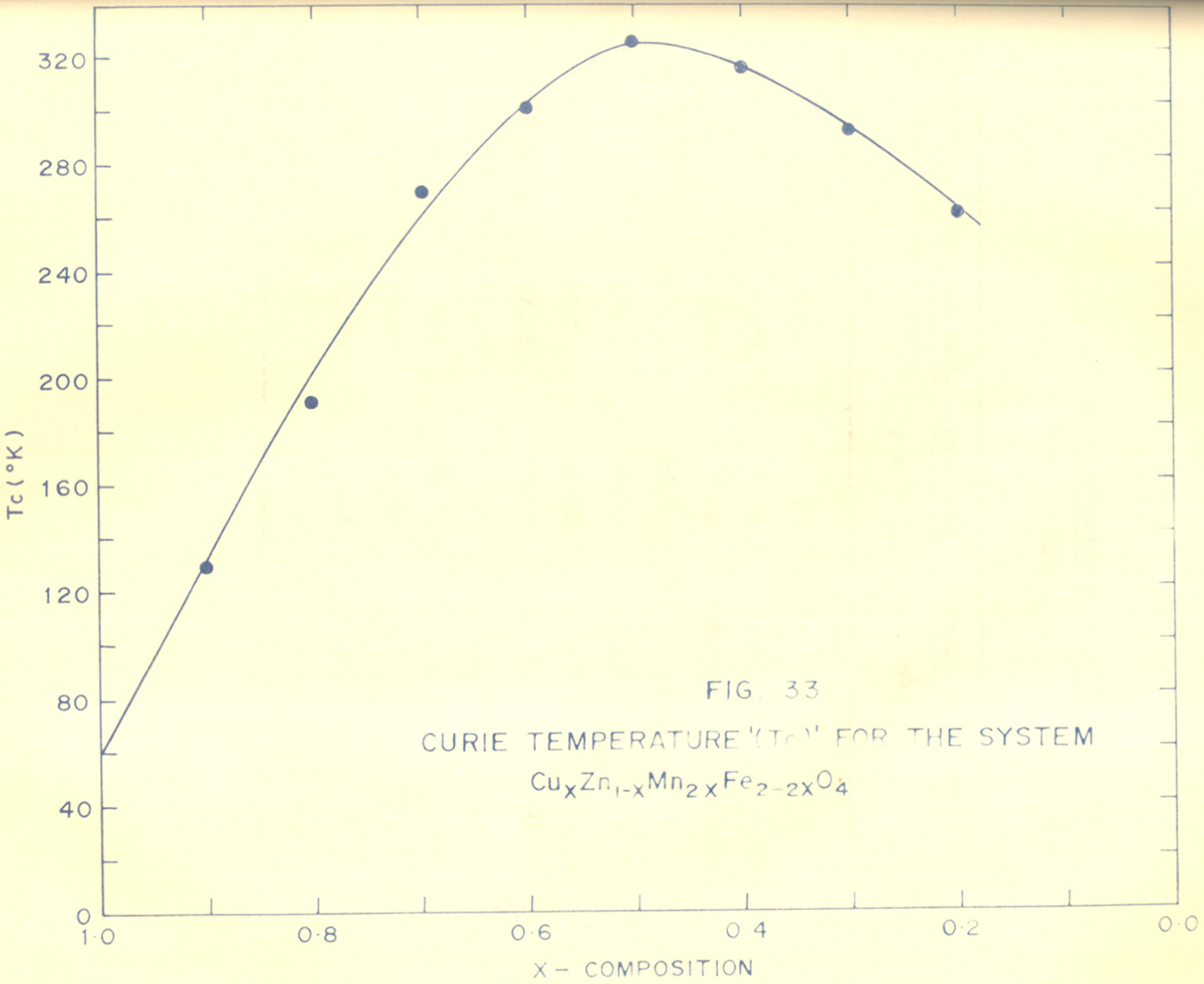

FIG. 33

CURIE TEMPERATURE ('Tc') FOR THE SYSTEM

$Cu_xZn_{1-x}Mn_{2x}Fe_{2-2x}O_4$

Table - 10

Copper manganite - Copper ferrite

$CuMn_2O_4$ - $CuFe_2O_4$ ($CuMn_{2x}Fe_{2-2x}O_4$)

Composition 'x'	σ gauss-cm^3/g, T = 300°K	σ gauss-cm^3/g, T = 77°K	σ gauss-cm^3/g, T = 0°K	n_B ($\frac{\sigma_{T=0^\circ K} \times M}{5585}$)	Curie Temp. (T_c)°K
1.0	0.48	5.2	15.00	0.68	25
0.9	0.96	4.06	10.00	0.425	100
0.8	6.8	7.78	8.50	0.431	150
0.7	15.8	28.6	41.00	1.74	373
0.6	19.4	34.75	46.25	1.97	419
0.5	24.5	39.35	45.50	1.947	468
0.4	27.35	40.30	47.00	2.00	500
0.3	31.16	42.0	45.50	1.94	568
0.2	30.35	38.65	40.75	1.74	612
0.1	30.35	36.50	37.50	1.61	662
0	25.30	29.35	31.20	1.33	729

Table - 11

Copper manganite - Nickel ferrite

$CuMn_2O_4$ - $NiFe_2O_4$ ($Cu_xNi_{1-x}Mn_{2x}Fe_{2-2x}O_4$)

Composition 'x'	σ gauss-cm^3/g at T = 300°K	σ gauss-cm^3/g at T = 82°K	σ gauss-cm^3/g at T = 0°K	$n_B = \frac{(\text{molecular wt.}) \times \sigma_{(T=0^\circ K)}}{5585}$	Curie temp. (T_c)°K
0.9	0.39	9.57	11.50	0.50	250
0.8	8.72	24.27	26.50	1.13	375
0.7	18.48	33.45	38.50	1.50	475
0.6	25.10	39.79	41.50	1.76	551
0.5	32.94	45.68	50.00	2.12	614
0.4	34.89	46.26	50.00	2.116	679
0.3	39.93	48.49	52.50	2.20	701
0.2	43.63	49.87	52.50	2.20	747
0.1	47.02	51.10	52.50	2.20	793
0.0	51.52	53.70	55.50	2.30	858

Table - 12

Copper Manganite -Cobalt ferrite

$CuMn_2O_4$ - $CoFe_2O_4$ ($Cu_xCo_{1-x}Mn_{2x}Fe_{2-2x}O_4$)

Composition 'x'	σ gauss-cm^3/g T = 300°K	σ gauss-cm^3/g T = 82°K	σ gauss-cm^3/g T = 0°K	n_B ($\sigma_{T=0^oK} \times M$ / 5585)	Curie temp. (T_c)°K
0.9	1.70	10.02	21.50	0.92	150
0.8	7.46	20.65	30.00	1.30	250
0.7	16.55	39.04	47.00	2.01	350
0.6	25.79	47.52	54.50	2.32	393
0.5	38.90	60.67	69.50	2.95	477
0.4	46.90	63.78	70.00	2.97	538
0.3	55.86	67.50	71.00	3.00	578
0.2	61.85	68.71	71.50	3.016	648
0.1	66.09	71.22	73.00	3.10	720
0.0	67.04	74.52	78.00	3.30	796

Table - 13

Copper manganite - Zinc ferrite

$CuMn_2O_4$ - $ZnFe_2O_4$ ($Cu_xZn_{1-x}Mn_{2x}Fe_{2-2x}O_4$)

Composition 'x'	σ gauss-cm^3/g T = 300°K	σ gauss-cm^3/g T = 82°K	σ gauss-cm^3/g T = 0°K	n_B ($\sigma_{T=0°K} \times M$)/5585	Curie temp. (T_c)°K
0.9	0.66	7.88	11.00	0.47	130
0.8	1.11	30.42	34.00	1.45	190
0.7	1.39	55.85	64.00	2.78	270
0.6	6.55	61.12	70.00	3.01	300
0.5	10.55	60.37	70.00	3.00	320
0.4	5.32	43.24	48.50	2.10	310
0.3	2.39	22.27	26.50	1.14	290
0.2	1.22	15.63	19.50	0.84	260
0.1	0.75	6.22	9.00	0.39	-

Table - 14

Copper manganite - Manganese ferrite

$CuMn_2O_4$ - $MnFe_2O_4$ ($Cu_xMn_{1+x}Fe_{2-2x}O_4$)

Composition 'x'	σ gauss-cm^3/g T = 300°K	σ gauss-cm^3/g T = 82°K	σ gauss-cm^3/g T = 0°K	n_B ($\sigma_{T=0^\circ K} \times M / 5585$)	Curie temp. (T_c)°K
0.9	1.08	5.2	7.00	0.30	235
0.8	2.70	6.67	8.50	0.36	305
0.7	6.08	12.45	15.00	0.63	390
0.6	11.65	20.45	24.00	1.01	450
0.5	27.40	45.50	53.00	2.23	480
0.4	35.53	61.41	72.50	3.04	498
0.3	44.58	71.00	86.50	3.61	523
0.2	54.76	78.98	96.00	4.00	556
0.1	58.68	81.81	99.50	4.10	583
0.0	61.41	82.19	112	4.62	603

3.3. Electrical conductivity

The A.C. electrical resistivity (ρ) of the circular pellets of composition $x = 0.3, 0.5, 0.7, 0.8$ and 0.9 for the systems $CuMn_2O_4$ - $CuFe_2O_4$, $CuMn_2O_4$ - $NiFe_2O_4$, $CuMn_2O_4$ - $CoFe_2O_4$ and $CuMn_2O_4$ - $MnFe_2O_4$ and $x = 0.3, 0.5, 0.6, 0.7$ and 0.9, for the $CuMn_2O_4$ - $ZnFe_2O_4$ system were measured at various temperatures in the range between 34°C to 450°C. The log ρ values were plotted against the reciprocal of the absolute temperature T (Figs. 34, 35, 36, 37, 38 and 39). The specific resistivity values at room temperature for different compositions are given in column 1 of Tables 15, 16, 17, 18 and 19.

The activation energy value ΔE in e.v. was calculated from the equation $\rho = \rho_0 \exp \frac{\Delta E}{kT}$. The values of ΔE in paramagnetic and ferromagnetic region are given in Tables 15, 16, 17, 18 and 19 in columns 2 and 3 together with the values of log ρ_0 (columns 4 and 5). It is observed that there is a break in the log ρ vs 1/T plot at the Curie temperature for the compounds which are ferromagnetic above room temperature.

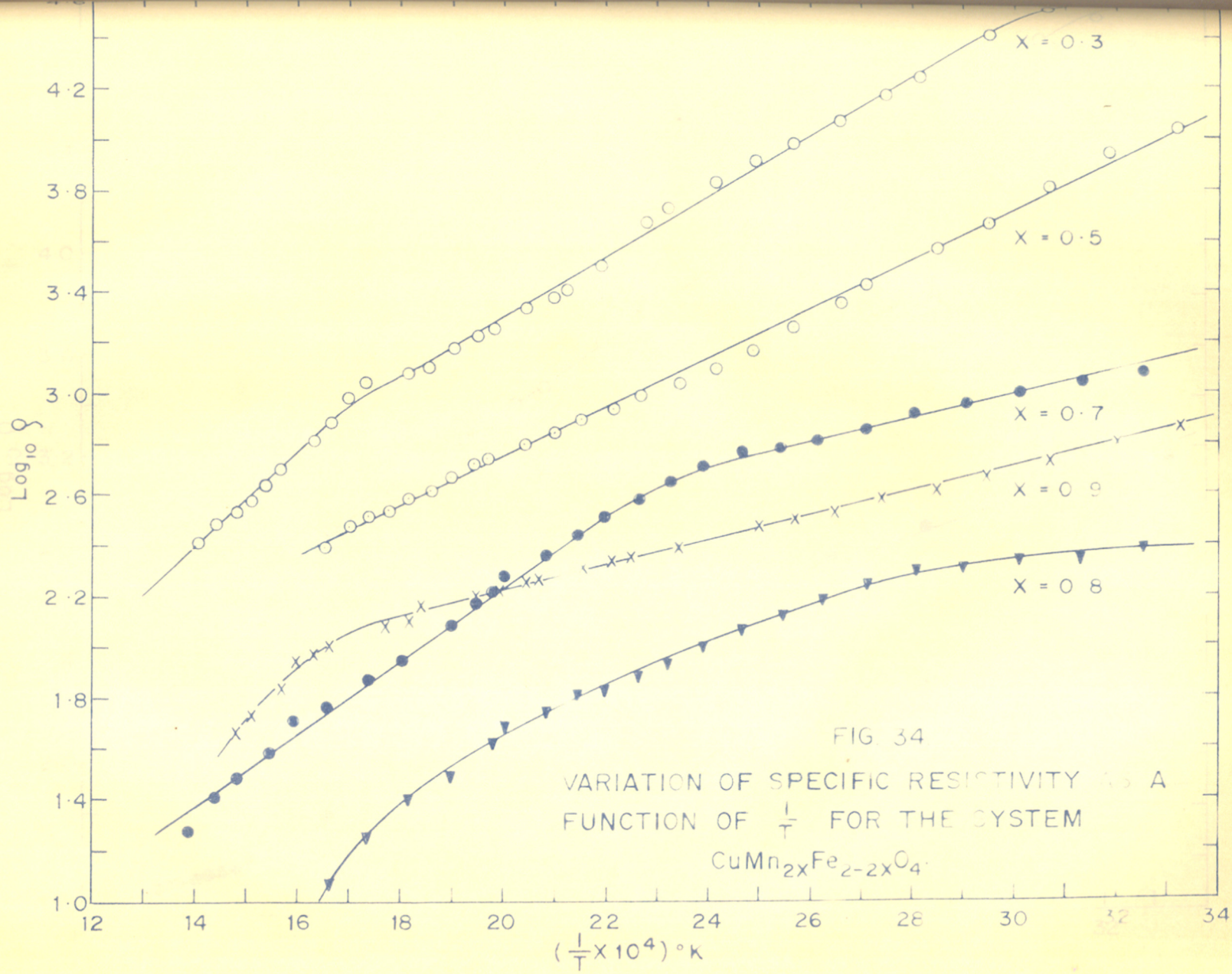

FIG. 34

VARIATION OF SPECIFIC RESISTIVITY AS A FUNCTION OF $\frac{1}{T}$ FOR THE SYSTEM $CuMn_{2x}Fe_{2-2x}O_4$

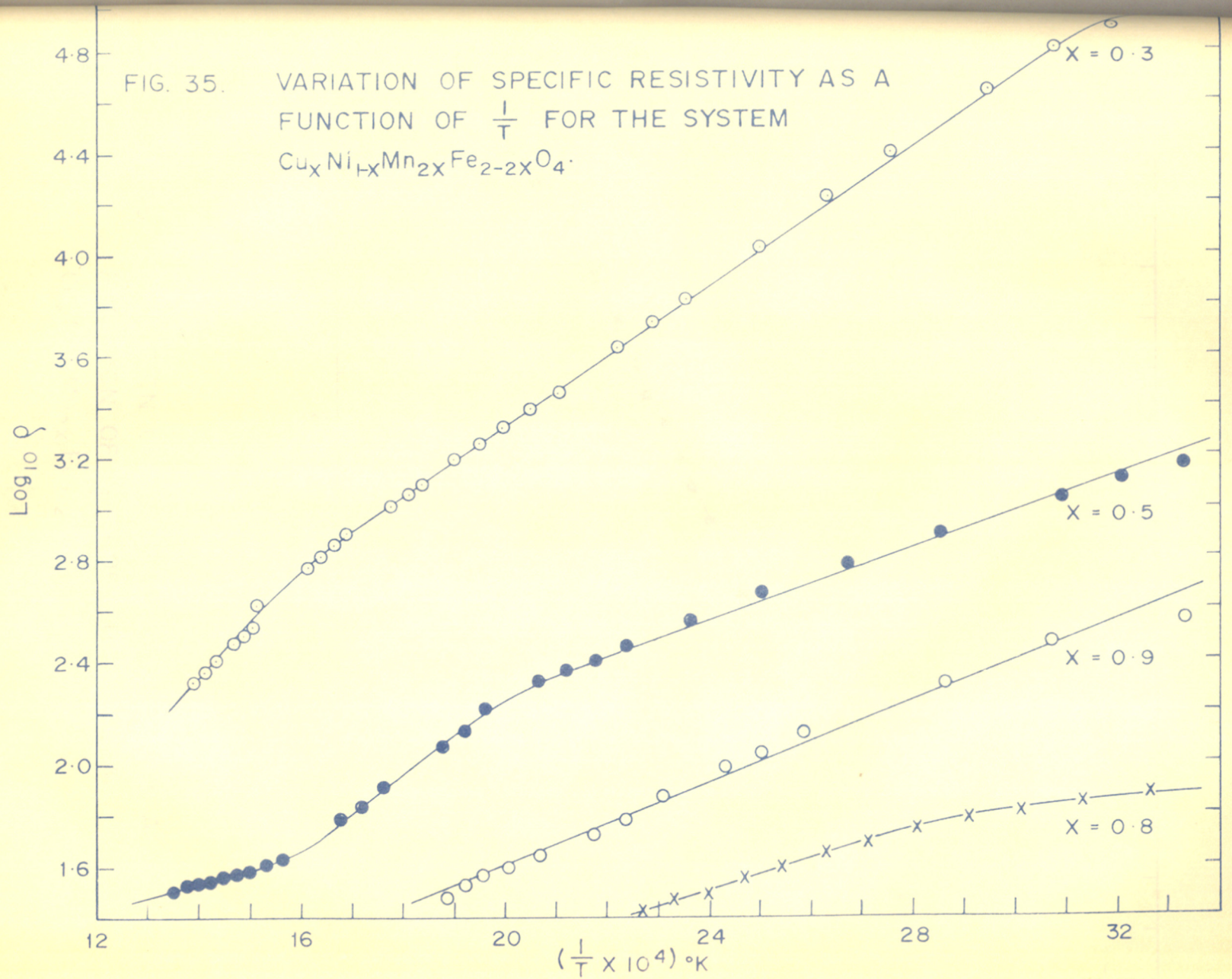
FIG. 35. VARIATION OF SPECIFIC RESISTIVITY AS A FUNCTION OF $\frac{1}{T}$ FOR THE SYSTEM $Cu_xNi_{1-x}Mn_{2x}Fe_{2-2x}O_4$.
X = 0·3
X = 0·5
X = 0·9
X = 0·8
$Log_{10}\rho$
4·8
4·4
4·0
3·6
3·2
2·8
2·4
2·0
1·6
12
16
20
24
28
32
$(\frac{1}{T} \times 10^4)\,°K$

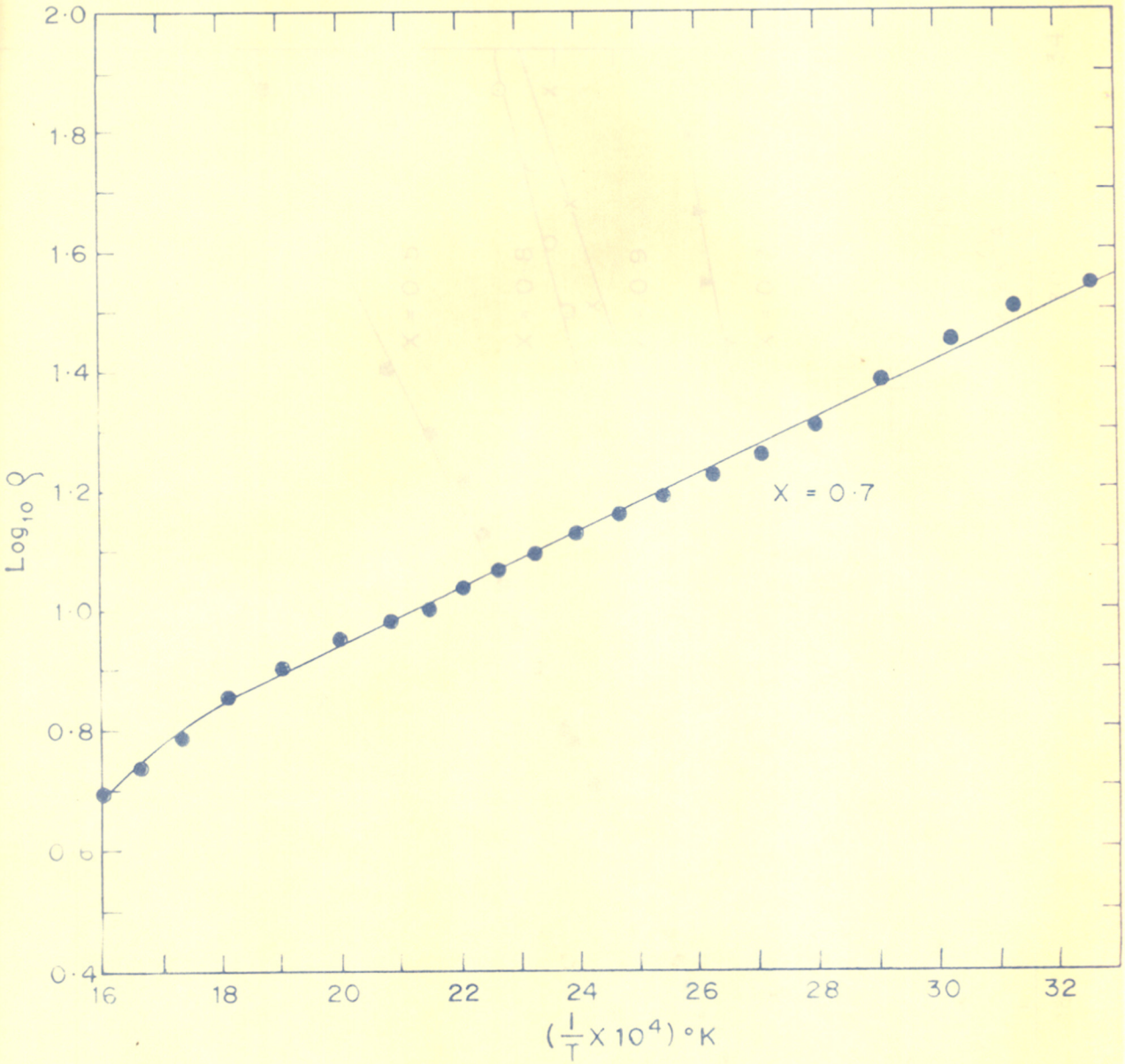

FIG 36. VARIATION OF SPECIFIC RESISTIVITY AS A FUNCTION OF $\frac{1}{T}$ FOR THE SYSTEM $Cu_xNi_{1-x}Mn_{2x}Fe_{2-2x}O_4$

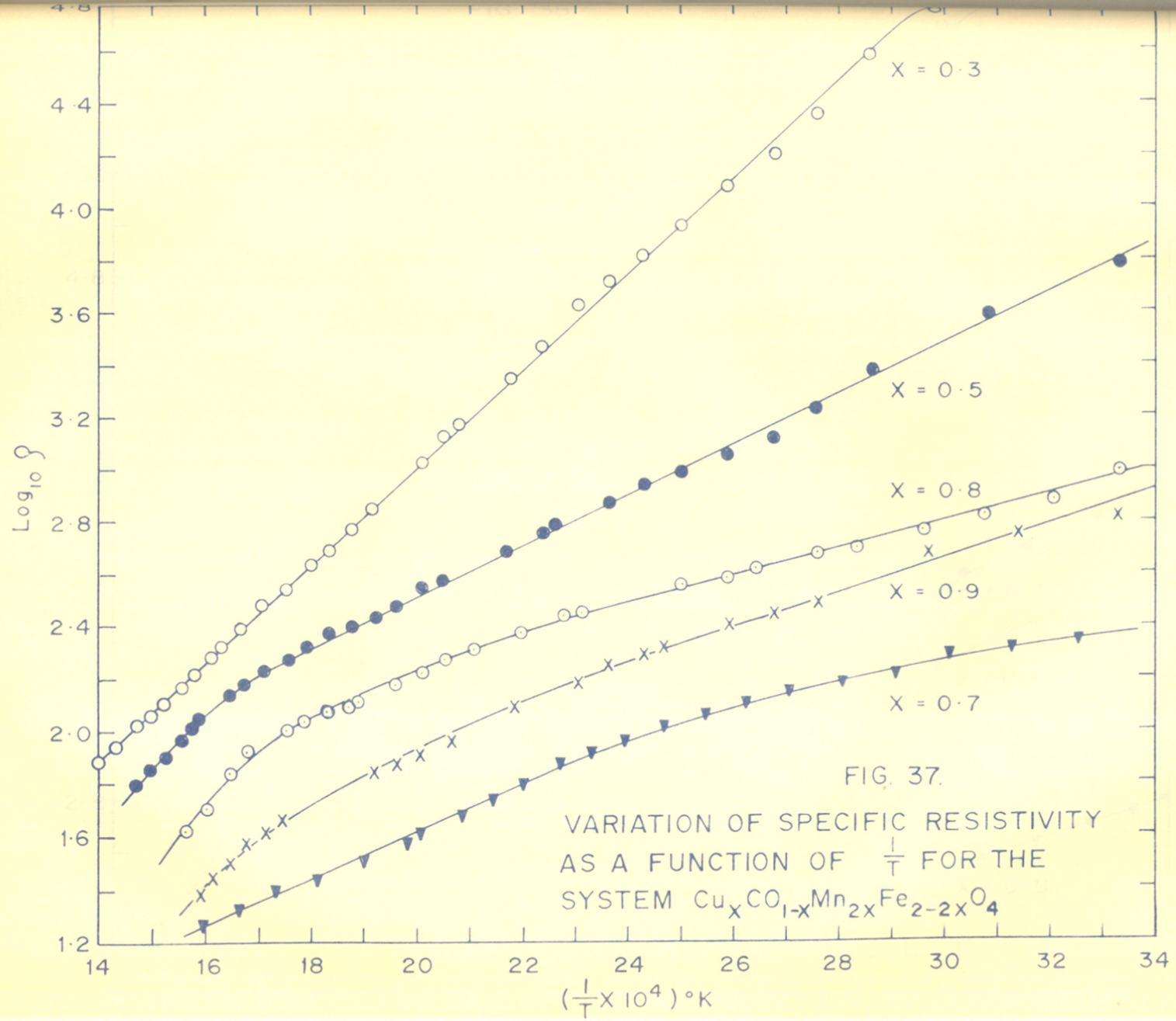

FIG. 37.

VARIATION OF SPECIFIC RESISTIVITY AS A FUNCTION OF $\frac{1}{T}$ FOR THE SYSTEM $Cu_xCO_{1-x}Mn_{2x}Fe_{2-2x}O_4$

FIG. 38.

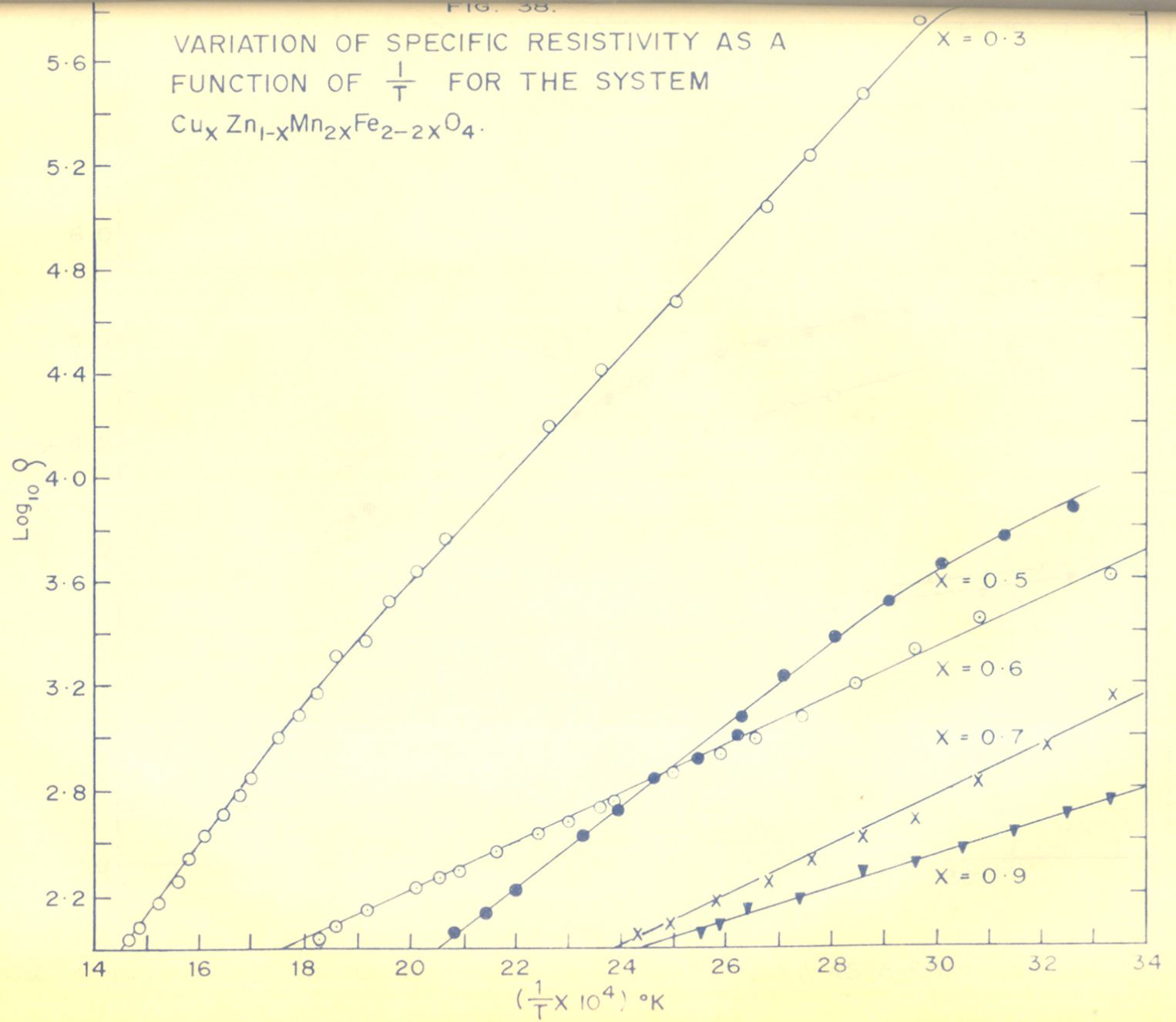
VARIATION OF SPECIFIC RESISTIVITY AS A FUNCTION OF 1/T FOR THE SYSTEM
Cu$_x$ Zn$_{1-x}$Mn$_{2x}$Fe$_{2-2x}$O$_4$.
X = 0·3
X = 0·5
X = 0·6
X = 0·7
X = 0·9
Log$_{10}$ ρ
5·6
5·2
4·8
4·4
4·0
3·6
3·2
2·8
2·2
14
16
18
20
22
24
26
28
30
32
34
(1/T X 10^4) °K

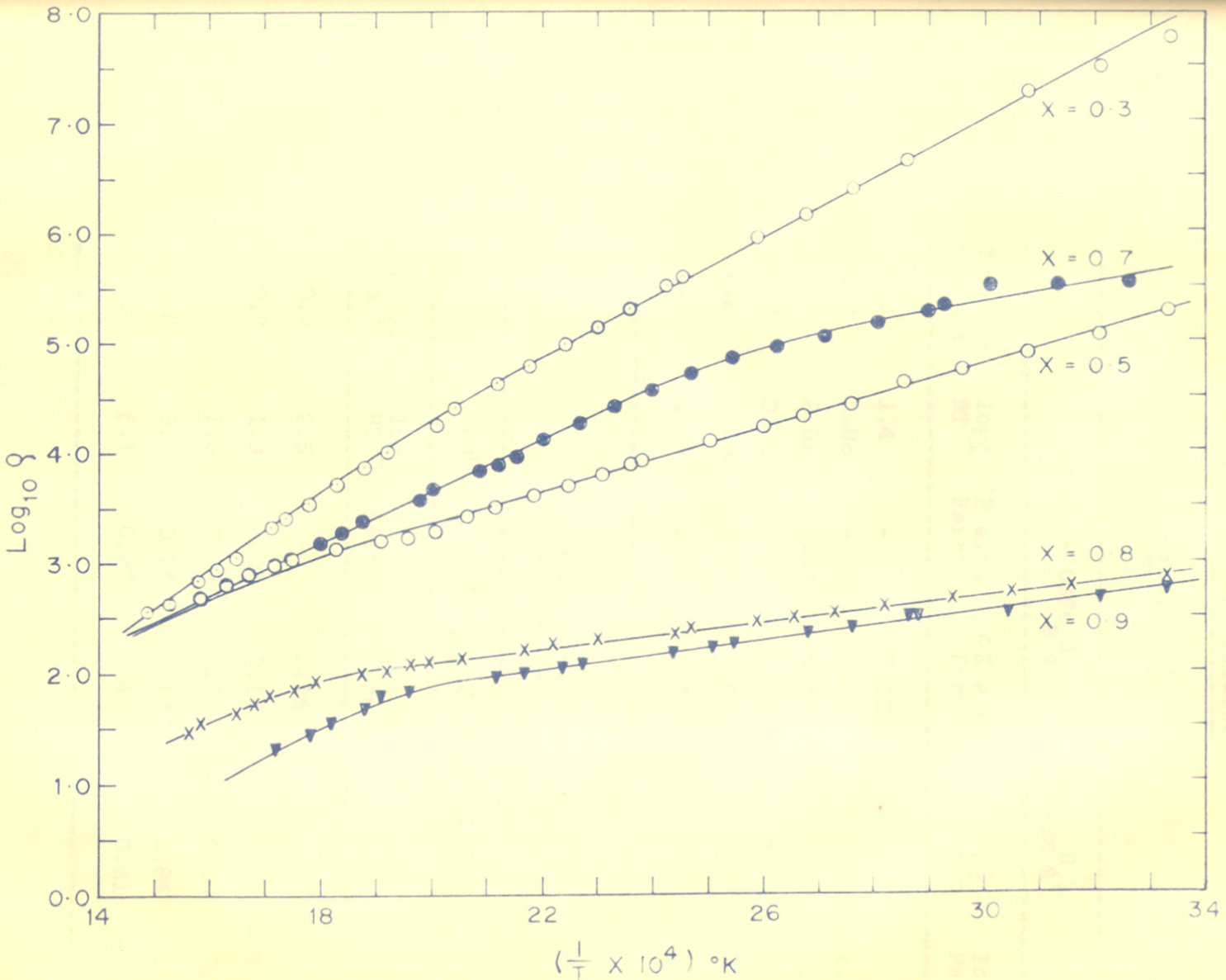

FIG. 39. VARIATION OF SPECIFIC RESISTIVITY AS A FUNCTION OF $\frac{1}{T}$ FOR THE SYSTEM $Cu_x Mn_{1+x} Fe_{2-2x} O_4$.

Conductivity results

Table - 15

$CuMn_2O_4$ - $CuFe_2O_4$ ($CuMn_{2x}Fe_{2-2x}O_4$)

Composition 'x'	$\log \rho$ RT	ΔE e.v. Ferro	ΔE e.v. Para	$\log \rho$ Ferro	$\log \rho$ Para
1.0	1.4	-	0.26	-	-
0.9	2.86	-	0.10	-	1.2
0.8	2.39	0.04	0.16	1.80	0.03
0.7	3.08	0.10	0.28	1.50	- 0.6
0.5	4.06	0.18	0.20	1.0	0.8
0.3	4.85	0.23	0.37	1.0	- 0.2

Table - 16

$CuMn_2O_4$ - $NiFe_2O_4$ ($Cu_xNi_{1-x}Mn_{2x}Fe_{2-2x}O_4$)

Composition 'x'	$\log \rho$ RT	ΔE e.v. Ferro	ΔE e.v. Para	$\log \rho$ Ferro	$\log \rho$ Para
0.9	2.5	-	0.16	-	0.02
0.8	1.9	0.07	0.14	0.79	- 0.1
0.7	1.5	0.09	0.09	0.09	0.6
0.5	3.2	0.14	0.13	0.84	0.60
0.3	5.1	0.27	0.46	0.61	-0.9

Conductivity results

Table 17

$CuMn_2O_4$ - $CoFe_2O_4$ ($Cu_xCo_{1-x}Mn_{2x}Fe_{2-2x}O_4$)

Composition 'x'	$\log \rho$ RT	ΔE e.v. Ferro	ΔE e.v. para	$\log_{10} \rho_o$ Ferro	$\log_{10} \rho_o$ Para
0.9	2.8	-	0.13	-	0.6
0.8	3.0	-	0.11	-	0.9
0.7	2.3	0.02	0.17	2.0	- 0.1
0.5	3.8	0.18	0.22	2.5	0.3
0.3	5.4	0.36	0.41	- 0.5	1.0

Table 18

$CuMn_2O_4$ - $ZnFe_2O_4$ ($Cu_xZn_{1-x}Mn_{2x}Fe_{2-2x}O_4$)

Composition 'x'	$\log \rho$ RT	ΔE e.v. Ferro	ΔE e.v. Para	$\log_{10} \rho_o$ Ferro	$\log_{10} \rho_o$ Para
0.9	2.7	-	0.13	-	0.70
0.7	3.2	-	0.19	-	-0.1
0.6	3.6	-	0.18	-	0.6
0.5	3.9	0.18	0.31	1.0	- 1.0
0.3	6.4	-	0.43	-	- 0.7

Conductivity results

Table 19

$CuMn_2O_4$ - $MnFe_2O_4$ ($Cu_xMn_{1+x}Fe_{2-2x}O_4$)

Composition 'x'	$\log_{10}\rho$ RT	ΔE e.v. Ferro	ΔE e.v. Para	$\log_{10}\rho$ Ferro	$\log_{10}\rho$ Para
0.9	2.8	-	0.14	-	0.6
0.8	2.9	-	0.12	-	0.9
0.7	5.5	0.06	0.47	4.6	- 1.0
0.5	5.3	0.28	0.53	0.6	- 1.5
0.3	7.7	0.53	0.71	- 1.1	- 2.8

3.4. Thermoelectric coefficient

The thermoelectric coefficient for the compositions x = 0.9, 0.8, 0.7 of the systems $CuMn_2O_4$ - $CoFe_2O_4$, $CuMn_2O_4$ - $MnFe_2O_4$; x = 0.9, 0.8 of $CuMn_2O_4$ - $NiFe_2O_4$, and x = 0.9, 0.7 of $CuMn_2O_4$ - $ZnFe_2O_4$ were measured at different temperatures in the range room temperature to 200°C. The conduction in all these cases was found to be p-type. The values of the thermoelectric coefficient S and ST are given in Tables 20 to 24 in columns 5 and 6.

The thermoelectric coefficient S rises as 'x' decreases in case of $CuMn_2O_4$ - $NiFe_2O_4$, $CuMn_2O_4$ - $CoFe_2O_4$ and $CuMn_2O_4$ - $MnFe_2O_4$ and decreases with 'x' in case of $CuMn_2O_4$ - $CuFe_2O_4$ and remains nearly constant in case of $CuMn_2O_4$ - $ZnFe_2O_4$.

It is observed that the thermoelectric coefficient is nearly independent of temperature for all the samples.

Table 20

Thermoelectric coefficient of $Cu_xNi_{1-x}Mn_{2x}Fe_{2-2x}O_4$ as a function of temperature

(Type of conduction p type)

Composition x = 0.9

t_1^oC	t_2^oC	T^oK	$T_{e.m.f.}$ in microvolts	S microvolts/degree	ST volts
77.5	83.5	353.5	400	66	0.023
100	109.25	377.62	590	64	0.024
107.5	117.5	385.5	650	65	0.025

Composition x = 0.8

107.5	122.5	388	1640	109	0.042
109.5	122.5	389	1470	113	0.044
134	151.5	415.75	1750	100	0.042
147	165.75	424.37	2000	106	0.045

t_1 = Temperature of the cold end.

t_2 = Temperature of the hot end.

Table - 21

Thermoelectric coefficient of $Cu_xCo_{1-x}Mn_{2x}Fe_{2-2x}O_4$ as a function of temperature

(Type of conduction : p type)

Composition x = 0.9

t_1^oC	t_2^oC	T^oK	$T_{e.m.f.}$ in micro-volts	S microvolts/ degree	ST volts
100	125	385.5	1500	60.0	0.023
130	157.5	416.75	1620	59.0	0.025
140	172.5	429.25	2200	67.0	0.029

Composition x = 0.8

115	127	395.25	760	61	0.024
115	137	399.25	1400	62	0.025
117.5	147.5	405.5	1000	61	0.025
140	150	418.0	671	67	0.028

Composition x = 0.7

169	206	460.5	2400	65	0.030
174	214	467.0	2500	63	0.029

Table - 22

Thermoelectric coefficient of $CuMn_{2x}Fe_{2-2x}O_4$ as a function of temperature

(Type of conduction : p type)

t_1^oC	t_2^oC	T^oK	$T_{e.m.f.}$ in micro-volts	S microvolts/ degree	ST volts
			Composition x = 0.9		
131	153.5	415.25	1700	76	0.031
167.5	185	449	1460	82	0.037
158	175.5	436.75	1440	82	0.036
			Composition x = 0.8		
40.5	46.5	316.5	400	67	0.021
117	139.5	401.25	1500	67	0.027
127	153.0	413.0	1700	65	0.027
191.5	209	473	1200	68	0.032
			Composition x = 0.7		
141.5	161.25	426.37	1460	62	0.026
154.25	177.0	438.6	1440	63	0.028
159.0	181.5	447.25	1460	65	0.029

Table - 23

Thermoelectric coefficient of $Cu_xZn_{1-x}Mn_{2x}Fe_{2-2x}O_4$ as a function of temperature

(Type of conduction : p type)

t_1^oC	t_2^oC	T^oK	$T_{e.m.f.}$ in micro-volts	S microvolts/ degree	ST volts
			Composition x = 0.9		
105	91.5	371	480	35	0.013
130	110	391	750	38	0.015
147	125	409	860	39	0.016
165	140.5	425	1000	40	0.017
180	147.5	436	1290	40	0.017
			Composition x = 0.7		
87	76.5	355	370	35	0.012
165	140	425	970	38	0.016
177	146	434	1120	36	0.016
182.5	155	442	1100	40	0.017
180	153	440	1080	40	0.018

Table - 24

Thermoelectric coefficient of $Cu_xMn_{1+x}Fe_{2-2x}O_4$ as a function of temperature

(Type of conduction: p type)

t_1^oC	t_2^oC	T^oK	$T_{e.m.f.}$ in micro-volts	S microvolts/ degree	ST volts
			Composition x = 0.9		
112	130	394	900	50	0.020
118	129	396.5	600	54	0.021
124	134	402	526	53	0.021
			Composition x = 0.8		
82	72.5	350	390	41.1	0.014
87.5	77	355	433	41	0.015
130.3	112	394	825	45	0.018
145	123	407	1000	44.8	0.018
192.5	160	449	1500	48.6	0.022
			Composition x = 0.7		
82.7	75	352	420	54	0.019
130.3	115	396	895	58.3	0.023
133.0	117	398	940	59	0.024
158	137.7	421	1200	58	0.025
172.8	150	434	1435	62	0.027

3.5. X-ray analysis

The x-ray diffraction patterns of the following selected compounds were taken using Mo-K_α radiation on a 14 cm. Debye-Scherrer Camera:

(i) $CuMn_2O_4$ - $CuFe_2O_4$: system x = 1.0, 0.6, 0.5, 0.3 and 0.2.

(ii) $CuMn_2O_4$ - $NiFe_2O_4$: system x = 0.5, 0.7 and 0.9.

(iii) $CuMn_2O_4$ - $MnFe_2O_4$: system x = 0.4 and 0.7.

The structure for the composition x = 0.7 in the $CuMn_2O_4$-$MnFe_2O_4$ series is tetragonal and all the other compounds are cubic. The unit cell values for cubic compounds were obtained using the formula $a = \frac{d}{\sqrt{h^2 + k^2 + l^2}}$. The a & c values for the tetragonal compound were calculated by successive refinements. The diffraction lines were quite broad hence the unit cell parameters could not be determined to an accuracy better than $\pm$ 0.02. The observed 'd' values and the intensities of the reflections for the various compounds are given in Tables 25 to 34, together with the calculated values of the lattice parameters. It is clear from the unit cell parameters, the absent reflections and the intensities of the various reflections, that the cubic compounds are isomorphous with spinel structure and the tetragonal compound is isomorphous with the hausmannite structure.

Table - 25

X-ray results for $CuMn_{2x}Fe_{2-2x}O_4$

Composition x = 1.0

hkl	Intensity	d(A^o)	Lattice parameter a(A^o)	
111	W	4.8201	8.35	
220	S	2.952	8.34	
311	V.S.	2.512	8.33	
222	W	2.405	8.33	
400	M	2.080	8.32	
331	-	-	-	a = 8.327Å
422	M	1.701	8.33	
511, 333	S	1.600	8.31	
440	S	1.472	8.32	
531	-	-	-	
620	V.W.	1.321	8.34	
533	M.S.	1.270	8.33	
444	V.V.W.	1.202	8.32	
711, 551	V.V.W.	1.167	8.33	
731, 553	M	1.083	8.32	

Table - 26

X-ray results for $CuMn_{2x}Fe_{2-2x}O_4$

Composition x = 0.6

hkl	Intensity	d(A^o)	Lattice parameter a(A^o)	
111	VVW	-	-	
220	M	2.984	8.44	
311	VS	2.548	8.44	
400	M	2.116	8.46	
422	VVW	-	-	a = 8.46Å
511,333	MS	1.626	8.45	
440	S	1.498	8.47	
533	M	1.292	8.47	
731, 553	W	1.103	8.47	
800	VVW	-	-	

Table - 27

X-ray results for $CuMn_{2x}Fe_{2-2x}O_4$

Composition x = 0.5

hkl	Intensity	d(A°)	Lattice parameter a(A°)	
111	VVW	4.865	8.42	
220	VW	2.973	8.40	
311	VVS	2.527	8.38	
222	VVW	2.430	8.41	
400	S	2.100	8.40	
331	-	-	-	a = 8.40Å
422	W	1.718	8.41	
511, 333	S	1.616	8.39	
440	VS	1.485	8.40	
531	-	-	-	
620	VVW	1.329	8.40	
533	VVW	1.282	8.40	
444	VVW	1.213	8.40	
711, 551	-	-	-	
642	VVW	1.124	8.41	
731, 553	VW	1.091	8.38	

Table - 28

X-ray results for $CuMn_{2x}Fe_{2-2x}O_4$

Composition x = 0.3

hkl	Intensity	d(A°)	Lattice parameter a(A°)	
220	S	2.9349	8.30	
400	MS	2.0751	8.30	
422	MS	1.6973	8.31	
511, 333	VS	1.6007	8.32	
440	VS	1.4721	8.33	a = 8.307Å
533	MS	1.2666	8.30	
800	VVW	1.0369	8.30	
751, 555	MS	0.95996	8.31	
840	VVW	0.92747	8.30	
844	MS	0.84802	8.30	

Table - 29

X-ray results for $CuMn_{2x}Fe_{2-2x}O_4$

Composition x = 0.2

hkl	Intensity	d(A°)	Lattice parameter a(A°)	
220	VS	2.9349	8.29	
311	VVS	2.4985	8.29	
400	MS	2.0668	8.27	
422	VVW	-	-	
511, 333	S	1.5970	8.30	
440	VS	1.4638	8.30	a = 8294Å
533	MS	1.2575	8.30	
731, 553	MS	1.0805	8.31	
800	VVW	1.0389	8.31	
751, 555	MS	0.9557	8.28	

Table - 30

X-ray results for $Cu_x Ni_{1-x} Mn_{2x} Fe_{2-2x} O_4$

Composition x = 0.9

hkl	Intensity	d(A°)	Lattice parameter a(A°)	
220	MS	2.9224	8.26	
311	VVS	2.4939	8.27	
400	MW	2.068	8.27	
422	MW	1.6918	8.29	
511, 333	MS	1.5958	8.29	a = 8.276Å
440	MS	1.4659	8.29	
533	MW	1.2575	8.25	
444	VW	1.1939	8.27	
731, 553	VW	1.0778	8.28	
751, 555	VVW	0.9591	8.29	

Table - 31

X-ray results for $Cu_x Ni_{1-x} Mn_{2x} Fe_{2-2x} O_4$

Composition x = 0.7

hkl	Intensity	d(A^o)	Lattice parameter a(A^o)	
220	S	2.9413	8.30	
311	VVS	2.5069	8.30	
222	VVW	2.3990	8.30	
400	VW	2.0730	8.29	
422	VVW	1.6918	8.28	
511, 333	MS	1.6007	8.30	
400	S	1.4608	8.29	
531	VVW	1.4022	8.29	a = 8.29A^o
622	VW	1.2523	8.30	
731, 553	MS	1.0767	8.28	
800	VW	1.0349	8.28	
751, 555	MW	0.9566	8.28	
931	MW	0.87052	8.30	
844	VVW	0.84546	8.28	

Table - 32

X-ray results for $Cu_xNi_{1-x}Mn_{2x}Fe_{2-2x}O_4$

Composition x = 0.5

hkl	Intensity	d(A^o)	Lattice parameter a(A^o)	
111	VVW	-	-	
220	W	2.982	8.43	
331	VS	2.540	8.43	
400	W	2.113	8.45	
422	VW	1.725	8.45	a = 8.44Å
511, 333	S	1.629	8.46	
440	S	1.490	8.43	
533	W	1.289	8.43	
731, 553	W	1.100	8.45	

Table - 33

X-ray results for $Cu_x Mn_{1+x} Fe_{2-2x} O_4$

Composition x = 0.7

hkl	Intensity	d(obs.)	d(cal.)	Lattice parameter
112	MS	2.97	2.99	
103	MS	2.64	2.63	
211	VS	2.46	2.46	a = 5.73 Å
220	VW	2.02	2.02	c = 8.87 Å
105	MS	1.68	1.70	a' = 8.09 Å
312			1.68	c' = 8.87 Å
321	MS	1.57	1.56	c'/a' = 1.10
224	MS	1.50	1.50	
400	VW	1.43	1.43	
413	W	1.26	1.26	

Table - 34

X-ray results for $Cu_x Mn_{1+x} Fe_{2-2x} O_4$

Composition x = 0.4

hkl	Intensity	d(A°)	Lattice parameter a(A°)	
220	MS	2.9733	8.41	
311	VVS	2.5293	8.39	
400	MW	2.0941	8.38	
422	MW	1.7113	8.38	
511, 333	MS	1.6168	8.40	
440	S	1.4825	8.39	
533	MW	1.2765	8.37	a = 8.39Å
444	VVW	1.2122	8.40	
731, 553	MW	1.0926	8.39	
800	VW	1.0489	8.39	
751, 555	VVW	0.96932	8.39	
931	VW	0.88053	8.40	
844	VVW	0.85581	8.39	

3.6. Permeability

The permeability μ for compositions x = 0.5, 0.4, 0.3 and 0.1 of the system $CuMn_2O_4$ - $MnFe_2O_4$, x = 0.5, 0.4, 0.3, 0.2 of $CuMn_2O_4$ - $NiFe_2O_4$ system and x = 0.5 and 0.6 of $CuMn_2O_4$ - $ZnFe_2O_4$, were measured. The values of μ, μQ are given in Tables 35 to 37. The permeability rises with decreasing 'x' in case of $CuMn_2O_4$ - $MnFe_2O_4$ and $CuMn_2O_4$ - $NiFe_2O_4$.

Table - 35

Copper manganite - Manganese ferrite

$Cu_x Mn_{1+x} Fe_{2-2x} O_4$

Frequency f kc/sec.	Comp. x = 0.1	Comp. x = 0.3	Comp. x = 0.4	Comp. x = 0.5
	μ = 58	μ = 77.5	μ = 33.65	μ = 26.85
1000	$\mu.Q$ = 114	$\mu.Q$ = 211	$\mu.Q$ = 157	$\mu.Q$ = 195

Table - 36

Copper manganite - Nickel ferrite

$Cu_x Ni_{1-x} Mn_{2x} Fe_{2-2x} O_4$

Frequency f kc/sec.	Comp. x = 0.2	Comp. x = 0.3	Comp. x = 0.4	Comp. x = 0.5
	μ = 13.6	μ = 15.0	μ = 11.2	μ = 8.6
1000	$\mu.Q$ = 37.25	$\mu.Q$ = 25.1	$\mu.Q$ = 22.6	$\mu.Q$ = 19.4

Table - 37

Copper manganite - Zinc ferrite

$Cu_x Zn_{1-x} Mn_{2x} Fe_{2-2x} O_4$

Frequency f mc/sec.	Comp. x = 0.5	Comp. x = 0.6
	μ = 8.5	μ = 2.6
7.0	$\mu.Q$ = 42.0	$\mu.Q$ = 33.4

CHAPTER - IV

D I S C U S S I O N

CHAPTER - IV

4 D I S C U S S I O N

4.1. Cation distribution in ferrite rich phases ($x < 0.5$)

Copper manganite is a cubic spinel with the "normal" cation distribution (Sinha, Sanjana and Biswas)[1], i.e. the Cu ions occupy the tetrahedral sites and the Mn ions the octahedral sites. One would expect that if the formula is $Cu^{2+}_{tet}\left[Mn_2^{3+}\right]_{oct} O_4$, the structure would be tetragonal as the Mn^{3+} ions are present at the octahedral sites. The observed cubic symmetry has been explained by Sinha et.al.(1957)[1,20] by assigning the structure $Cu^{1+}\left[Mn^{3+}Mn^{4+}\right] O_4$ to the compound. The number of Mn^{3+} ions is then less than that required to give the cooperative distortion (1 against 1.2 required for distortion,(Irani, Sinha and Biswas[33,38]). Miyahara[39](1962) on the other hand has explained the cubic structure as due to the opposing influence of the tetrahedral Cu^{2+} and octahedral Mn^{3+} ions. The former tends to distort the cubic structure to $c/a < 1$, whereas the latter to $c/a > 1$. The two effects are supposed to balance exactly and no distortion is therefore observed. However, recent results on electrical (Sabane, Sinha and Biswas(1966)[95] and magnetic (Blasse(1966)[68]) properties of copper manganite and related compounds have supported the formula $Cu^{1+}\left[Mn^{3+}\ Mn^{4+}\right] O_4$.

Copper ferrite is tetragonal and has the "inverse" cation distribution given by the formula $Fe^{3+}\left[Cu^{2+}Fe^{3+}\right]O_4$. For the copper ferrite - manganite systems of the general formula $x\,CuMn_2O_4 + (1-x)CuFe_2O_4$ i.e. $CuMn_{2x}Fe_{2-2x}O_4$ the cation distribution should be

$$Fe^{3+}_{1-x}Cu^{1+}_{x}\left[Cu^{2+}_{1-x}Mn^{3+}_{x}Mn^{4+}_{x}Fe^{3+}_{1-x}\right]O_4$$

if the ions are assumed to maintain the same valence state which they had in the parent compounds $CuMn_2O_4$ and $CuFe_2O_4$. In the ferrite rich range, i.e. $x < 0.5$, Neel theory is expected to be valid i.e. the magnetic moments at the tetrahedral sites are aligned antiparallel to those on the octahedral sites. Thus the resultant magnetic moment for the above distribution would be $(6x + 1)$ Bohr magnetons per formula unit if the magnetic moments of individual ions are taken as follows:

$$\begin{aligned} Fe^{3+} &= 5\ \mu_B \\ Mn^{3+} &= 4\ \mu_B \\ Mn^{4+} &= 3\ \mu_B \\ Cu^{2+} &= 1\ \mu_B \\ Cu^{1+} &= 0\ \mu_B \end{aligned}$$

This, however, does not agree with the observed variation of n_B with x, the experimental result being

$$n_B = (1 + 2x)\ \mu_B.$$

If the spinel contains Fe^{3+}, Cu^{1+}, Cu^{2+}, Mn^{3+} and Mn^{4+} ions then an unambiguous method to determine the cation distribution would be:

(i) To place the Fe^{3+} and Cu^{1+} ions at the tetrahedral sites in an arbitrary ratio (1-a); a, (where the value of a is to be determined). These ions are known to have a strong preference for the tetrahedral sites (Miller[9], 1959).

(ii) To place the remaining ions at the octahedral sites. The cation distribution would then be

$$Fe^{3+}_{1-a}Cu^{1+}_{a}\left[Cu^{2+}_{1-a}Mn^{3+}_{2x-a}Mn^{4+}_{a}Fe^{3+}_{1+a-2x}\right]O_4.$$

The octahedral copper ions have been assumed to be Cu^{2+} following Blasse(1966)[68], who has shown that at the octahedral sites $(Cu^{2+} + Mn^{3+})$ couple is more stable than the $(Cu^{1+} + Mn^{4+})$ couple. The calculated value of the resultant magnetic moment for the above formula unit turns out to be $n_B = (1 + 8a - 2x)\ \mu_B$. Equating this to the observed value of $(1 + 2x)\ \mu_B$, we get $a = x/2$. Thus the cation distribution is

$$Fe^{3+}_{1-\frac{x}{2}}Cu^{1+}_{\frac{x}{2}}\left[Cu^{2+}_{1-\frac{x}{2}}Mn^{3+}_{\frac{3x}{2}}Mn^{4+}_{\frac{x}{2}}Fe^{3+}_{1-\frac{3x}{2}}\right]O_4 \qquad \ldots(A1)$$

If, on the other hand, the spinel contains only Fe^{3+}, Cu^{2+} and Mn^{3+} ions, then, following the above arguments, one can write the general formula as:

$$Fe^{3+}_{1-a}Cu^{2+}_{a}\left[Cu^{2+}_{1-a}Mn^{3+}_{2x}Fe^{3+}_{1+a-2x}\right]O_4$$

Then $n_B = 1 + 8a - 2x = 1 + 2x$. So $a = x/2$ and the formula becomes

$$Fe^{3+}_{1-\frac{x}{2}}Cu^{2+}_{\frac{x}{2}}\left[Cu^{2+}_{1-\frac{x}{2}}Fe^{3+}_{1-\frac{3x}{2}}Mn^{3+}_{2x}\right]O_4 \qquad \ldots(B1)$$

On comparing A1 and B1 it turns out that the pair ($Cu^{1+}_{tet.}$ + $Mn^{4+}_{oct.}$) of A1 has been replaced by ($Cu^{2+}_{tet.}$ + $Mn^{3+}_{oct.}$) in B1. It is easy to see that this change leads to no change in the resultant magnetic moment because both pairs give a resultant value of 3 μB only (3 - 0 or 4 - 1 μB respectively). Thus the magnetic data will not be able to resolve this ambiguity and we have to take help from the electrical conductivity and structural data.

Verwey and coworkers[75] (1936) have found that the electrical conductivity in a transition metal oxide is high if it contains, at crystallographically equivalent sites, an element in two different ionisation states, q and q + 1. For example, Fe_3O_4 which has Fe^{2+} and Fe^{3+} ions at the octahedral sites of the spinel structure shows a very high conductivity whereas $ZnFe_2O_4$ which has only Fe^{3+} ions at the octahedral sites has a very low conductivity. This arises from the fact that an electron exchange between the two ions in Fe_3O_4 [illegible],

$$Fe^{2+} \overset{e}{\curvearrowright} + Fe^{3+} \longrightarrow Fe^{3+} + Fe^{2+}$$

leaves the total system unchanged, hence very little activation energy is required for the electron transfer. On the other hand, the electron exchange between the octahedral Fe^{3+} ions of $ZnFe_2O_4$ leads to the formation of Fe^{2+} and Fe^{4+} ions,

$$Fe^{3+} \overset{e}{\curvearrowright} + Fe^{3+} \longrightarrow Fe^{4+} + Fe^{2+}$$

requires a high energy, so the rate of electron transfer becomes much reduced.

Furthermore, it can be seen that in the spinel structure the distance between tetrahedral-octahedral or tetrahedral - tetrahedral cations is so large that the overlap between the electronic wave functions on adjacent pairs is negligible and the probability of electron exchange between cations on these sites is small. Thus the electron conduction in spinels takes place mainly by electron exchange amongst the octahedral ions and when these sites are occupied by an element in two different ionisation states, q and q + 1, then the conductivity is high.

If we examine the two formulae A1 and B1 in the light of what has been said above, the sample should show a fairly high conductivity if formula A1 is correct because in this case both Mn^{3+} and Mn^{4+} ions are present at the octahedral sites. Furthermore, the conductivity σ should go on increasing as x increases because the number of Mn^{3+} ions and that of Mn^{4+} increase with x. This indeed is what is experimentally observed as can be seen from the following table.

Composition x	Log σ	$\triangle$E(e.v.)
0	- 6	-
0.3	- 5	0.23
0.5	- 4	0.18

The formula B1, on the other hand, does not predict any such variation with composition.

Furthermore, formula B1 is inconsistent with the known site preference energies of the ions. Cu^{2+} ion has a stronger preference for the octahedral site than the Fe^{3+} ions[Miller[9], (1959) Cu^{2+} = -0.1, Fe^{3+} = - 13.3 K.cal/g. at wt.] but in this

formula there are some Cu^{++} ions at the tetrahedral sites whereas there are some Fe^{3+} ions at the octahedral sites.

In view of the above, thus it appears reasonable to conclude that the correct formula for $CuMn_{2x}Fe_{2-2x}O_4$ in the range $x < 0.5$ is

$$Fe^{3+}_{1-0.5x}Cu^{1+}_{0.5x}\left[Cu^{2+}_{1-0.5x}Mn^{3+}_{1.5x}Mn^{4+}_{0.5x}Fe^{3+}_{1-1.5x}\right]O_4.$$

For nickel ferrite - copper manganite systems of the general formula $x\,CuMn_2O_4+(1-x)\,NiFe_2O_4$ (or $Cu_xNi_{1-x}Mn_{2x}Fe_{2-2x}O_4$) we proceed to determine the cation distribution and the valence state of the ions in the range $x < 0.5$ by following the method outlined above. As is well-known nickel ferrite has an "inverse" spinel structure given by the formula $Fe^{3+}\left[Ni^{2+}Fe^{3+}\right]O_4$. If the ions are assumed to have the same distribution and the same valence state which they had in the parent compounds then the formula would be:

$$Fe^{3+}_{1-x}Cu^{1+}_{x}\left[Ni^{2+}_{1-x}Mn^{3+}_{x}Mn^{4+}_{x}Fe^{3+}_{1-x}\right]O_4$$

The resultant magnetic moment for the above formula is equal to $2.2 + 5x$ assuming the atomic moment of Ni^{2+} as 2.2 μ_B. This, however, does not agree with the experimental observations that $n_B = 2.2\ \mu_B$ and is constant and independent of x in the range $x < 0.5$ (Fig.30).

The two formulae which give the correct magnetic resultsare:

$$Fe^{3+}_{1-0.4x}Cu^{1+}_{0.4x}\left[Cu^{2+}_{0.6x}Mn^{3+}_{1.6x}Mn^{4+}_{0.4x}Fe^{3+}_{1-1.6x}Ni^{2+}_{1-x}\right]O_4 \quad ..(A2)$$

and

$$Fe^{3+}_{1-0.4x}Cu^{2+}_{0.4x}\left[Cu^{2+}_{0.6x}Mn^{3+}_{2x}Fe^{3+}_{1-1.6x}Ni^{2+}_{1-x}\right]O_4 \quad .... (B2)$$

For this system also the first formula is preferred because:

(i) It predicts the correct electrical behaviour.

(ii) The location of the ions does not conflict with the well-known site preference energies.

The electrical conductivity and the activation energy are functions of x as can be seen from the following table.

Composition x	Log ρ	ΔE (e.v.)
0	- 6	-
0.3	- 5	0.27
0.5	- 3	0.14

This behaviour can be best explained on the basis of formula A2.

The analysis of results on cobalt ferrite - copper manganite solid solutions (x) $CuMn_2O_4$ + (1-x) $CoFe_2O_4$ with $x < 0.5$, is slightly more complicated in view of the fact that the tetrahedral site preference energies of Co^{2+} and Cu^{1+} ions are comparable[9] (Co^{2+} = 10.5, Cu^{1+} = 8.6 K.cal/g. atom) and it is not justified to exclude the possibility of the presence of Co^{2+} ions at these sites. We, however, rule out the possibility of the presence of Cu^{2+} ions at the tetrahedral sites in view of the results obtained in the ~~case of~~ above two cases. The general formula for this case would then be:

$$Fe^{3+}_{1-a-b}Cu^{1+}_{a}Co^{2+}_{b}\ Cu^{2+}_{x-a}Mn^{3+}_{2x-a}Mn^{4+}_{a}Fe^{3+}_{1+a+b-2x}Co^{2+}_{1-x-b}\ O_4$$

The resultant magnetic moment for this formula is (3-4x + 8a + 4b). The experimentally observed value for this is 3.0 B and is independent of x (for x 0.5). Thus putting 3 - 4x + 8a + 4b = 3, we get 2a + b = x. Taking the two extreme cases of b = 0 and a = 0, we get the two of the possible formulae as:

(i) $$Fe^{3+}_{1-\frac{x}{2}}Cu^{1+}_{\frac{x}{2}}\ Cu^{2+}_{\frac{x}{2}}Mn^{3+}_{\frac{3x}{2}}Mn^{4+}_{\frac{x}{2}}Fe^{3+}_{1-\frac{3x}{2}}Co^{2+}_{1-x}\ O_4 \qquad \ldots(A3)$$

and

(ii) $$Fe^{3+}_{1-x}Co^{2+}_{x}\ Cu^{2+}_{x}Mn^{3+}_{2x}Fe^{3+}_{1-x}Co^{2+}_{1-2x}\ O_4 \qquad \ldots(C3)$$

The other possibilities correspond to solid solutions of A3 and C3 in various proportions. The electrical conductivity results (Table 17) support formula A3 because the conductivity rises and E falls appreciably with rise in x. This suggests that both Mn^{3+} and Mn^{4+} ions are present at the octahedral sites, which is consistent with formula A3.

Summarising, we can write the cation valence state and distribution in the systems $x\ CuMn_2O_4 + (1-x)\ AFe_2O_4$ as follows (for A = Cu^{2+}, Ni^{2+}, Co^{2+}, x 0.5)

$$Fe^{3+}_{1-mx}Cu^{1+}_{mx}\ Cu^{2+}_{(1-m)x}Mn^{3+}_{(2-m)x}Mn^{4+}_{mx}Fe^{3+}_{1-(2-m)x}A^{2+}_{1-x}\ O_4$$

where m lies in the range 0.4 to 0.5. It is interesting to find that the solid solutions based on the three inverse ferrites have the same type of general formula. We now turn our attention to the solid solutions based on "normal" ferrites. The first

series in this class is the $xCuMn_2O_4 + (1-x)MnFe_2O_4$ solid solution systems. As usual, we write the general formula in which the three tetrahedral preferring ions viz. Cu^{1+}, Mn^{2+} and Fe^{3+} are placed at the tetrahedral sites in an arbitrary ratio a:b:1-a-b and the remaining ions at the octahedral sites. The general formula turns out to be:

$$Cu_a^{1+}Mn_b^{2+}Fe_{1-a-b}^{3+}\left[Cu_{x-a}^{2+}Mn_{2-a-2b}^{3+}Mn_{a+b+x-1}^{4+}Fe_{1+a+b-2x}^{3+}\right]O_4$$

As discussed earlier the possibility of Cu^{2+} ions at the tetrahedral sites has been ruled out. The calculated value of the resultant magnetic moment for this formula unit is $n_B = (5-6x+8a)\mu B$. It is interesting to find that n_B is independent of 'b'. This arises from the fact that both Mn^{2+} and Fe^{3+} have the atomic moment of 5 μB and one cannot distinguish between them on the basis of the magnetic moment data, one can only find out the sum of $Mn^{2+} + Fe^{3+}$ ions at a given site. The observed variation of the magnetic moment with x follows the relationship:

$$n_B = 5-6x$$

Thus a = 0 and the general formula is:

$$Mn_b^{2+}Fe_{1-b}^{3+}\left[Cu_x^{2+}Mn_{2-2b}^{3+}Mn_{b+x-1}^{4+}Fe_{1-b-2x}^{3+}\right]O_4$$

The value of 'b' is determined with the help of electrical conductivity results. The values of ρ and ΔE are set out in Table 19.

Composition x	Log σ	ΔE (e.v.)
0	- 4	-
0.3	- 8	0.53
0.5	- 5	0.28

It is found that the conductivity of the solid solutions is much lower than that of pure $MnFe_2O_4$ and the activation energy is high. These results rule out the possibility of simultaneous presence of Mn^{3+} and Mn^{4+} ions at the octahedral sites. Thus: $b + x - 1 = 0$ or $b = 1 - x$ and the final formula for the solid solutions ($x < 0.5$) is

$$Mn^{2+}_{1-x}Fe^{3+}_{x}\left[Cu^{2+}_{x}Mn^{3+}_{2x}Fe^{3+}_{2-3x}\right]O_4$$

For zinc ferrite-copper manganite system, it is difficult to determine the cation distribution from the magnetic data because in the range $x < 0.5$, the tetrahedral sites are expected to be predominantly occupied by the diamagnetic Zn^{2+} ions. Thus the A-B interaction becomes much weakened and comparable to A-A or A-B interactions. Under this situation, Neel type arrangement is no longer stable. As the analysis of the above type is based on the validity of the Neel model, it cannot be applied the Zn ferrite-copper manganite solid solutions. However, on analogy with the Mn ferrite-copper manganite solid solution, the cation distribution is expected to be:

$$Zn^{2+}_{1-x}Fe^{3+}_{x}\left[Cu^{2+}_{x}Mn^{3+}_{2x}Fe^{3+}_{2-3x}\right]O_4$$

Thus the following formulae appear to represent the cation distribution in the present systems ($x < 0.5$):

(1) $x\,CuMn_2O_4 - (1-x)CuFe_2O_4$

$$Fe^{3+}_{1-\frac{x}{2}}\,Cu^{1+}_{\frac{x}{2}}\left[Cu^{2+}_{1-\frac{x}{2}}\,Mn^{3+}_{\frac{3x}{2}}\,Mn^{4+}_{\frac{x}{2}}\,Fe^{3+}_{1-\frac{3x}{2}}\right]O_4$$

(2) $x\,CuMn_2O_4 - (1-x)NiFe_2O_4$

$$Fe^{3+}_{1-0.4x}\,Cu^{1+}_{0.4x}\left[Cu^{2+}_{0.6x}\,Mn^{3+}_{1.6x}\,Mn^{4+}_{0.4x}\,Fe^{3+}_{1-1.6x}\,Ni^{2+}_{1-x}\right]O_4$$

(3) $x\,CuMn_2O_4 - (1-x)CoFe_2O_4$

$$Fe^{3+}_{1-\frac{x}{2}}\,Cu^{1+}_{\frac{x}{2}}\left[Cu^{2+}_{\frac{x}{2}}\,Mn^{3+}_{\frac{3x}{2}}\,Mn^{4+}_{\frac{x}{2}}\,Fe^{3+}_{1-3\frac{x}{2}}\,Co^{2+}_{1-x}\right]O_4$$

(4) $x\,CuMn_2O_4 - (1-x)MnFe_2O_4$

$$Fe^{3+}_{x}\,Mn^{2+}_{1-x}\left[Cu^{2+}_{x}\,Mn^{3+}_{2x}\,Fe^{3+}_{2-3x}\right]O_4$$

(5) $x\,CuMn_2O_4 - (1-x)ZnFe_2O_4$

$$Fe^{3+}_{x}\,Zn^{2+}_{1-x}\left[Cu^{2+}_{x}\,Mn^{3+}_{2x}\,Fe^{3+}_{2-3x}\right]O_4$$

The interesting features of these formulae are:

(i) Fe^{3+} and Cu^{1+} have a comparable preference for the tetrahedral sites so that some Cu^{1+} are present at these sites after displacing some Fe^{3+} ions to the octahedral sites.

(ii) When some ions with much stronger preference for the tetrahedral sites (e.g. Mn^{2+}) are present then Cu ions are completely removed from the tetrahedral sites.

It thus appears that in the spinels containing Cu and Mn the following four pairs are stable under different conditions.

(a) $Cu^{1+}_{tet.} + Mn^{4+}_{oct.}$

(b) $Cu^{2+}_{oct.} + Mn^{3+}_{oct.}$

(c) $Cu^{2+}_{tet.} + Mn^{3+}_{oct.}$

(d) $Cu^{1+}_{oct.} + Mn^{4+}_{oct.}$

Generally (a) and (b) appear to be more stable than (c) and (d.) The choice between (a) and (b) which are of comparable, stability depends on the other ions present in the structure. Thus, for example, if the third ion is Mn^{2+} (or Zn^{2+}) which has a stronger preference for tetrahedral site then the Cu ion is forced to the octahedral site and formula (b) becomes stable. On the other hand if the third ion has a preference for the octahedral site (e.g. Mn^{3+} in $CuMn_2O_4$) then the Cu ion is forced to tetrahedral site and the formula (a) becomes stable. These general conclusions enable us to predict the valence states in some known copper-manganese spinels which are as follows:

Compound	Predicted valence state	Reason	Obs. C_M 96	Calcd. C_M	
				Cu^{2+} Mn^{3+}	Cu^{1+} Mn^{4+}
$CuCrMnO_4$	$Cu^{1+}\left[Cr^{3+}Mn^{4+}\right]O_4$	Cr^{3+} has a preference for B site	3.54	5.25	3.75
$Zn_{0.5}Ge_{0.5}CuMnO_4$	$Zn_{0.5}Ge_{0.5}\left[Cu^{2+}Mn^{3+}\right]O_4$	Zn^{2+}, Ge have a preference for A site	2.97	3.38	1.88
$GaCuMnO_4$	$Ga^{3+}\left[Cu^{2+}Mn^{3+}\right]O_4$	Ga^{3+} has a preference for A site.	2.97	3.38	1.88

It can be seen that these predicted formulae are consistant with observed Curie constants of the compounds[96].

One interesting consequence of above formulae (1-5) is that there are two distorting ions at the octahedral sites viz. Mn^{3+} and Cu^{2+}. $Mn^{3+}(d^4)$ and $Cu^{2+}(d^9)$ ions, when put at octahedral sites lead to a doubly degenerated orbitals state which is unstable (Jahn-Teller[31], 1937). The system therefore distorts such that this degeneracy is removed. In case Mn^{3+} and Cu^{2+} ions at octahedral sites of spinels at tetragonal distortion with $c/a > 1$ is usually observed. This distortion is a cooperative phenomenon and is absent if the percentage of octahedral sites occupied by distorting cations is less than a certain critical value.

To fix our ideas let us take the specific case of copper ferrite - manganite system which has the cation distribution:

$$Fe^{3+}_{1-\frac{x}{2}}\,Cu^{1+}_{\frac{x}{2}}\left[Cu^{2+}_{1-\frac{x}{2}}\,Mn^{3+}_{\frac{3x}{2}}\,Mn^{4+}_{\frac{x}{2}}\,Fe^{3+}_{1-\frac{3x}{2}}\right]O_4$$

for $x < 0.5$.

It is well known that in case of manganites the system changes from cubic to tetragonal structure when the number of Mn^{3+} ions at the octahedral sites becomes greater than 1.2 per formula unit. This critical number in case of spinels containing Cu^{2+} ions is not known, but is expected to be less than 1 because, $CuFe_2O_4$, where the number of Cu^{2+} ions at the octahedral

sites per formula unit is one, is tetragonal. Thus in systems which contain both Cu^{2+} and Mn^{3+} the critical concentrations would be between 1 and 1.2 if both Mn^{3+} ions and Cu^{2+} ions act cooperatively. Thus it is clear that the transformation to tetragonal structure in the present copper ferrite manganites system should occur at $0 < x < 0.2$ and the compositions $x = 0.2$ and 0.3 should clearly be tetragonal. However, contrary to expectations, the observed structure is cubic. For each Cu^{2+} ion removed from the octahedral sites three Mn^{3+} ions are brought in. So the only reason why the tetragonal structure of pure $CuFe_2O_4$ should change to cubic structure in the solid solution could be that the Cu^{2+} ions and Mn^{3+} ions do not act cooperatively to cause Jahn-Teller distortion.

The number of distorting cations per formula unit in the various solid solutions determined from the cation distribution arrived at earlier, is as follows:

		$Cu^{2+} + Mn^{3+}$	Mn^{3+} only
1.	$x\ CuMn_2O_4 - (1-x)CuFe_2O_4$	$1 + x$	$\frac{3x}{2}$
2.	$x\ CuMn_2O_4 - (1-x)NiFe_2O_4$	$2.2x$	$1.6x$
3.	$x\ CuMn_2O_4 - (1-x)CoFe_2O_4$	$2x$	$\frac{3x}{2}$
4.	$x\ CuMn_2O_4 - (1-x)MnFe_2O_4$	$3x$	$2x$
5.	$x\ CuMn_2O_4 - (1-x)ZnFe_2O_4$	$3x$	$2x$

If Cu^{2+} and Mn^{3+} ions do not act cooperatively and only Mn^{3+} ions are operative in causing the distortion, then in the range $x < 0.5$ (where the above cation distribution is valid) the structure should be cubic (because $\left[Mn^{3+}\right] < 1.2$) as is indeed the case. This would also explain the cubic symmetry of $Zn_{0.5}Ge_{0.5}CuMn\ O_4$ and $GaCuMnO_4$ observed by Baltzer and Lopatin[96]. Although the compounds contain Cu^{2+} and Mn^{3+} ions at the octahedral sites but these two ions do not act cooperatively to cause the distortion.

4.2. Solid solution $x\ CuMn_2O_4 - (1-x)AFe_2O_4 (x > 0.5)$

At this stage it is worthwhile discussing the magnetic structure of copper manganite. As the cation distribution and valence state of ions in this compound have been clearly established to be $Cu^{1+}\ \left[Mn^{3+}\ Mn^{4+}\right] O_4$, the observed ferrimagnetic behaviour is worth some analysis. As the 'A' sites are occupied by the diamagnetic Cu^{1+} ions it is clear that the A-B interaction is absent and the cause of the spin alignments must be the mutual interaction between the B-B ions only. A parallel alignment of all the B ions would give a net resultant magnetic moment of 7 μ_B whereas the experimentally observed value is 0.6 μ_B only[96]. Furthermore, the variation of $1/\chi$ with 'T' is not linear as is to be expected for a ferromagnetic material, but is hyperbolic characteristic of a ferrimagnetic substance. Ferrimagnetism of $CuMn_2O_4$ can arise if:

(i) Mn^{3+} and Mn^{4+} ions are ordered over the two sublattices B1 and B2, and

(ii) The spins on lattice B1 are aligned antiparallel to those on B2. This would give a net magnetic moment of 1 μ_B which is close to the experimentally observed value.

The other possible cause of the ferrimagnetism could be the presence of a small proportion of some paramagnetic ions such as Mn^{3+} or Cu^{2+} at the tetrahedral sites. In this case the A-B interaction is negative but weak due to the dilution of A moments by the large concentration of the paramagnetic Cu^{1+} ions. Thus the A-B and B-B interactions are of comparable magnitude and the Neel type collinear alignment would no longer be stable and a triangular spin alignment (Yafet-Kittel type) would result.

The spin alignment in solid solutions containing excess of $CuMn_2O_4$ would also be different from simple Neel type arrangement. In fact for many pure manganites the experimentally observed magnetic moment is less than that calculated on the basis of Neel theory (Mn_3O_4, $n_B = 1.56 \pm 0.04$, Jacobs[60],1959) indicating that Neel arrangement does not hold in these compounds. It is generally believed that Yafet-Kittel type or helical spin arrangement exist in manganites (Jacobs[60],1959; Kaplan[45],1960). Therefore, it is not possible to get an idea about the cation distribution from the observed magnetic moments in manganite rich compositions (i.e. $x > 0.5$). A qualitative idea about the cation distribution can however be obtained from the electrical conductivity results. It can be seen that generally the

electrical resistance of the x $CuMn_2O_4$ + (1-x)AFe_2O_4 solid solutions is low (20-1000Ω) in the range ($1 > x > 0.7$).

In view of what has been said earlier it appears clear that these phases contain both Mn^{3+} and Mn^{4+} ions at the octahedral sites. The following two formulae appear plausible for $xCuMn_2O_4 + (1-x)AFe_2O_4$ solid solution($x > 0.8$) where AFe_2O_4 is an inverse spinel:

(1) $Cu_x^{1+}Fe_{1-x}^{3+}\left[Mn_x^{3+}Mn_x^{4+}Fe_{1-x}^{3+}A_{1-x}^{2+}\right]O_4$

(2) $Cu_{2x-1}^{1+}Fe_{2-2x}^{3+}\left[Mn_1^{3+}Mn_{2x-1}^{4+}Cu_{1-x}^{2+}A_{1-x}^{2+}\right]O_4$

The first formula is based on the assumption that in solid solutions the cations maintain the same distribution as they had in the parent compounds. Formula 2 is derived if Fe^{3+} ions are assumed to have a stronger preference for the tetrahedral site than the Cu^{1+} ions so that they come to the A sites and displace an equal amount of Cu^{1+} to the octahedral sites and the Cu^{1+} ions displaced to the octahedral site change their valance state to Cu^{2+} by an electron exchange with Mn^{4+} ions.

Similarly for the cases in which the ferrite AFe_2O_4 is "normal" we would get the following two formulae (based on the above arguments).

(1') $Cu_x^{1+}A_{1-x}^{2+}\left[Mn_x^{3+}Mn_x^{4+}Fe_{2-2x}^{3+}\right]O_4$

(2') $\begin{cases} Fe_{2-2x}^{3+}Cu_{3x-2}^{1+}A_{1-x}^{2+}\left[Cu_{2-2x}^{2+}Mn_{2-x}^{3+}Mn_{3x-2}^{4+}\right]O_4 & (x > 2/3) \\ Fe_x^{3+}A_{1-x}^{2+}\left[Cu_x^{2+}Mn_{2x}^{3+}Fe_{2-3x}^{3+}\right]O_4 & (\frac{1}{2} < x < 2/3) \end{cases}$

We first take up the case of $CuMn_2O_4$ - $MnFe_2O_4$ system where we have conclusive evidences in support of formula 2'. As is well-known, the electrical conductivity σ is given by the relationship $\sigma = ne\mu$ where 'n' is the number of charge carriers per unit volume. μ is the mobility. The number of charge carriers is equal to the number of Mn^{4+} ions at the octahedral sites per unit volume in these p-type semiconductors. The electronic wave function is localised around these charge carriers. Furthermore, due to an interaction of these localised charge carriers with the lattice polarisation of the lattice, takes place. The total energy of the system is lowered due to the polarisation and the charge carrier gets trapped. Due to interaction with phonons these charge carriers (holes) are able to hop from one Mn^{4+} ion to the adjacent Mn^{3+} ions. The transition probability and thus mobility will therefore be strongly temperature dependent. Furthermore, it will also be directly proportional to the probability of finding a Mn^{3+} ion adjacent to the Mn^{4+} ion which in turn depends on the concentration of Mn^{3+} ions at the octahedral sites. Thus:

$$\sigma = ne\mu\alpha\left[Mn^{4+}\right] \times \left[Mn^{3+}\right]$$

and

$$\text{Log}\,\rho = k - \log\left[Mn^{3+}\right]\left[Mn^{4+}\right]$$

The value of $\left[Mn^{3+}\right] \times \left[Mn^{4+}\right]$ calculated from formula (1') and (2') for different values of x are given in Table 38. The value of Log ρ has been normalised by choosing the value of k such that the calculated and observed values of log ρ for pure $CuMn_2O_4$ (x = 1) agree. The calculated values of log ρ

are presented in Table 38 and results are plotted in figure 40 together with the experimentally observed values.

Table - 38

Composition x	Formula 1'				Formula 2'			
	Mn^{3+}	Mn^{4+}	$Mn^{3+} \times Mn^{4+}$	Log ρ	Mn^{3+}	Mn^{4+}	$Mn^{3+} \times Mn^{4+}$	Log ρ
1.0	1	1	1	1.4	1	1	1	1.4
0.9	0.9	0.9	0.81	1.5	1.1	0.7	0,77	1.5
0.8	0.8	0.8	0.64	1.6	1.2	0.4	0.48	1.8
0.7	0.7	0.7	0.49	1.7	1.3	0.1	0.13	2.3
0.69	-	-	-	-	1.31	0.07	0.09	2.5
0.68	-	-	-	-	1.32	0.04	0.05	2.7
0.67	-	-	-	-	1.33	0.01	0.01	3.4
0.66	-	-	-	-	1.332	0	0	∞
0.60	0.6	0.6	0.36	1.8	1.2	0	0	∞

In view of the fact that the composition dependence of conductivity is not fully understood and that the equation is very approximate, the agreement between the observed and the calculated values for formula 2' is considered to be good. Furthermore, as mentioned earlier the manganites in which the number of Mn^{3+} ions per formula unit is 1.2 or more the structure is tetragonal otherwise it is cubic. Thus according to formula 1 all the compositions listed in Table 38 should be cubic. On the other hand according to formula 2' the composition in the range

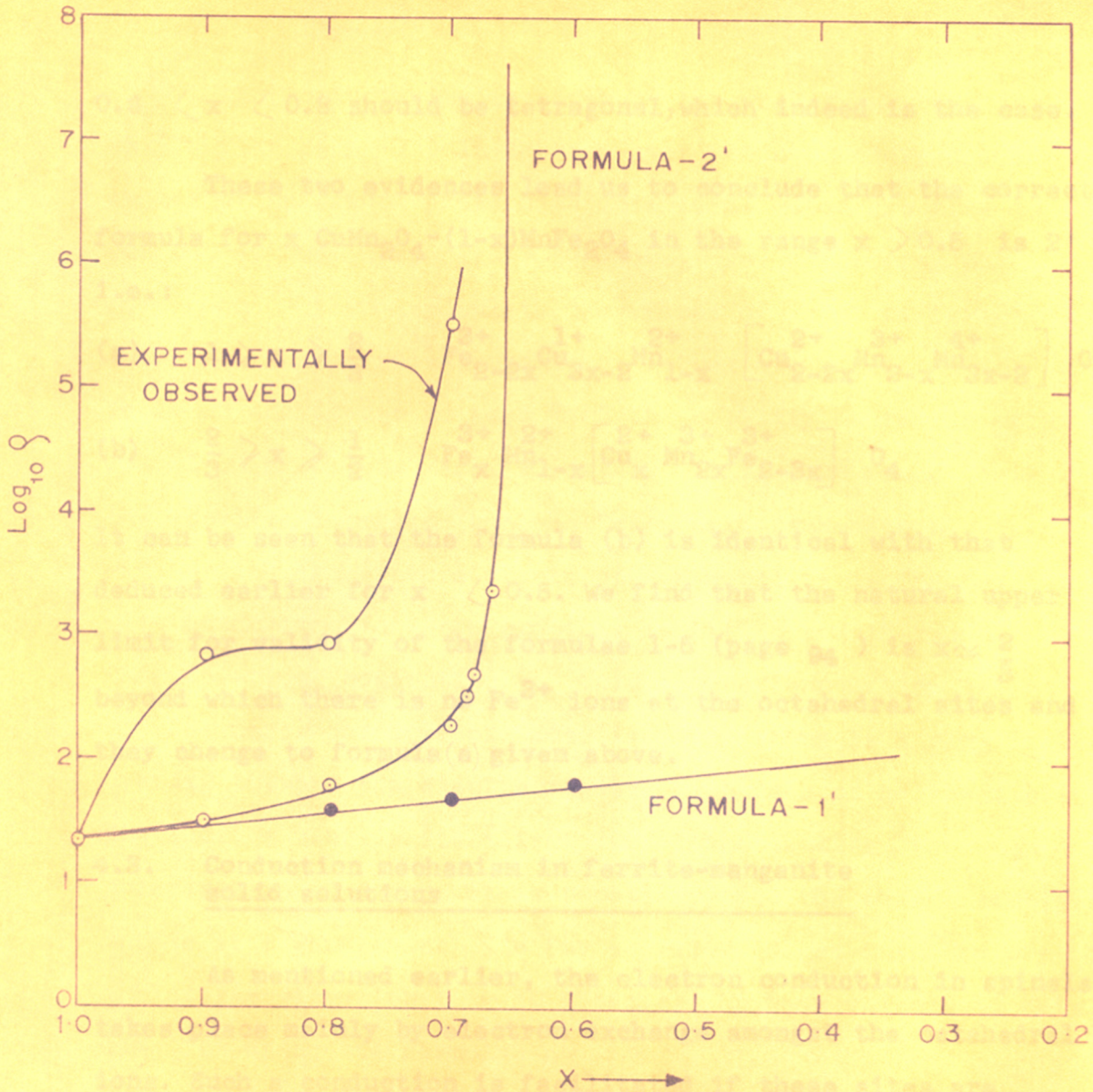

FIG 40

VARIATION OF SPECIFIC RESISTIVITY AS A FUNCTION OF 'X' AT ROOM TEMPERATURE FOR THE SYSTEM $Cu_xMn_{1+x}Fe_{2-2x}O_4$

$0.6 < x < 0.8$ should be tetragonal, which indeed is the case.

These two evidences lead us to conclude that the correct formula for $x\,CuMn_2O_4-(1-x)MnFe_2O_4$ in the range $x > 0.5$ is 2', i.e.:

(a) $\quad 1 \geqslant x \geqslant \frac{2}{3} \qquad Fe^{3+}_{2-2x}Cu^{1+}_{3x-2}Mn^{2+}_{1-x}\left[Cu^{2+}_{2-2x}Mn^{3+}_{2-x}Mn^{4+}_{3x-2}\right]O_4$

(b) $\quad \frac{2}{3} \geqslant x \geqslant \frac{1}{2} \qquad Fe^{3+}_{x}Mn^{2+}_{1-x}\left[Cu^{2+}_{x}Mn^{3+}_{2x}Fe^{3+}_{2-3x}\right]O_4$

It can be seen that the formula (b) is identical with that deduced earlier for $x < 0.5$. We find that the natural upper limit for validity of the formulae 1-5 (page 94) is $x \simeq \frac{2}{3}$ beyond which there is no Fe^{3+} ions at the octahedral sites and they change to formula(a) given above.

4.3. Conduction mechanism in ferrite-manganite solid solutions

As mentioned earlier, the electron conduction in spinels takes place mainly by electron exchange amongst the octahedral ions. Such a conduction is facilitated if these sites are occupied by an element in two different ionisation states q and q + 1. From the formulae established above, it is clear that in many compositions we have, at the octahedral sites, both Mn^{3+} and Mn^{4+} ions and it is reasonable to assume that conduction takes place by electron exchange between these ions.

The conductivity is given by the well-known relationship $\sigma = ne\mu$. In these p-type semiconductors n = the number of Mn^{4+} ions present at octahedral sites are free to conduct at room temperature or above. We, therefore, put $n = [Mn^{4+}]$ and calculate the values of μ at different temperature. The room temperature values are presented in Table 39 and it can be seen that the mobility is really very low (10^{-5} - 10^{-7} cm^2/sec. x volts). It is also found that the mobility increases exponentially with temperature. This exponential temperature dependence of mobility is inconsistent with conduction in bands and fits in with the well-known "hopping-type" conduction. This type of conduction arises if the charge carriers are localised and there is a very little overlap between the electronic wave functions on adjacent sites. The localisation is stabilised due to the lattice polarisation. For such polarisation to occur, it is necessary that the charge carriers reside at a particular site for a period longer than the period of lattice vibration ($\simeq 10^{-13}$sec.). We have calculated this time "t" using the formula

$$t = \frac{ed^2}{\mu kT}$$

and the value is found to lie in the range 10^{-7} to 10^{-9}sec. at room temperature. It is thus clear that the condition for polarisation and self-trapping is fulfilled in these compounds. These localised carriers move from site to site by means of a phonon assisted process. Various mechanisms have been suggested

Table - 39

Mobility μ x 10^{-7} cm^2/sec. x volt at room temperature

Composition x	Systems				
	$CuMn_{2x}Fe_{2-2x}O_4$	$Cu_xCo_{1-x}Mn_{2x}Fe_{2-2x}O_4$	$Cu_xZn_{1-x}Mn_{2x}Fe_{2-2x}O_4$	$Cu_xMn_{1+x}Fe_{2-2x}O_4$	$Cu_xNi_{1-x}Mn_{2x}Fe_{2-2x}O_4$
0.9	7	8	10	8	10
0.8	20	6	-	7	100
0.7	5	33	4	-	300

in the literature and from our present data it is not clear as to which process predominates in our case. Jogalekar and Sinha[97] have pointed out that in manganites containing Mn^{3+} and Mn^{4+} ions, trapping is enhanced due to the presence of local Jahn-Teller distortion. This arises from the fact that oxygen octahedron around Mn^{3+} ion is distorted whereas that around Mn^{4+} ions is not. Thus an electron exchange of electrons between neighbouring Mn^{3+} and Mn^{4+} ions will lead to an unstable configuration as the new Mn^{4+} (at the old site of Mn^{3+}) would be surrounded by a distorted octahedral arrangement of oxygen ions and the new Mn^{3+} ion by a cubic octahedron of O^{2-} ions. So each electron exchange will have to be associated with a rearrangement of surrounding oxygen ions which would require an additional activation energy. Furthermore, our experimental results point to the existance of a pronounced effect of spin ordering on electrical conductivity.

A comparison of the ΔE and log ρ_0 in the ferro and paramagnetic regions can be made from the values given in Tables 15 to 19. Quite generally, it is found that ΔE is lower and ρ_0 higher in the ferromagnetic region. It is to be expected that the number of current carriers remain unchanged on paramagnetic to ferromagnetic transition. The lower value of ΔE in the ferromagnetic phase is to be expected on the basis of the hopping mechanism of conduction. Let us take the case of a spinel structure containing Mn^{3+} and Mn^{4+} ions at the octahedral sites. The distribution of the octahedral ions in space is shown

figure 1. It can be seen that each Mn ion is surrounded by six oxygen ions as its first nearest neighbour and six Mn ions as its second nearest neighbour. The field due to oxygen ions causes the five fold degenerate 'd' levels to split up into a triply degenerate lower level and doubly degenerate upper level. The trigonal field due to the next nearest metal ions and due to the deviation of oxygen ion parameter from the ideal value $u = 0.375$ cause a further splitting of the levels. The energy levels for electrons on the two adjacent Mn^{3+} and Mn^{4+} ions would then be as shown in the following figures.

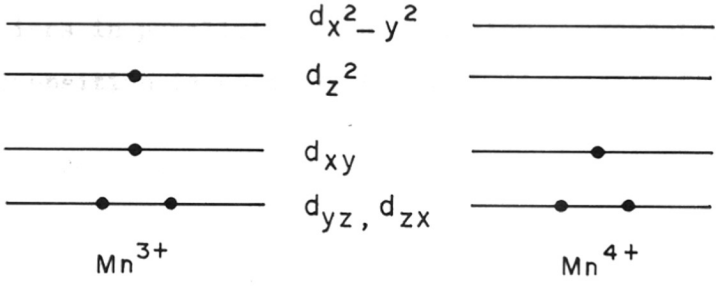

It can be seen that the electron responsible for conduction is the one occupying the dz^2 orbital in the Mn^{3+} ions. This hops on the adjacent Mn^{4+} ions where the dz^2 orbital is empty. If the substance is ferromagnetic then the spin on the adjacent ions will be parallel so the hopping

electrons can move from one site to another without changing the direction of its spin angular momentum. If on the other hand the adjacent ions are aligned antiferromagnetically, then the hopping probability will be greatly diminished because the electron must change its spin direction when it jumps to the next site. This has to be achieved through the spin-orbit coupling which make the transition probability much less. In the case of paramagnetic substances the spin orientation of each ion takes up one of the quantum mechanically allowed values at random so there is a finite probability of finding two adjacent ions in parallel spin orientation. Therefore, the hopping transition is possible but with diminished frequency.

---0---

SUMMARY

SUMMARY

A number of $Cu_xMe_{1-x}Mn_{2x}Fe_{2-2x}O_4$ systems (where Me = Cu, Ni, Co, Mn and Zn) have been prepared and their structural, magnetic and electrical properties have been studied.

The compounds of the above general formula were prepared by reacting x $CuMn_2O_4$ + (1-x)$MeFe_2O_4$ in appropriate proportion at elevated temperatures. X-ray diffraction patterns indicate the formation of a homogeneous phase. Saturation magnetization (σ) of the above systems was measured as a function of temperature in the range between 300°K to 77°K in a magnetic field of 6500 oe. The value of $\sigma(T = 0°K)$ was obtained by extrapolation and its value n_B was calculated in Bohr magneton units. It has been found that for $CuMn_{2x}Fe_{2-2x}O_4$, and $Cu_xZn_{1-x}Mn_{2x}Fe_{2-2x}O_4$ n_B increases as x decreases from x = 1 and reaches the maximum at x = 0.5 and 0.6 respectively beyond which it starts falling and attains the value of 1.3 at x = 0. In the case of $Cu_xNi_{1-x}Mn_{2x}Fe_{2-2x}O_4$ and $Cu_xCo_{1-x}Mn_{2x}Fe_{2-2x}O_4$ n_B increases as x decreases from x = 1 and reaches the maximum at x = 0.5 in both cases and remains nearly constant for further decrease in 'x'. The maximum values of n_B in two cases are 2.12 and 2.95 respectively. For $Cu_xMn_{1+x}Fe_{2-2x}O_4$ on the other hand n_B increases regularly as 'x' changes from 1 to 0.

In all cases except $Cu_xZn_{1-x}Mn_{2x}Fe_{2-2x}O_4$ system Curie temperature has been found to decrease with increase in 'x'. At low values of x ($0 < x < 0.5$) the decrease in Curie temperature is linear with respect to 'x'. For $x > 0.5$, however, T_c vs x plot

is non-linear and Curie temperature decreases, rapidly with increasing 'x'. For $Cu_xZn_{1-x}Mn_{2x}Fe_{2-2x}O_4$ system the T_c vs x plot shows a maximum at x = 0.5 (T_c = 320°K).

In many systems it has been found that σ - T plot becomes asymptotic to the temperature axis near the Curie temperature and no sharp transition point is observed. This may be due to magnetic inhomogeneties, in an apparently homogeneous solid solution.

The saturation magnetization results appear to indicate the following cation distributions for these compounds in the range $0 < x < 0.5$.

(1) $$\underline{x\ CuMn_2O_4 - (1-x)CuFe_2O_4}$$

$$Fe^{3+}_{1-x}Cu^{1+}_{x}\left[Cu^{2+}_{1-x}Mn^{3+}_{3x}Mn^{4+}_{x}Fe^{3+}_{1-3x}\right]O_4$$

(2) $$\underline{x\ CuMn_2O_4 - (1-x)NiFe_2O_4}$$

$$Fe^{3+}_{1-0.4x}Cu^{1+}_{0.4x}\left[Cu^{2+}_{0.6x}Mn^{3+}_{1.6x}Mn^{4+}_{0.4x}Fe^{3+}_{1-1.6x}Ni^{2+}_{1-x}\right]O_4$$

(3) $$\underline{x\ CuMn_2O_4 - (1-x)CoFe_2O_4}$$

$$Fe^{3+}_{1-x}Cu^{1+}_{x}\left[Cu^{2+}_{x}Mn^{3+}_{3x}Mn^{4+}_{x}Fe^{3+}_{1-3x}Co^{2+}_{1-x}\right]O_4$$

(4) $$\underline{x\ CuMn_2O_4 - (1-x)MnFe_2O_4}$$

$$Fe^{3+}_{x}Mn^{2+}_{1-x}\left[Cu^{2+}_{x}Mn^{3+}_{2x}Fe^{3+}_{2-3x}\right]O_4$$

(5) $$\underline{x\ CuMn_2O_4 - (1-x)\ ZnFe_2O_4}$$

$$Fe^{3+}_{x}Zn^{2+}_{1-x}\left[Cu^{2+}_{x}Mn^{3+}_{2x}Fe^{3+}_{2-3x}\right]O_4$$

It has been concluded that:

(1) Fe^{3+} and Cu^{1+} have a comparable preference for the tetrahedral sites.

(2) When some ions (e.g. Mn^{2+} or Zn^{2+}) with much stronger preference for the tetrahedral sites are present then Cu^{1+} ions are completely removed from the tetrahedral sites.

(3) At tetrahedral sites Cu ions are present as Cu^{1+} and at octahedral sites as Cu^{2+}.

(4) The pairs ($Cu^{1+}_{tet.}$ + $Mn^{4+}_{oct.}$) and ($Cu^{2+}_{oct.}$ + $Mn^{3+}_{oct.}$) are of comparable stability and the choice is governed by the other ions present. Thus in presence of Mn^{2+} or Zn^{2+} ions the Cu ions are removed to the octahedral sites and the second pair is stabilised. On the other hand, if the other ion has a preference for the octahedral site (e.g. Mn^{3+} in $CuMn_2O_4$) then the Cu ion occupies the tetrahedral site and the first pair stabilised.

Electrical conductivity measurements on some of these solid solutions show:

(1) A break in the log vs 1/T plot at the Curie temperature.

(2) The activation energy in the ferromagnetic region is lower than that in the paramagnetic region.

(3) The resistivity is high in the range $0 < x < 0.5$ and falls rapidly as x changes from 0.5 to 0.8. In the range $0.8 < x < 1.0$ the electrical resistivity of the samples is very low ($<$ 100 ohms x cm).

These results suggest the presence of Mn^{3+}, Mn^{4+} ions at octahedral sites in the compositions ranges $0.5 < x < 1.0$. The magnetisation data for these compositions afford no clue for the distribution and the valence states of the cations because in this range the Neel arrangement may not be present.

The high electrical conductivity in this region is attributed to the electrons hopping between Mn^{3+} and Mn^{4+} ions at the octahedral sites.

REFERENCES

(1) Sinha, A.P.B., Sanjana, N.R. and Biswas, A.B., Acta.Cryst., 10, 439 (1957).

(2) Bragg, W. H., Nature, 15, 531, (1915).

(3) Nishikawa, S., Proc.Tokyo Math.Phys.Soc.,8, 199-209 (1915).

(4) Aminoff, G., Zeitschr f. Krist., 64, 475 (1926).

(5) Barth, T.F.W. and Posnjak, F., Zeitschr f. Krist.,82,325(1932).

(6) Verwey, E.J.W. and Heilmann, E.L., J.Chem.Phys., 15, 174-180 (1947).

(7) Gorter, E. W., Philips Res.Rept., 9, 229 (1954).

(8) McClure, D.S., J.Phys.Chem.Solids, 3, 311 (1957).

(9) Miller A., J.Appl.Phys.Suppl.to Vol.30, 24(S) (1959).

(10) Hastings, J.M. and Corliss, L. M., Phy.Rev.,104, 328-331(1956).

(11) Shull, C.G., Wollan, E.O. and Kochler, W.C., Phy.Rev., 84, 912-921 (1951).

(12) Claassen, A., Proc.Phys.Soc., 38, 482-87 (1925-1926).

(13) Prince, E., Phy.Rev., 102, 674-676 (1956).

(14) Hastings, J. M. and Corliss, L. M., Revs.Mod.Phys., 25, 114-119 (1953).

(15) Prince, E. and Treuting, R.G., Acta.Cryst., 9, 1025-1028(1956).

(16) Verwey, E. J.W. and Heilmann, E.L., J.Chem.Phys., 15, 174-180 (1947).

(17) Bacon, G.E. and F.P. Roberts, Acta.Cryst., 6, 57-62 (1953).

(18) Corliss, L. M. Hastings, J. M. and Brockman, F.G., Phy.Rev., 90, 1013-1018 (1953).

(19) Braun, P.B., Nature, 170, 1123, (1952).

(20) Sinha, A.P.B., Sanjana, N.R. and Biswas, A.B., Zeitschr f. Krist., 109, 410-420 (1957).

(21) Sinha, A.P.B., Sanjana, N.R. and Biswas, A.B., J.Phys.Chem., 62, 191 (1958).

(22) Sanjana, N.R.,Thesis, University of Bombay (1958).

(23) Bongers, P.F., Thesis, University of Leiden (1958).

(24) Mason, B., Amer.Min., 32, 426 (1947).

(25) Mason, B. Goel Foren Stockholm, Forch, 65, 97 (1943).

(26) Wickham, D.G. and Croft, W.J., Quarterly Progress Reports of Solid State Research Group, Lincoln Laboratory, M.I.T. (1958).

(27) Baltzer, P.K. and White, J.G., J.Appl.Phys., 29, 445 (1958).

(28) Kurlina, E.V., Prokhvatilov, V.G. and Sheftel, I.T., Doklady Akad Nauk, USSR, 86, 305 (1952).

(29) Dunitz, J.D. and Orgel, L.E., J.Phys.Chem.Solids, 3, 20(1957).

(30) McMurdic, H. and Golovato, E.J. J.Res.Nat.Bur.Stand., 41, 589 (1948).

(31) Jahn, H.A. and Teller, E., Proc.Roy.Soc.A-161, 220(1937).

(32) Romeijn, F.C., Philips Res.Rept., 8, 304-20 (1953).

(33) Irani, S. K., Sinha, A.P.B. and Biswas, A.B., J.Phys.Chem. Solids, 23, 711-727 (1962).

(34) Finch, G.I., Sinha, A.P.B. and Sinha, K.P., Proc.Roy.Soc., (London) A-242, 28 (1957).

(35) Wojtowicz, P.J., Phy.Rev., 116, 32 (1959).

(36) Kanamori, J., J.Appl.Phys., 31S, 14, (1960).

(37) Wickham, D.G. and Croft, W.J., J.Phys.Chem.Solids, 7, 351-60 (1958).

(38) Irani,S. K.,Sinha, A. P.B. and Biswas, A.B., J.Phys. Chem. Solids, 17, 101 (1960).

(39) Miyahara, S., J.Phys.Soc. Japan, 17, Suppl. B-1, 181(1962).

(40) Miyahara, S., Muramori, K. and Tokuda, N., J.Phys.Soc. Japan, 16, 1490 (1961).

(41) Weiss, P. and Forrer, R., Ann.Phys.Paris(10) 12, 279-374 (1929).

(42) Hilpert, G., Ber.dtsch.chem. Ges., 42, 2248 (1909).

(43) Neel, L., Ann.Phys.Paris, 3, 137-198 (1948).

(44) Yafet, Y and Kittel, C., Phys.Rev., 87, 290-294 (1952).

(45) Kaplan, T.A., Phys.Rev., 119, 1460 (1960).

46) Kaplan, T.A., Dwight, K., Lyones, D.H. and Menyuk, N., J.Appl. Phys., 32, 13(s) (1961).

(47) Pölder, D., J.Instn. Elect. Engrs., 97(II), 246-256 (1950).

(48) Gorter, E.W., C.R.Acad.Sci. Paris, 230, 192-194 (1950).

(49) Gorter, E.W., Nature, 165, 798-800(1950).

(50) Guillaud, C. and Roux, M., C.R.Acad.Sci.Paris, 229, 1133-35 (1949).

(51) Guillaud, C. and Creveaux, H., C.R.Acad.Sci. Paris, 230, 1256-58 (1950).

(52) Guillaud, C. and Creveaux, H.,C.R.Acad. Sci. Paris, 230, 1458-60 (1950).

(53) Guillaud, C. and Sage, M., C.R.Acad.Sci. Paris, 232, 944-46 (1951).

(54) Guillaud, C., J.Phys.Radium, 12, 239-248 (1951).

(55) Pauthenet, R., C.R.Acad.Sci. Paris., 230, 1842-1843(1950).

(56) Pauthenet, R., and Bochirol, L., J.Phys. Radium, 12, 249-251 (1951).

(57) Pauthenet, R., Ann.Phys. Paris, 7, 710-747 (1952).

(58) Gorter, E. W., Philips Res. Reports, 9, 295-320, 321-365 and 403-443 (1954).

(59) Borovik, A.S., Romanov, V. and Orlova, M.P., Soviet Phys. JETP, USSR, 5, 1023 (1957).

(60) Jocobs, I.S., J.Appl. Phys. Suppl. 30, 301S (1959).

(61) Bernard, Boucher, Cmpt. Reudus, 249 (4), 514 (1959).

(62) Wickham, D.G. and Croft, W.J., J.Phys.Chem.Solids, 7, 351-60 (1958).

(63) Jocobs, I.S. and Kouvel, J.S., Phy.Rev., 122, 412 (1961).

(64) Dwight, K. and Menyuk, N., Phy.Rev., 119, 1470 (1960).

(65) Sabane, C.D., Ph.D. Thesis, University of Poona,(1960).

(66) Jogalekar, P. P., Ph.D. Thesis, University of Poona,(1965).

(67) Blasse, G., Solid State Communication, 3, 67-69 (1965).

(68) Blasse, G., J.Phys.Chem.Solids, 27, 383-89 (1966).

(69) Philips, K., Baltzer and John, G. White, J.Apply. Phys., 29(3), 445 (1958).

(70) Andrew, H., Eschenfelder, J.Appl. Phys., 29(3),378 (1958).

(71) Arthur Miller, J.Apply.Phys.,31,(5)Suppl. 261-262(5) (1960).

(72) Victor, L. Moruzzi, J.Appl. Phys.,Suppl. to Vol.32(3), 59(5) (1961).

(73) M. O'Keeffe, Phys.Chem.Solids, 21(3-4), 172-178 (1961).

(74) Smit, J. and Wijn, H.P.J., "Ferrite" John Wiley and Sons Publications Inc., New York, p.229-36 (1959),

(75) Verwey, E.J.W., Roc-Trav Chim. (Pays-Pas) 55, 531 (1936).

(76) Van Uitert, L.G., Proc. I.R.E., 44, 1294-1303(1956).

(77) Guillaud, C. and Bertrand, R., J. des recherches du centre Nationale de la Recherche Scientifique,3, 73(1950).

(78) Belov, K. P. and Nikitin, S.A., Sov.Phys.Cryst., 5, 694 (1961).

(79) Lotgering, F. K., J.Phys.Chem.Solids, 25, 95 (1964).

(80) Morin, F. J. and Geballe, T. H., Phys.Rev., 99, 467 (1955).

(81) Elwell, D., Parker, R. and Sharkey,A., J.Phys.Chem.Solid, 24, 1325 (1963).

(82) Jonker, G. H., J. Phys.Chem.Solids, 9 No.2) 165-175 (1959).

(83) Larson, E.G., Arnott, R. J. and Wickham, D.G., J.Phys.Chem. Solids, 23, 1771 (1962).

(84) Rosenberg, M., Nicolau, P., Manaila, R and Pasescu, P., J.Phys.Chem.Solids, 24, 1419 (1963).

(85) Vewey, E. J.W. and De Boer, J. H., Proc.Phys.Soc., 49 Suppl. 59 (1937).

(86) Bloch, F., Z.Phys. 52, 555 (1928).

(87) Bloch, F., Z.Phys., 59, 208 (1930).

(88) Wilson, A. H., Proc.Roy.Soc., 133A, 458 (1931).

(89) Mott, N.F., Proc. Phys.Soc., 62A, 416 (1949).

(90) Yamashita, J. and Kurosawa, T., J.Phys.Chem.Solids, 5, 34-53 (1958).

(91) Yamashita, J. and Kurosawa, T., J.Phy.Soc. of Japan 15, 802 (1960).

(92) Yamashita, J., J.Appl. Phys. Suppl. 32, 221S (1961).

(93) Sinha, A.P.B. and Sinha, K.P., Indian Journal of Pure and Applied Physics, 1, 286-290 (1963).

(94) Rathenau, G.W. and Snoek, J. L., Philips Res.Rep., 1, 239 (1946).

(95) Sabane, C.D., Sinha, A.P.B. and Biswas, A.B., Indian Journal of Pure and Applied Physics, 4, No.5, 187-190, (1966).

(96) Baltzer, P. K. and Lopatin, E., paper read at "International Conference on Magnetism" (held at Nottingham, U.K.), September, 1964.

(97) Jogalekar, P. P. and Sinha, A.P,B., Indian Journal of Pure and Applied Physics (in press).

---0---